Aus dem Max-Planck-Institut für Polymerforschung in Mainz

The fabrication and application of semi-crystalline and thermoset-thermoplastic composite colloidal particles with well-defined microstructures

Dissertation

zur Erlangung des Grades

"Doktor der Naturwissenschaften"

Im Promotionsfach Physikalische Chemie

eingereicht am

Fachbereich Chemie, Pharmazie und Geowissenschaften

der Johannes Gutenberg-Universität in Mainz

Yang Zhang

geboren in Anhui, China

Mainz, Dezember 2013

Dekan:

Prodekan:

1. Berichterstatter:

2. Berichterstatter:

Tag der Prüfung: 07. Februar 2014

Table of Contents

1. Introduction

Composite materials, which are made from two or more constituent materials with different properties, are used widely from construction to transportation along the development of human history, because they can offer properties of each component and possibly synergetic properties depending on fabrication process. The concept of composite materials is not new, but rather ancient. The first use of composite materials can be dated back to as early as the 1500s B.C., when the Egyptians and Mesopotamian settlers started to use a mixture of mud and straw to build strong and durable dwellings.[1] Dried mud in brick shape is hard but brittle, while straw is strong in growing direction but easy to be crumpled up. When they are mixed together, bricks for buildings that are resistant to both squeezing and tearing are generated. Another example of ancient composite is the composite bow invented by the Mongols in 1200 A. D., which is made from wood, bone and "animal glue" created by boiling animal connective tissue for long time.[1] These bows probably were the most powerful weapons before the invention of gunpowder.

After the development of various synthetic plastic materials in the early 1900s, such as vinyl, polystyrene, phenolic, polyester and so on, modern composite materials started to arise from 1930s, when Owens Corning Fiberglass Company began to sell fiberglass in U.S.[1] The matrix of fiberglass is a plastic material, which is reinforced by glass fibers. Although glass itself is hard but brittle, the plastic matrix can bind the glass fibers together and protect them from damage. Thus a composite material with more comprehensive properties is obtained. After that, the development of modern composite materials is accelerated during the Second World War due to military requirements. Since the end of the war, many companies started to shift their attentions on composite materials from military applications to the needs in daily life. Brandt Goldsworthy, who is often called as "grandfather of composites", developed the first fiberglass reinforced surfboard, which revolutionized the sport industry.[2] In the next 20 years till 1970s, various composites with better plastic resins and improved reinforcing fibers emerged in the market, which marked the mature of composites industry. Dupont developed an aramid fiber known as Kevlar that become the standard for armor application.[1] Also, carbon fibers were developed to replace glass fibers for better mechanical performances.

Conventional composites are consisted of components that are mixed at the macroscopic level. With the arising of nanoscience in the last two decades, composite materials combining different materials at microscopic scale, or even nanoscopic scale, have attracted more and more research interests. With the decrease of the size of reinforcement, the contact area of reinforcement with matrix is increased, which means that the efficiency of the reinforcement can be improved significantly. However, to “mix” different components in microscopic and nanoscopic level is far more difficult than macroscopic level due to the drastic increase of surface energy derived from the increase of interfacial areas. On the other hand, polymer composites can be generated from polymer melts, solutions and dispersions through various methods. Due to the consideration of processing cost and the environmental effect of the manufacturing processes, water-based system are more and more preferred, especially in coating and adhesive industries. Therefore, polymer composites are produced in the form of colloidal particles, which can become bulk composites and composite films through direct drying. This type of colloidal particle is frequently called composite latex particle. The importance of this novel material class can be indicated by the amazing amount of related scientific articles and patents released in recent years. The synergistically combination of different polymers, easy processing to obtain solid functional composite materials, less negative effect on environments leads to the wide application of composite latex particles from structural composites over functional coatings to high-end packaging materials.

The objective of this thesis is the exploration of new approaches to fabricate structured composite particles in aqueous environment, which can be seen as the formation of well-defined heterogeneous structures in colloids. In general, two different routes have been carried out based on the property of the source of colloidal heterogeneous structure: heterogeneity and homogeneity. The first one is based on the assembly of heterogeneous phases to form structured colloidal particles with heterogeneity in chemistry, while the latter one is based on the creation of heterogeneous structures in colloidal particles from homogeneous mixtures through a controlled phase separation process.

In detail, the major focus of this thesis is the formation of raspberry-shaped or core-shell shaped composite particles with semi-crystalline polyacrylonitrile or epoxy thermoset embedded in soft thermoplastic polymers, which can form continuous films with

comprehensive properties. The major challenges for the preparation of such particles are the prohibition of the crystallization process in hybrid systems due to decreased regularity and the difficulty to synthesize well-dispersed thermoset colloidal particles directly in aqueous phase. The first challenge can be overcome by assembling highly semi-crystalline colloidal particles with other materials rather than copolymerization. In this thesis, polyacrylonitrile based semi-crystalline hybrid polymer particles with raspberry-shaped and core-shell shaped morphologies were fabricated by a two-stage assembly method, which is based on the assembly of reactive monomer liquid droplets and semi-crystalline polyacrylonitrile solid particles with subsequent morphology fixation step through polymerization. Attributing to the existence of polyacrylonitrile homopolymer core and soft polymer particles outside, composite particles with strong semi-crystalline feature were obtained, which could form continuous films by drying.

For the second point, the miniemulsion technique is a suitable method to prepare thermoset colloidal particles. Various processes including phase separation, free radical polymerization and polyaddition can be carried out inside miniemulsion droplets to form composite particles with well-defined microstructures. In this thesis, core-shell shaped thermoset-thermoplastic hybrid particles were prepared by combining polyaddition and free radical polymerization in individual miniemulsion droplets. It was shown that, epoxy thermoset seed particles containing reactive monomers as solvent could be generated by chemically induced phase separation process, in which epoxy thermoset network separate from reactive monomer upon curing. After monomer feeding and free radical polymerization, core-shell shaped particles were generated. As-prepared thermoset-thermoplastic particles could form continuous and transparent films with significantly improved mechanical properties compared with pure thermoplastic films.

2. Abstracts

2.1. From heterogeneity to well-defined heterogeneous structure

The synthesis of structured semi-crystalline composite colloidal particles based on liquid-solid assembly and their applications

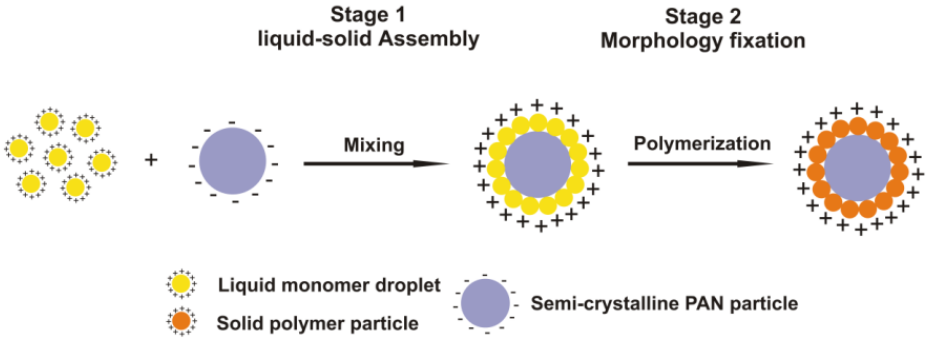

The first concept in this thesis deals with creating well-defined heterogeneous structures in colloids by precisely assembling heterogeneous species. A novel fabrication method of structured semi-crystalline composite colloidal particles with high colloidal stability based on the assembly of liquid monomer droplets and solid semi-crystalline polyacrylonitrile particles are presented. Unlike classic heterocoagulation, which is the assembly between solid particles, positively charged liquid methacylic monomer droplets are assembled with negatively charged solid polyacrylonitrile particles. Highly stable dispersions with structured semi-crystalline composite particles have been generated after free-radical polymerization, whereas direct blending of PAN dispersion with methacrylic polymer dispersion leads to immediate coagulation. Depending on the T_g of the methacrylic polymer, subsequent free-radical polymerization triggers the formation of raspberry shaped particles or core-shell shaped particles. A two-step formation mechanism describing the mobility of surfactants at the particle/droplet interfaces has been proposed, which includes the assembly of liquid droplets with solid particles driven by electrostatic interaction and the subsequent morphology fixation by free-radical polymerization. As-prepared composite particles are able to form continuous films embedded with semi-crystalline domains, which can be used in the application of oxygen barrier. The versatility of the composition of miniemulsion droplets makes this method potentially applicable for other systems.

2.2. From homogeneity to well-defined heterogeneous structure

The preparation of structured thermoset-thermoplastic composite colloidal particles and derived thermoset reinforced thermoplastic films

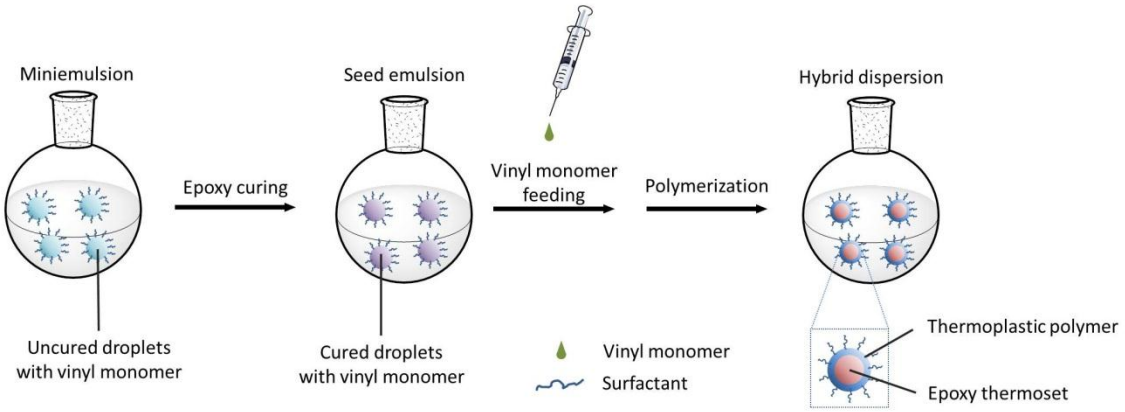

The second concept of this thesis deals with creating well-defined heterogeneous structures in colloids from homogeneous mixtures. A new preparation method of structured thermoset-thermoplastic composite colloidal particles is presented. The formation of thermoset network and thermoplastic shell has been achieved in two steps through two different polymerization mechanisms separately: polyaddition and free radical polymerization. Stable miniemulsion containing bisphenol F based epoxy resin, phenalkamine based curing agent and vinyl monomers has been prepared by ultrasonication and cured at various temperatures to obtain seed emulsions. More vinyl monomers have been added afterwards and polymerized, which leads to the formation of core-shell shaped thermoset-thermoplastic composite particles. Chemically induced phase separation between thermoset phase and thermoplastic phase takes place in both steps, which is the essence for the creation of heterogeneous structures. As-prepared composite particles can form transparent films under proper conditions, which possess much better mechanical properties compared to pure thermoplastic films. Besides an epoxy thermoset and a styrene-methacrylic thermoplastic copolymer, other thermoset and thermoplastic species have the potential to be combined together through this novel approach benefitting from the generality of this method.

3. Theories and Introduction

3.1. Polymer composite

3.1.1. Composites

Composites are an important class of engineering materials, which are widely used in various fields, such as structural applications (materials for buildings, aircraft, automobiles…), thermal applications (materials for thermal conductors, heat retention…), and so on. Nature has already offered us numerous examples of composite materials. For instance, wood is a typical fibrous composite with cellulose fibers embedded in lignis matrix. The earliest use of composite materials by human beings can be dated back to thousands of years ago when our ancient ancestors found that clay bricks can be reinforced by the incorporation of straw and sticks.

Composite materials can be defined as multiphase materials that combine two or more components with different properties.[3] There is one component acting as continuous phase, which is called the *matrix*; while other components play the role as discontinuous phases, which are called *reinforcement*, as illustrated in **Figure 1**. In the case of several species with different natures as discontinuous phases, the composite can be called *hybrid*. Compared to conventional single-phase materials, composite materials integrate the features of individual phases to exhibit a set of performance characteristics that cannot be provided by separate components.

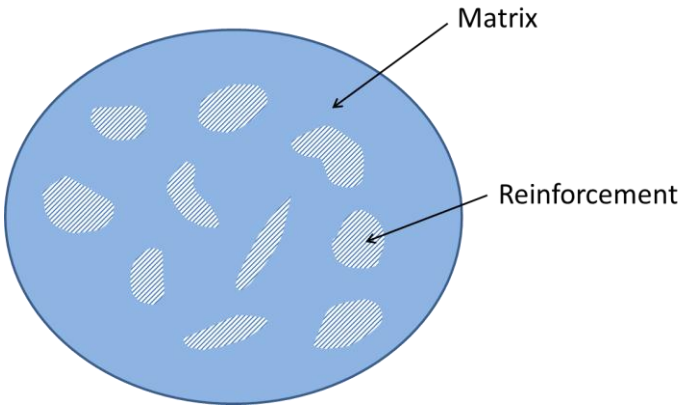

Figure 1. Schematic description of the basic composition of composite materials. Generally speaking, composite materials are consisted of two phases: matrix, which is the continuous phase; and reinforcement, which is the dispersing phase.

In general, composite materials are classified by the matrix materials, which include polymer-matrix, cement-matrix, metal-matrix, carbon-matrix and ceramic-matrix composites.[4] Due to the low cost of fabrication and easy processing, the most commonly used matrix for composites are polymers.

3.1.2. Thermosets and thermoplastics

Polymeric materials are generally classified into two categories: thermosets and thermoplastics.[5] Thermosets are polymers with network structures that are formed by the chemical reactions between multifunctional monomers, at least one of which has three or more reactive groups. The formation reaction is usually called curing, which can be induced by heating or suitable radiation. There are a variety of different thermosetting resins that can be cured to form highly crosslinked networks, including Bakelite, epoxy resin, melamine resin, polyester, and so on.[6] The properties of thermosets are majorly dependent on the structure and composition of crosslinked networks.

In contrast, thermoplastic polymers usually have high molecular weight linear chains which are not chemically linked. Therefore, from a macroscopic perspective, the most obvious difference between thermoset and thermoplastic polymers is the reprocessability. Thermosets cannot be dissolved or melted once polymerized, while thermoplastic behaves like a fluid above a certain temperature that means thermoplastics can be melted and molded several times. Depending on the requirement of final application, the matrices for polymer composite can be either thermosets or thermoplastics.

3.1.3. Polymerization mechanism

There are two major mechanisms for polymerization: chain-growth polymerization and step-growth polymerization.[5, 7] Step-growth polymerization is featured as building up polymer chains in a stepwise manner by bonding monomers to form dimers, trimers, and higher species. Polyaddition and polycondensation are typical types of step-growth polymerization. While there is no loss of molecules during reaction for polyaddition, polycondensation loses small molecules during the polymerization process. These two polymerization mechanisms are widely used in the preparation of thermosets. According to the step-wise growth mechanism, there are at least two different functional groups in every monomer molecule, which can react with each other directly to form a polymer network without the use of

initiator, which means that monomer consumes rapidly without apparent molecular weight increase. With the consumption of functional groups, the polymerization rate decreases steadily. Theoretically, there is no termination of step-growth polymerization, because the end groups are still reactive. However, many kinetic parameters like viscosity can halt the reactions in real practice. In contrast, chain-growth polymerization constructs polymers by successive binding monomers to the end of growing chains. Free-radical polymerization is the most important technique in chain-growth polymerization, which is commonly used in the preparation of thermoplastics. There are three stages in free-radical polymerization: initiation, chain propagation, and chain termination. Polymerization rate increases initially in the beginning with the creation of free radicals, which remains constant until the depletion of the monomers. In this thesis, free radical polymerizations are used to create semi-crystalline polymers and various thermoplastics, while polyaddition is utilized to fabricate epoxy thermosets.

3.1.4. Epoxy polymer

Epoxy polymer is one of the most important thermoset materials in industry due to their unique properties, including minimum fabrication pressure of products, low cure shrinkage, various choices of raw materials and curing conditions, and so on. First epoxy polymer was invented by Schlack in 1934.[8] The research and development in the field of epoxy polymers boosted in the 1970s and 1980s benefitting from the establishment of most of the fundamental knowledge in thermosets. In the same period, new formulations and processing methods for different applications of epoxy polymers, such as adhesives, coatings, structural polymers, and composites, have been developed. In the last 20 years, due to the emergence of nanoscience, various new concepts have been applied in the field of epoxy, such as the incorporation of nano- and submicro-sized inorganic and organic fillers in epoxy polymers to further improve the performance of traditional epoxy based materials[9].

There are a number of different types of epoxy resins from difunctional to multifunctional resins, as shown in **Figure 2**.

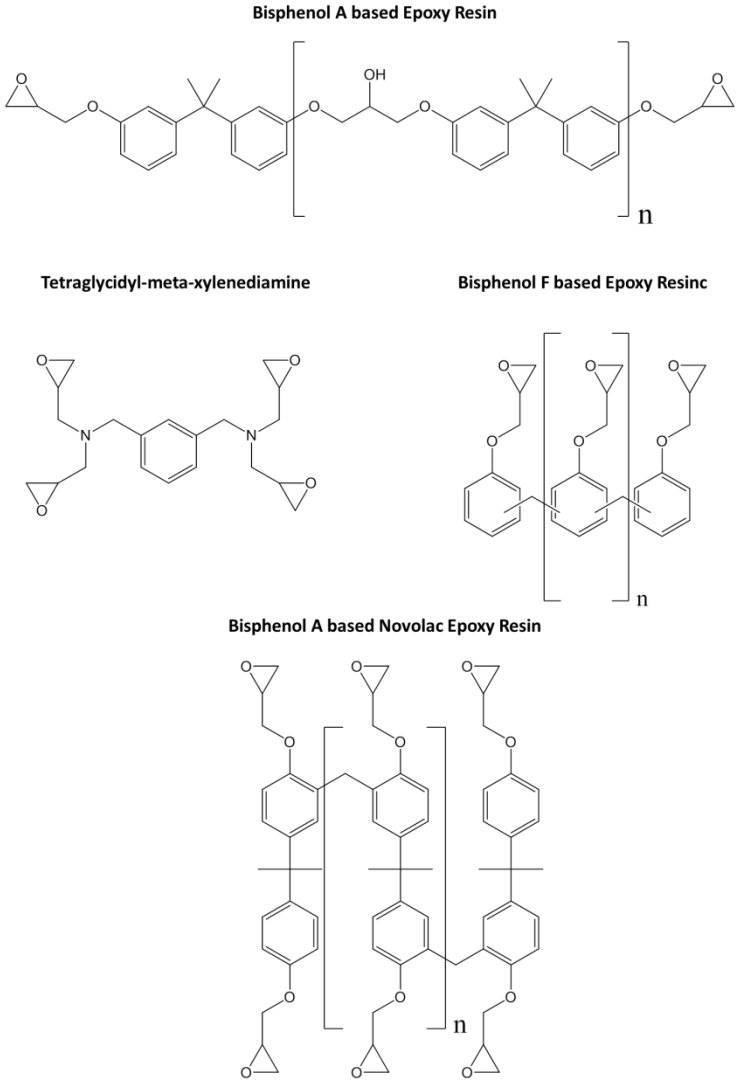

Figure 2. Chemical structures of commonly used difunctional and multifunctional epoxy resins.

Except for ultrahigh molecular weight phenoxy resins and epoxy thermoplastic resins, almost all epoxy resins need to be converted to a solid thermosetting polymer in real industrial applications.

Regarding to the curing of epoxy resins, two reactive groups in epoxy resins, epoxy and hydroxyl are involved. From the mechanism perspective, there are two basic curing mechanisms: coreactive and catalytical curing.[10] For coreactive curing, commonly used curing agents (usually called hardners) are amines, polyamides, anhydrides, etc. Because the reactions between epoxy resin and many hardeners are not fast enough, Lewis acids like alcohols, phenols or carboxylic acids are usually used as accelerators for the curing reactions. A typical curing mechanism of epoxy resin by amine is illustrated in **Figure 3**. For catalytic curing, Lewis bases containing unshared electron pairs can act as nucleophilic catalytic curing

agents for epoxy curing. A tertiary amine is the most commonly used catalyst for curing. **Figure 4** demonstrated the curing process of epoxy resin by tertiary amine based on catalytic mechanism.

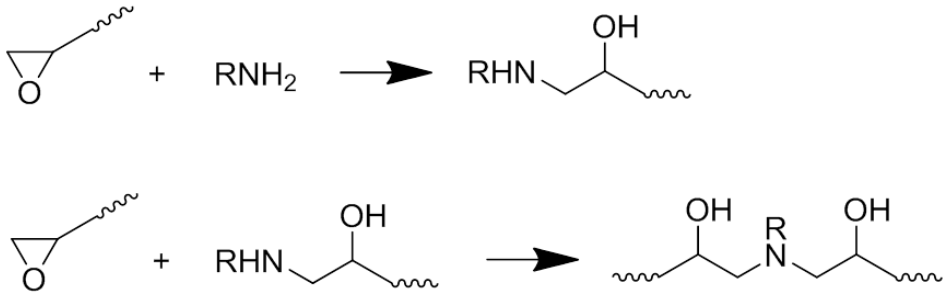

Figure 3. Epoxy curing with coreactive mechanism

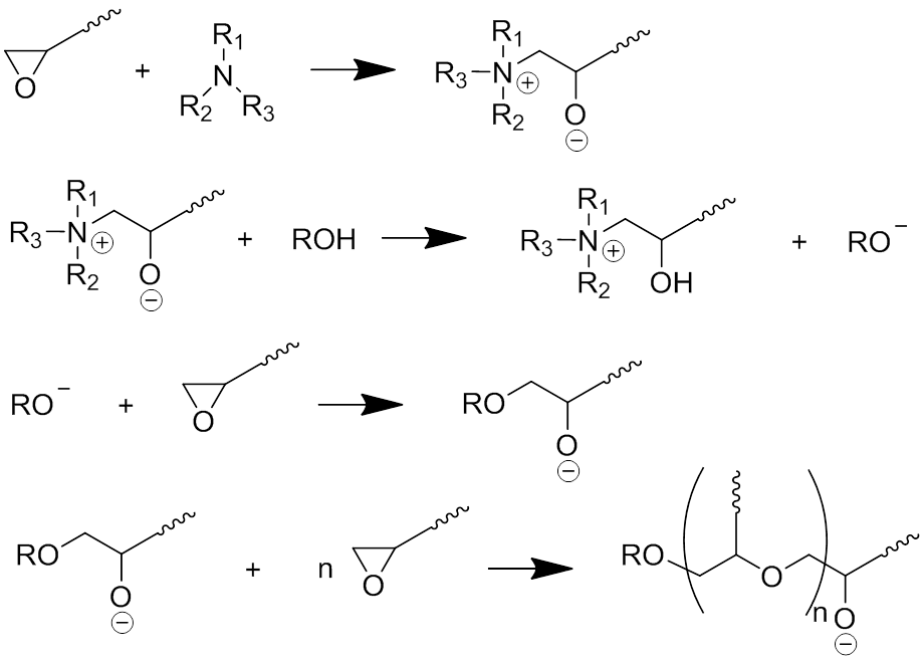

Figure 4. Epoxy curing with catalytic mechanism.

In this dissertation, epoxy thermoset has been synthesized by using primary and secondary polyamines as curing agents. Therefore more details regarding to this specific type of curing pairs are provided in the following paragraph.

For epoxy-amine curing reactions, there are two important terms related to the characterization of epoxy resin and amine curing agents respectively: the epoxy equivalent weight (EEW) and the amine hydrogen equivalent weight (AHEW). The EEW is defined as the weight of epoxy resin required to obtain one equivalent of the epoxy functional group. The AHEW is defined as the weight of an amine curing agent containing one equivalent of N-H

groups. For the stoichiometric ratio of functional groups, the amount of amine that is required to cure epoxy resin can be calculated by following equation:

$$m_{\text{Amine}} = \frac{AHEW \times m_{\text{Epoxy}}}{EEW}$$

The properties of an epoxy thermoset are determined by the structure of the repeating units that consist of a crosslink network and the distance between crosslinking joints. As shown in **Figure 5**, high EEW and AHEW of the epoxy resin and the amine curing agent leads to the formation of a less dense network, and vice visa.

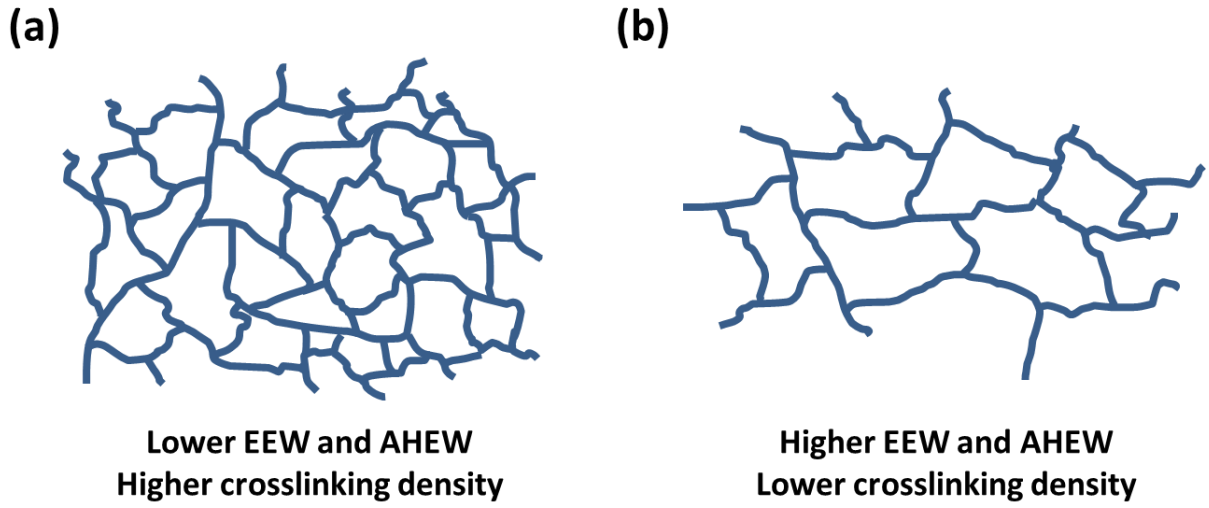

Figure 5. Schematic drawing of epoxy thermoset networks with different crosslinking densities which are determined by the EEW of the epoxy resin and the AHEW of the amine curing agent. Epoxy thermoset networks with higher crosslinking density usually have a higher glass transition temperature, which leads to an improvement in hardness of the materials. However, the major drawback of a highly crosslinked epoxy thermoset is its brittleness.

Phenalkamines are a special class of amine curing agents, which are hydrophobic and react fast with epoxy resins at relative low temperature (<5 ^{o}C) in humid atmosphere. They can be obtained by the reaction of Cardanol with formaldehyde and a polyamine through the Mannich reaction, as shown in **Figure 6**.[11] In this dissertation, a Cardanol-based phenalkamine is utilized as standard amine curing agent.

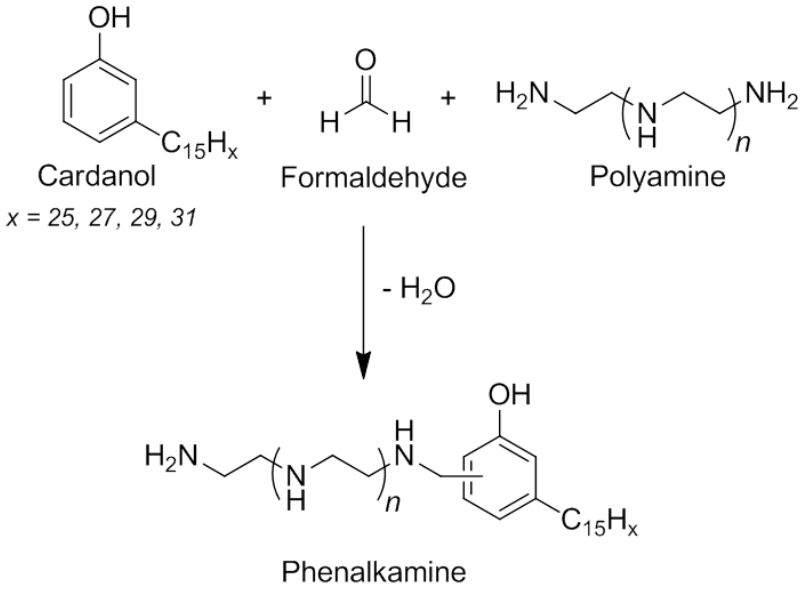

Figure 6. The synthesis route of a cardanol-based phenalkamine by Mannich reaction.

3.1.5. Phase separation in thermoset-thermoplastic composite

For polymer composites, one of the most important phenomena is phase separation. The discussion of phase separation could be started from polymer blends. When any two materials are mixed together, the properties of the mixture are strongly dependent on the level of miscibility of the two species. Most polymers cannot be mixed homogeneously like low molecular weight compounds.[12] Therefore polymer blends can be generally categorized into two types: miscible polymer blends and immiscible blends. For the former, the miscibility and homogeneity of the blend stays at the molecular level, which indicates no phase separation. In contrast, there is phase separation in the immiscible polymer blend. An immiscible blend can be called compatible if the inhomogeneity is only on the micro-scale rather than macro-scale. Most polymer mixtures are immiscible but can be made to be compatible through various compatibilization techniques.

In general the necessary condition for two substances to mix is described by the Gibbs energy of mixing (G_{mix}) which is expressed by:

$$\Delta G_{mix} = \Delta H_{mix} - T\Delta S_{mix},$$

where *H* is the enthalpy and *S* is the entropy. When the Gibbs free energy of the mixture is less than the sum of the Gibbs free energies of the individual constituents, i.e. $\Delta G_{mix} < 0$, these two substances can be mixed homogeneously.

For two small-molecule compounds, the change in enthalpy during mixing is small, therefore, the free energy of mixing is almost entirely dependent on the entropy change in mixing. The increase of entropy is usually sufficient enough to allow mixing to take place spontaneously in a certain concentration range, even when the ΔH_{mix} is positive. On the contrary, the entropy of mixing two polymers is usually much smaller than it would be for the mixing of the corresponding monomers. So the enthalpy term is of key importance in determining the sign of the Gibbs free energy change of mixing. In most case, even a small positive value of ΔH_{mix} would hinder the homogeneous mixing.[12]

The phase separation of polymer mixtures is theoretically described by Flory-Huggins theory, according to which the molar entropy change S^m_{mix} is given by:

$$\Delta S^m_{mix} = -R\,[(\phi_1/X_1)\ln\phi_1 + (\phi_2/X_2)\ln\phi_2]$$

Where X is the degree of polymerization, ϕ the volume fraction and R the molar gas constant and the molar enthalpy change H^m_{mix} is given by:

$$\Delta H^m_{mix} = RT\,\chi_{12}\,\phi_1\,\phi_2$$

Where χ_{12} is the Flory-Huggins interaction parameter.

Combining two equations, the molar Gibbs energy change of mixing can be calculated as:

$$\Delta G^m_{mix} = \Delta H^m_{mix} - T\Delta S^m_{mix} = RT\,[\chi_{12}\,\phi_1\,\phi_2 + (\phi_1/X_1)\ln\phi_1 + (\phi_2/X_2)\ln\phi_2]$$

There are two basic types of phase separation in composite materials, thermally induced phase separation and chemically induced phase separation, which are defined by the trigger.[13]

Thermally induced phase separation (TIPS)

As described above, if the phase separation inside materials is triggered by a temperature quench, such a process is called thermally induced phase separation. It is not surprising that temperature plays an important role in the occurrence of phase separation, because both items in the Flory-Huggins equation, $T\Delta S^m_{mix}$ and ΔH^m_{mix}, are strongly dependent on temperature. Moreover, the Flory-Huggins interaction parameter is not constant. In contrast, it is determined also by temperature and other factors like composition, temperature, and the

molecular weight of the polymer. According to this, phase diagrams are utilized for the characterization and predication of phase behaviors. For TIPS, there are basic phase diagrams, as demonstrated in **Figure 7**, which are related to two behaviors: the upper critical solution temperature (UCST) and the lower critical solution temperature (LCST).

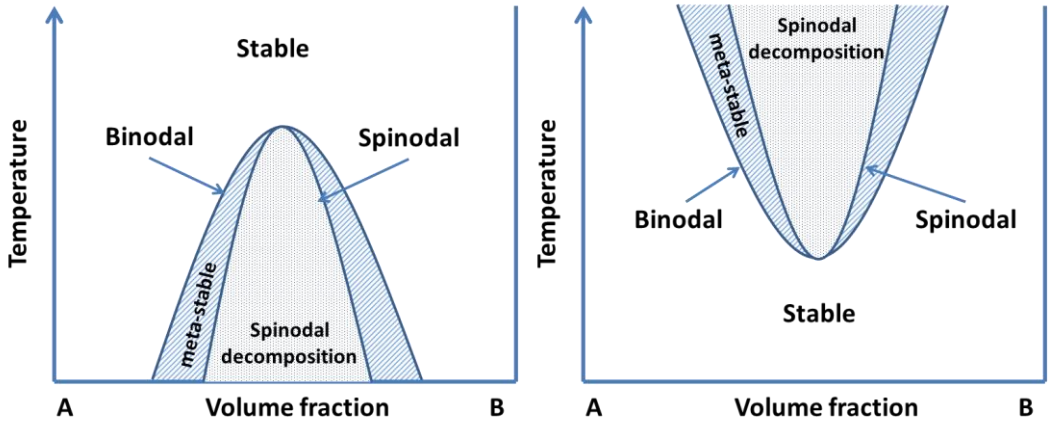

Figure 7. Schematic phase diagrams of upper critical solution temperature (UCST) in (a) and lower critical solution temperature (LCST) in (b).

In the phase diagrams, the stable region and the metastable region is separated by the binodal line. Inside the metastable region, the spinodal line separates it into two regions defined by different mechanisms for the initiation of phase separation. The area enclosed by spinodal line represents the phase separation process following spinodal decomposition mechanism. In this process, the rapid cooling can be seen as a quench that favors the formation of phase separated clusters or domains without a nucleation step due to the lack of an energy barrier for the formation of new phases. In contrast, the intermediate area between the binodal line and the spinodal line is the place where the phase separation is initiated via a nucleation and growth mechanism. This process is usually very slow because the formation of microscopic domains involves the crossing of a large free energy barrier.

Chemically induced phase separation (CIPS)

Besides temperature, the change of free energy can be triggered by chemical reactions such as polymerization. This is called chemically induced phase separation, the schematic phase diagram of which is demonstrated in Figure **8**. For thermoplastic polymers, when the polymerization is carried out in solvents, with the increase of molecular weight, the miscibility between polymer and solvents decreases, which leads to the precipitation of the polymer. For

thermoset polymers, a curing process leads to the formation of a highly crosslinked structure that is accompanied by the drastic molecular weight build-up during polymerization, which can be seen as “quench” that leads to the phase separation with spinodal decomposition mechanism. In this thesis, the CIPS concept is used to carry out the curing reaction of an epoxy by amine curing agents with the existence of vinyl monomers, which phase separate out to form thermoset domains during curing reaction.

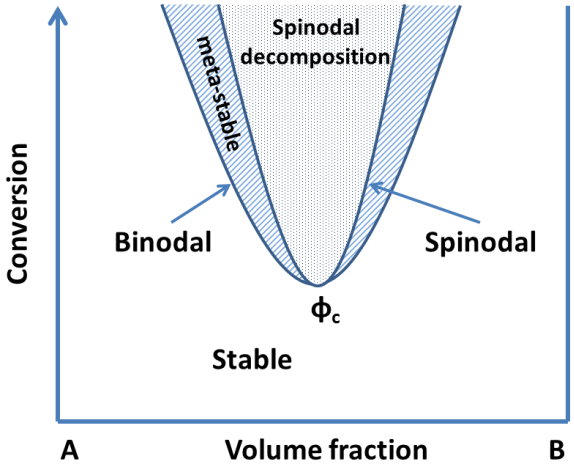

Figure 8. Schematic phase diagram of chemically induced phase separation (CIPS).

Depending on the phase separation mechanism, different morphologies can be generated in the cured thermoset-thermoplastic composites. If the phase separation is following a nucleation and growth mechanism, the phase separation process is dominated by the energy barrier for the creation of new surfaces, which leads to a spherical shape of the dispersing phase, because spherical shape offers the largest volume to surface ratio. For the phase separation process following spinodal decomposition, the morphology evolution proceeds through several stages, as shown in **Figure 9**. The key feature is that the shape of domains is not uniform.

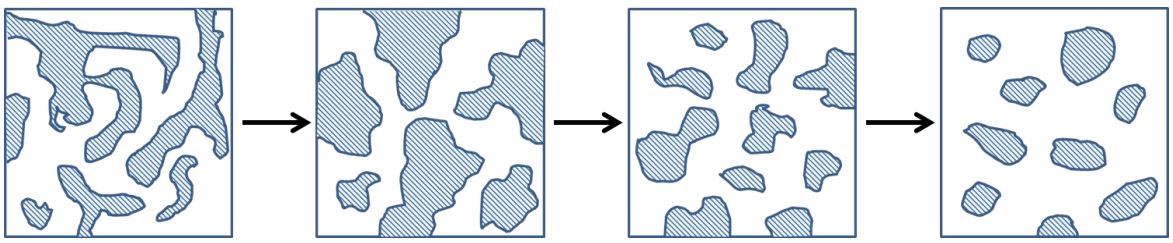

Figure 9. Morphology evolution of composite materials obtained from chemically induced phase separation through spinodal decomposition mechanism.

3.2. Emulsions and dispersions

Emulsions can be defined as heterogeneous mixtures of at least one immiscible liquid as dispersed phase (in the form of droplets) and another liquid as continuous phase. Unlike emulsions, solid particles are the dispersed phase in dispersions. Depending on the feature of the dispersed phase and the continuous phase, emulsions can be divided into two categories: oil-in-water (o/w) and water-in-oil (w/o) emulsions. Most commonly used emulsions belong to the o/w type with water as continuous phase.

In general, conventional emulsions, which are also mentioned as macroemulsions, are metastable colloidal systems, which usually possess a minimal stability with a droplet size between 100 nm and 10 µm in diameter. The formation of such emulsions is not spontaneous, but needs energy input such as stirring, shaking and homogenization. Additives like surfactants, nano/submicro-scaled solid particles and polymers are added during the emulsion preparation process, which is named as emulsification. Thermodynamically stable emulsions, which are named as microemulsions, can be formed spontaneously with an extremely high amount of surfactants added (>10 wt% related to the dispersing phase).

3.2.1. Emulsions stability

The most influential theory related to the stability of emulsions is the DLVO theory, which is developed by the four different scientists Derjaguin, Landau, Vervey and Overbeek independently in 1940s.[14-21] This theory suggests that the stability of a colloidal particle is determined by the total potential energy of interactions V_T, which includes attraction part V_A and repulsion part V_R:

$$V_T = V_A + V_R$$

The attraction interaction V_A between particles is derived from Van der Waals forces which are given by:

$$V_A = \frac{-Aa}{12H}$$

Where A is the Hamaker constant, a is the radius of the particle, and H is the shortest interparticle distance.

The repulsion part V_R usually arises from the charges on the surface of particles, which is given by:

$$V_R = \frac{\varepsilon_r a^2 \psi^2 \exp(-\kappa H)}{2a + H}$$

Where ε_r is the dielectric constant of the dispersing phase, ψ is the surface potential of the particle, a is the radius of the particle, H is the shortest interparticle distance, κ is the inverse of the Debye length that is defined as the distance to which the surface potential of the charged particle falls to its 1/exp value.

According to DLVO theory, repulsive forces between two particles prevent them approaching each other and adhering together, which creates an energy barrier, as shown in **Figure 10**. However, if the particles are endowed with energy that is enough to overcome the energy barrier, the attractive force will pull them into contact and bind them together irreversibly. Therefore, the colloidal stability of emulsion is strongly dependent on the repulsion mechanism. If the repulsive forces between particles are strong enough, flocculation (reversible aggregation) and coagulation (irreversible aggregation) can be avoided that brings stable emulsions.

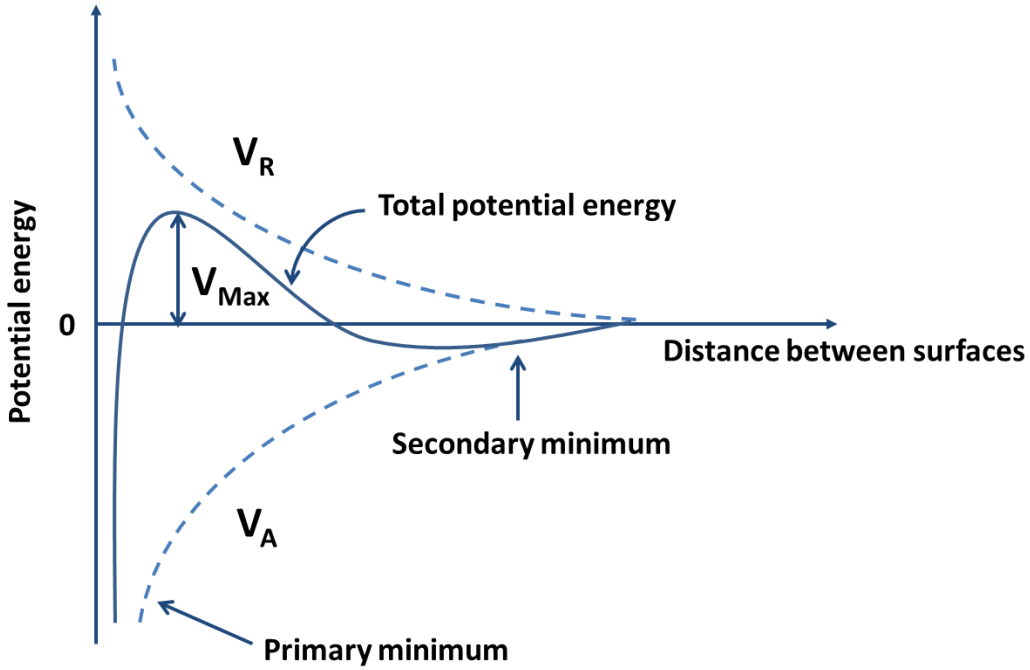

Figure 10. Schematic diagram of free energy change between particles with different separation distances according to DLVO theory.

In practice, the stability of emulsions is usually achieved through two basic mechanisms: the steric repulsion and the electrostatic repulsion, as shown in **Figure 11**. For electrostatic repulsion, usually ionic surfactants are added into the dispersion, which are adsorbed on the particles to offer strong electrostatic repulsions to counterbalance the attractive forces. For the steric stabilization mechanism, non-ionic surfactants and polymers are used and expected to be adsorbed on the surface of particles to prevent particles coming into close contact. The repulsive forces here include two major types: entropic force and osmotic repulsion. When non-ionic surfactants and polymers from different particle surfaces approach and overlap, the entropy in the interface will decrease, this is unfavorable for the system. Therefore, particles turn to separate from each other to increase entropy, which is the entropic force. On the other hand, when particles collide to each other, solvent molecules between particles are expelled out, which results in the increase of the osmotic pressure. So the solvent will diffuse back from the bulk to this region to reduce the osmotic pressure. This is the so-called osmotic repulsion. Recently, nano-sized and micro-sized solid particles that are partially wettable by oil and water are utilized as novel stabilizers for emulsion, which are known as Pickering stabilizers. The repulsive forces for the stabilization are determined by the surface properties of Pickering particles, which are still based on the two basic stabilization mechanisms described above.

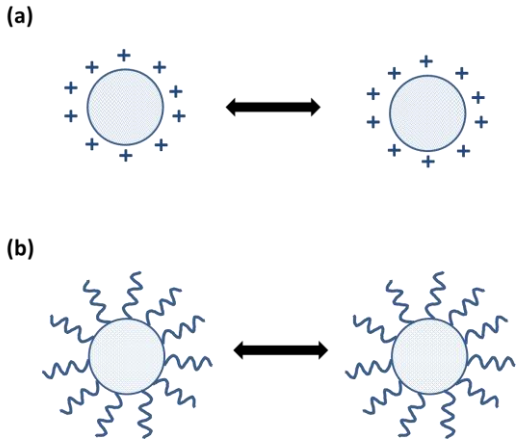

Figure 11. Schematic display of two stabilization mechanisms for colloidal particles: (a) electrostatic repulsion; (2) steric repulsion. It is common that many colloidal systems are stabilized by these two mechanisms simultaneously.

Regarding the stabilization mechanism based on electrostatic repulsion, the electrical double layer is a term that must be clarified with in more detail. In colloidal particles or droplets, the electrical double layer is a structure that describes the variation of the electric potential near

a surface of particles or droplets, which is schematically demonstrated in **Figure 12**. Based on the Stern model, the electrical double layer is consisted of a Stern layer and a diffuse layer. These two layers are separated by a plane, which is named as the Stern plane. The Stern plane is located at about a hydrated ion radius from the surface, because the center of an ion can only approach the surface within the range of its hydrated radius without being specifically absorbed. Adsorbed ions are attached to the surface of particles or droplets through electrostatic and/or van der Waals forces and are located in the Stern layer, between the surface of particles or droplets and the Stern plane, while ions are distributed according to the influence of electrical forces and the random thermal motion in the outer diffuse region. Within the diffuse layer there is a boundary which is called slipping plane. The ions between the slipping plane and the Stern plane form a stable entity which means that ions in this area move together with particles or droplets when they move. In contrast, the ions beyond this boundary do not travel with particles or droplets together.

Since the concept of the electrical double layer is explained, it is necessary to explain another term that is important for this thesis, the zeta potential. The zeta potential is the potential at the slipping plane, which gives an indication of the potential stability of the colloidal system in practice. As a thumb of rule for the colloids that are stabilized by electrostatic repulsion, significant aggregation occurs in emulsions and dispersions when the absolute value of the zeta potential of the droplets or particles is below a threshold of ca. 20 mV.[22]

The electrophoresis phenomenon of charged particles or droplets is commonly utilized to measure the zeta potential. In principle, when the charged particles or droplets are suspended in an electrolyte solution, they tend to move with constant velocity when an electric field is applied. The zeta potential can be calculated from the Henry equation when the velocity of the particles or droplets is known:

$$U_E = \frac{2\varepsilon z f(ka)}{3\eta}$$

where z is zeta potential, U_E is the velocity of the particle or droplet (also called electrophoretic mobility), ε is dielectric constant, η is viscosity, $f(ka)$ is Henry's function. For electrophoresis in aqueous media with moderate electrolyte concentration, $f(ka)$ is 1.5, which is referred as the *Smoluchowski* approximation. For small particles in low dielectric

constant media, like non-aqueous media, $f(ka)$ becomes 1.0, which is referred as *Hückel* approximation.

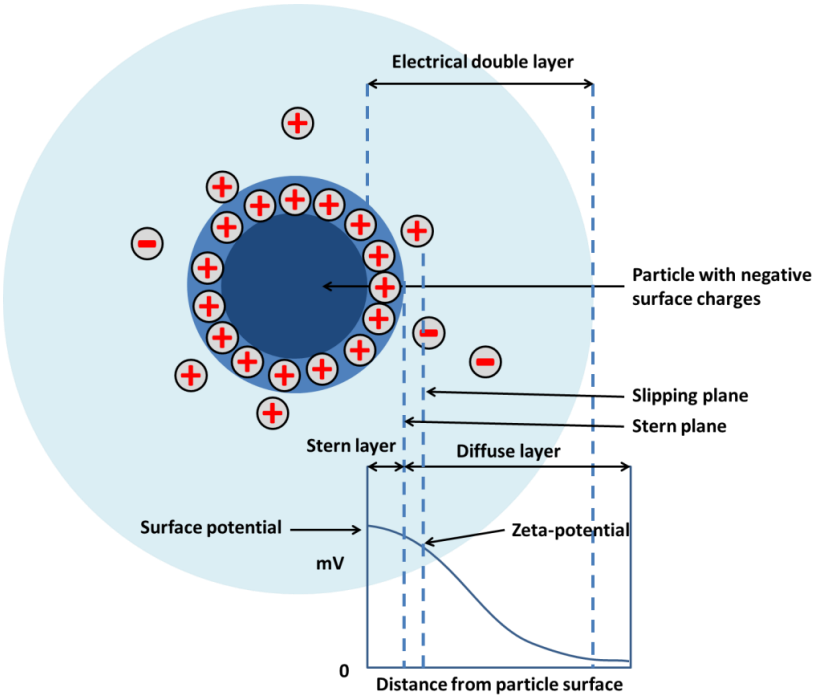

Figure 12. Schematic display of electrical double layer and related academic terms.

3.2.2. Film formation of emulsion polymers

Film formation of emulsion polymers is a process through which solid films are obtained by evaporating the water out of the latexes. Continuous films can form when film formation process is completed, while incomplete film-formation leads to powdery layers. A schematic demonstration of this process is shown in **Figure 13**. In principle, the evaporation of water upon time during drying brings polymer particles closer, which leads to the formation of "capillary tubes" between particles. With the decrease of the diameter of the "capillary tubes", when particles approach to each other further, the force originating from surface tension to collapse the tube increases, which cause the coalescence of particles and film-formation. The rate of coalescence is strongly dependent on the particles size and the T_g of the polymer. Generally speaking, the smaller the particle and lower the T_g is, the faster the coalescence, which accelerates the film-formation. [23]

Normally, the minimum film formation temperature (MFFT) of the latexes with core-shell morphology follows the trend below:

Soft-hard (core-shell) > medium-medium > hard-soft

However, the above trend is only valid when the shell is thick enough. For the core-shell particles with thin and soft shells, a higher temperature is required for successful film formation compared to the ones possessing thick shells and the same chemical composition. This is because more deformation of particles is needed for the film formation process, which involves core particles at the same time.

Coalescence agents, including 2,2,4-trimethyl-1,3-pentanediol monoisobutyrate (Texanol), henxanediol, ethyleneglycol monoethyl ether, diethyleneglycol butyl ether and xylene, are commonly used to assist the film formation process when the application temperature is below the minimum film formation temperature. The function of the coalescence agents is to soften polymer particles similar to plasticizers that can decrease the T_g of the polymers, the extent of which is defined by the difference between solubility parameters of coalescing agents and emulsion polymers. The smaller the difference is, the better the film formation is. In addition, a certain amount of coalescing agents exists in aqueous phase also, which could decrease the evaporation rate of water, thus benefit the leveling properties of the latexes.

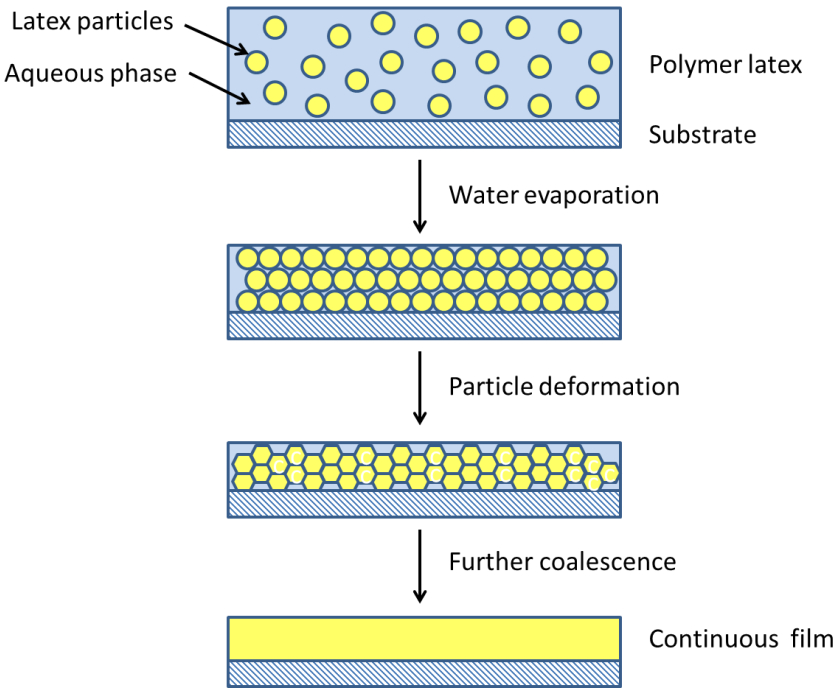

Figure 13. Schematic display of the film formation process of water-based latexes. Upon water evaporation, latex particles start to come close to each other. When the distance between particles is small enough, the capillary force originated from the particle interfaces causes the deformation of particles and induces further coalescence to form continuous films.

3.3. Heterophase polymerization

Heterophase polymerization can be defined as polymerization reactions that are carried out under nonhomogeneous conditions, which implies the existence of different phases and gradients in chemical compositions.[24] Generally speaking, heterophase polymerizations are utilized to produce polymer dispersions, in which fine polymer particles are dispersed in a continuous phase. Heterogeneity here requires the formation of materials in the disperse phase that are insoluble/immiscible in the continuous phase. Therefore, almost all combinations of the state of matter, except the gas-gas combination, can be used to carry out the heterophase polymerization, which includes precipitation polymerization, dispersion polymerization, emulsion polymerization, miniemulsion polymerization, microemulsion polymerization, and so on. Among them, miniemulsion polymerization and emulsion polymerization are of key importance to this dissertation, which are discussed separately in the following part.

3.3.1. Emulsion polymerization

Emulsion polymerization is one of the most widely applied heterophase polymerization techniques since the commercialization of this process in the early 1930s. It involves the emulsification of a monomer in water by an emulsifier and the subsequent initiation of free radical polymerization by water-soluble and oil-soluble initiators. The most differentiable feature of emulsion polymerization, if compared with other free radical polymerization methods like bulk polymerization and solution polymerization, is the existence of micelles and the fact that the locus of the polymerization are the micelles. A micelle can be defined as an aggregate of surfactants dissolved in a continuous liquid phase, which forms when a certain concentration threshold is achieved. This boundary concentration of surfactants is named as critical micelle concentration (CMC).

In a typical emulsion polymerization process, there are monomer droplets with the size of 1 to 10 mm, monomer-swollen micelles with the size of 5 to 10 nm, micelles with the size of 4 to 5 nm and a very small amount of dissolved monomers in the continuous phase, as shown in **Figure 14**.[25] When discussing about the mechanism of emulsion polymerization, it is important to know where the three steps of free radical polymerization (initiation, propagation, and termination) take place.

To answer this question, the locus of nucleation for the particle formation should be clarified first. There are three different types of nucleation mechanisms, depending on the solubility of the monomer in the continuous phase, the surfactant concentration, the solubility of the initiator in the monomer and the continuous phase, and so on. The first nucleation mechanism is micelle nucleation, which is also the most classic nucleation mechanism for emulsion polymerization. This is most suitable for monomers that are difficult to dissolve in water. Due to the extremely large oil-water interfacial area, micelles are much more competitive than monomer droplets in capturing the free radicals that are generated by initiators. Therefore, after nucleation from micelles, the propagation of polymer chains continues inside the micelles. Classic emulsion polymerization is characterized by the fact that all three steps of free radical polymerization take place in discrete micelles or monomer-swollen micelles. This ubiquity decreases the chances of a bimolecular termination, which in turn endow classic emulsion polymerization two advantages, high molecular weight and fast polymerization speed, if compared with solution polymerization and bulk polymerization. When the size of monomer droplets is comparable to monomer-swollen micelles, they can directly capture free radicals formed in continuous phase, which is the second type of the nucleation mechanism: the droplet nucleation mechanism. When initiators are dissolved in monomers before polymerization, the polymerization also takes place inside monomer droplets, which is also following a droplet nucleation mechanism. Miniemulsion polymerization is a typical type of a polymerization technique that follows the droplet nucleation mechanism, which will be described later with more details. The third type of nucleation is homogenous nucleation in continuous phase, which is mostly applied for hydrophilic monomers.

Generally speaking, the classic emulsion polymerization process can be divided into three distinct intervals, as illustrated in **Figure 15**.[23] Interval I is the nucleation stage. During this period of time, free radicals formed in continuous phase polymerize with dissolved monomers to form oligomeric radicals first, which become more and more hydrophobic that tend to enter monomer-swollen micelles to form a nucleus. Meanwhile, those micelles that do not contribute to the nucleation process dissociate to fulfill the increasing demand for surfactant molecules to stabilize growing particles. In this stage, micelles convert to particle nuclei continuously. With the disappearance of micelles and the appearance of particle nuclei, both the conversion of polymerization and polymerization rate increases, till all micelles disappear.

In this point, the number of particle nuclei turns to be constant, which means that the final particle number is determined and remains constant along the following two intervals. It also marks the end of Interval I.

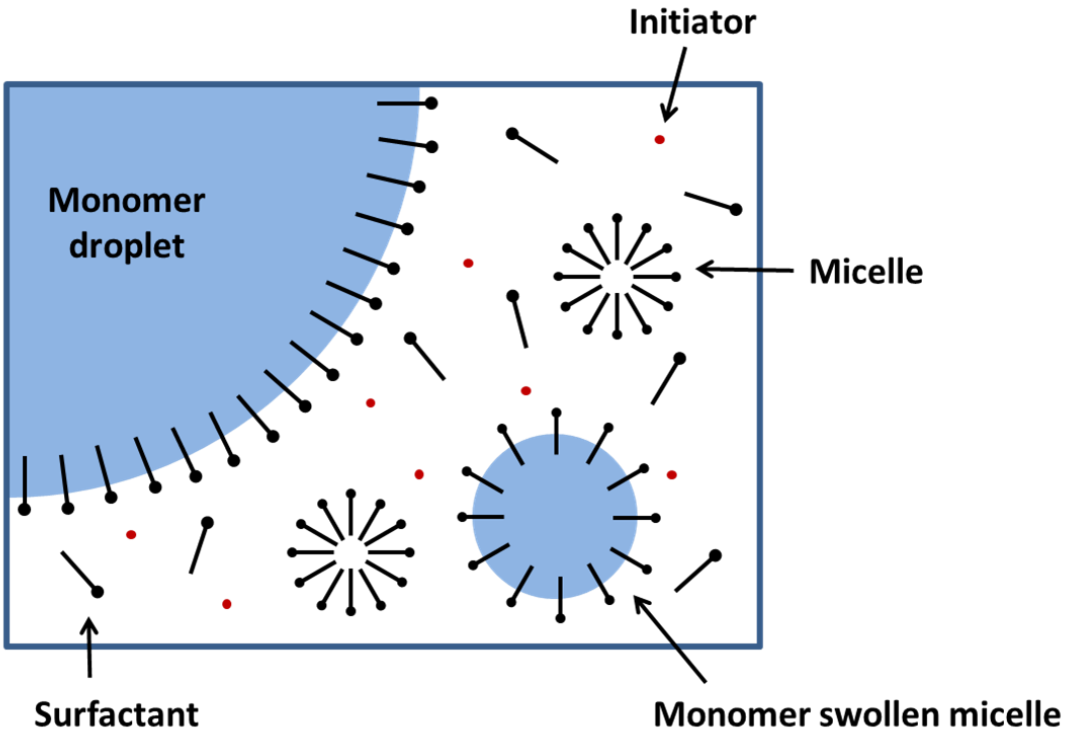

Figure 14. Schematic display of the phases existing in the emulsion polymerization systems: monomer droplets, monomer swollen micelles and micelles.

Interval II is the particle growth stage, where there are only particle nuclei and monomer droplets. Monomers keep diffusing through the continuous phase from monomer droplets to nuclei to keep the monomer concentration inside the nuclei constant, which means the polymerization rate is constant also. With the increase in the size of nuclei, monomer droplets become smaller and smaller. The end of this stage is marked by the disappearance of monomer droplets.

In Interval III, all monomers are inside particle nucleus. Along with the polymerization of these residual monomers, the polymerization rate decreases gradually till the end.

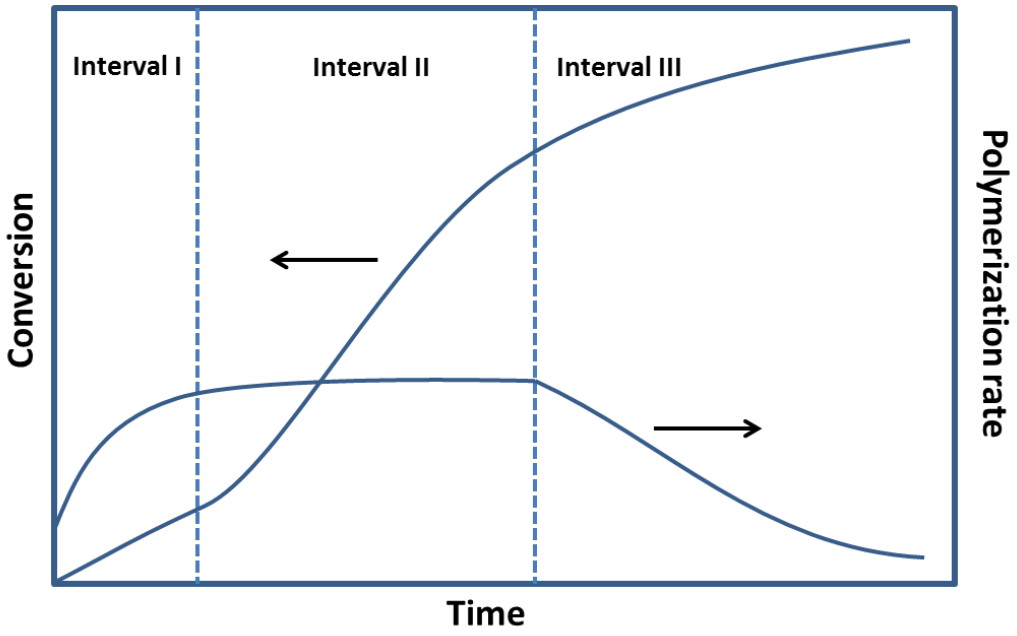

Figure 15. Schematic display of the kinetics of classic emulsion polymerization process. Interval I – nucleation; interval II – growth of latex particles; interval III – Consumption of residual monomers.

3.3.2. Miniemulsion polymerization

The first report on the preparation of miniemulsion was published by Ugelstad *et al* in 1973. [26] They have demonstrated that the reduction in average size makes the monomer droplets more competitive in capturing radicals generated in the aqueous phase. Miniemulsion is named as a stable emulsion of very small droplets due to historical reasons.[27] According to more a precise and strict definition, miniemulsions are specially formulated heterophase systems where stable droplets ranging between 30 and 500 nm in size as one phase are dispersed in a second, continuous phase.[28] High energy homogenization methods like ultrasound and high-pressure homogenization are commonly used to create such small droplets.[29] During homogenization, large droplets are broken down to small droplets and stabilized by the adsorbed surfactant. The polydispersity decreases through fission and fusion processes till an equilibrium state is reached, as shown in **Figure 16**.[30]

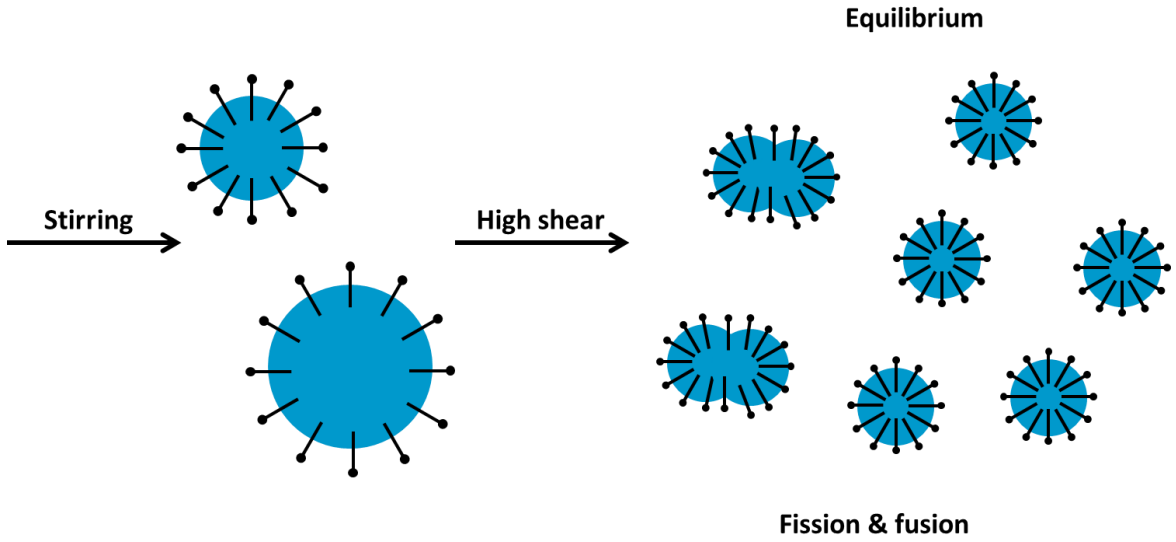

Figure 16. Formation process of droplets in an equilibrium state through the miniemulsification process.

Compared to thermodynamically stable microemulsions, miniemulsions are not thermodynamically stable, but kinetically stabilized. The stability of miniemulsions relies on the hindrance of two major destabilization processes: coalescence and Ostward ripening.[31] Coalescence is the fusion of multiple droplets due to collisions, which can be suppressed by the use of proper surfactants. It has to be emphasized that the amount of free surfactant (not adsorbed to interfaces) in miniemulsion is lower than the CMC, even when the total surfactant concentration in the formulation is higher than CMC, because most of the surfactants are adsorbed on the continuously created surfaces of small droplets by homogenization process. Ostward ripening denotes as the process in which larger droplets grow at the expense of smaller droplets. [29, 31, 32] Higher Laplace pressure in smaller droplets results in a net mass flux by diffusion, which is the driving force of this aging process. Therefore, hydrophobes like long-chain alkanes and lipophobes such as inorganic salts are commonly used as osmotic agent to build up an osmotic pressure that can counterbalance the Laplace pressure. [31, 32] Thus the diffusion process of ingredients from smaller droplets to larger droplets can be suppressed.

If there are reactive monomers in the droplets, they can be polymerized inside the droplets. This process is called miniemulsion polymerization. A typical miniemulsion polymerization process is illustrated in **Figure 17**. To understand the importance of the miniemulsion polymerization technique for the fabrication of structured latex particles, a short introduction on the “nanoreactor” concept has to be given. As discussed in 3.3.1, classic emulsion

polymerization process is featured by the particle nucleation from micelles and continuous diffusion of monomer into the nucleus through the continuous phase, which is because it is much easier for micelles to capture radicals than monomer droplets attributing to larger interfacial surface areas. When the droplet size is closer to the size of micelles, like the case in miniemulsion, nucleation and polymerization processes can take place directly inside monomer droplets. Therefore, these discrete droplets can be considered as nanoreactors. Polymerizations proceed easily in these nanoreactors like in bulk but with more advantages, such as heat transferring. Benefitting from restricted diffusion, heterophase polymerization can be extended from conventional free radical polymerization to a much broader range, including step-growth polymerization like polyaddition and polycondensation, ionic polymerization, catalytic polymerization and so on.[33]

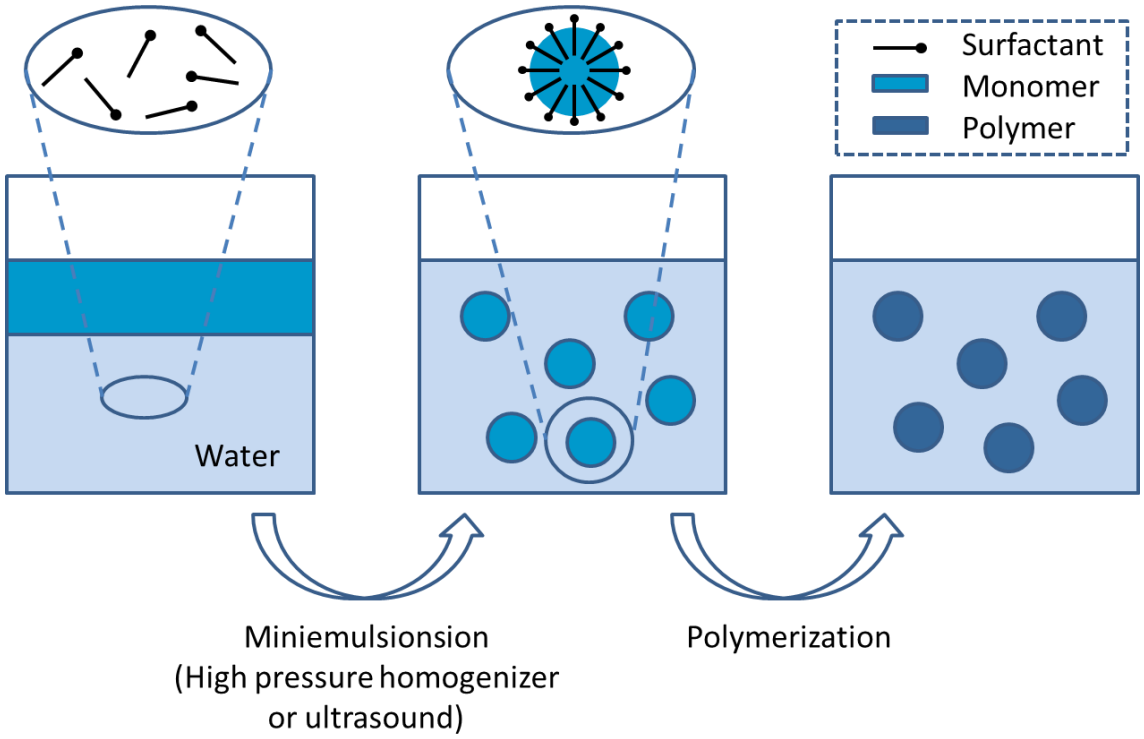

Figure 17. A typical process of miniemulsion polymerization.

For example, Antonietti, Landfester et al. have reported the pioneer work on applying miniemulsion polymerization technique to produce epoxy thermoset following a polyaddition mechanism by reacting epoxy resin with different types of curing agents from diamine to dimercaptans and polyurethane by reacting isophorone diisocyanate with hydrophobic diols.[34, 35] Also polyesters latex nanoparticles have been synthesized with a high yield through miniemulsion polymerization, benefiting from the expelling of water generated in

condensation reactions out of hydrophobic droplets due to incompatibility.[36] In this thesis, miniemulsion polymerization technique is utilized to produce semi-crystalline polymer particles following free radical polymerization mechanism and epoxy thermoset following polyaddition mechanism, which will be described thoroughly later.

3.4. Structured composite latexes

Since the first commercial product of composite polymer latex, K-120, which is produced by Rohm & Hass Co. in 1957 as a plastic modifier,[37] a variety of composite polymer latexes with well-defined microstructures has been developed and used in both numerous academic and industrial applications. Hybrid polymer latexes are defined as colloidal dispersions in which at least two distinct polymers exist within each particle.[38] The most attractive property of such composite latexes is that the special properties of individual components can be combined and optimized in a convenient way.

3.4.1. Colloidal morpholgies

Depending on the compatibility between different polymers and synthesis routes, hybrid polymer latex particles with a variety of microstructures can be obtained, such as core-shell, raspberry-like, Janus, etc., as shown in **Figure 18**.

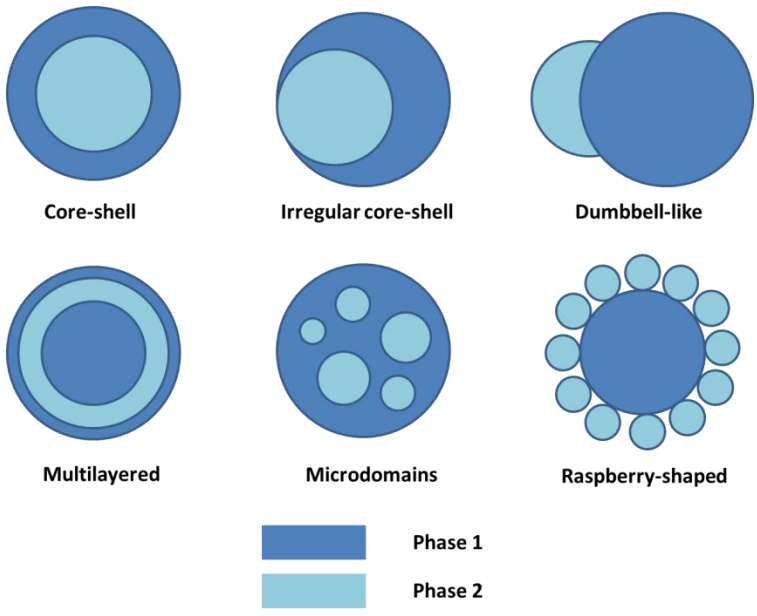

Figure 18. Schematic drawings of possible morphologies of composite colloidal particles containing two distinguishable phases.[39]

3.4.2. Synthesis approaches of structured composite latex particles

Structured composite latex particles with a variety of different morphologies can be prepared from various monomers and polymers through numerous methods, such as heterocoagulation,[40-42] Pickering emulsion polymerization,[43-48] in-situ polymerization,[49-53] to fulfill a wide range of applications. The key question is how to combine different materials together. In general, there are two ways to combine different materials in microscopic scale: through covalent bonds[40-42] and non-covalent bonds.[54-56] This section lists some of the most commonly used techniques for the preparation of such structured composite latex particles.

3.4.2.1. Layer-by-layer colloidal templating

Sequential layer-by-layer deposition of various materials from charged particles to charged molecules on macroscopically flat surfaces has been widely investigated since the report of layer-by-layer deposition of particles with opposite charges onto solid substrates in 1960s by Iler et al.[57] Since the early 1990s, Decher et al. have extended this process to the combination of polycations and polyanions by depositing polyelectrolyte layers from diluted solutions onto solid substrates.[58-60] Several years later, Sukhorukov et al. reported that two polyelectrolytes with opposite charges can be deposited consecutively onto colloidal particles like polystyrene latex particles also, which shows a new way for the preparation of structured composite latex particles.[61, 62] Caruso et al. synthesized a series of core-shell shaped composite particles and derived hollow capsules by layer-by-layer deposition of multilayers of polyelectrolytes on various core particles.[63-68] One point that has to be mentioned here is that the layer-by-layer assembly is not restricted to electrostatic attraction between polyelectrolytes. Other forces like covalent bond, coordination bond, and Van de Waals forces can also be utilized. The reason that electrostatic attraction is far more common in the layer-by-layer assembly is its versatility in the selection of polymers and the least steric demand of bonds.[58]

In a typical procedure, as displayed in **Figure 19**, an excess amount of polyelectrolyte solution is added into the oppositely charged colloidal dispersion to completely cover the surface of core particles. After the saturation of adsorption, excess polyelectrolyte is removed by centrifugation or filtration with subsequent washing by water. Then the sequential deposition of oppositely charged polyelectrolytes is conducted in the same way to obtain the required

shell thickness, which is determined by the number of polyelectrolyte layers. The thickness of each polyelectrolyte layer is around 1-2 nm.[64] The key to achieve a consecutive deposition is to ensure that not all the ionic groups on polyelectrolytes interact with the layer or core particle beneath.

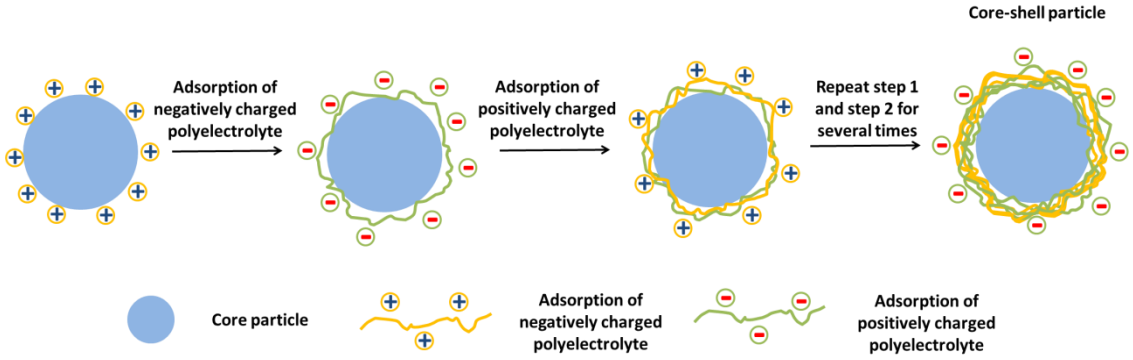

Figure 19. Scheme of a typical preparation route for core-shell particles through the layer-by-layer method.[63]

The layer-by-layer assembly method possesses many advantages, such as precise control of shell thickness and layered structure in the shells in nanoscopic scale, wide selection of polymers for adsorption and core particles. However, the most significant limitation of this method, which prevents the application of this technique in large-scale, is the tedious sequential polyelectrolyte deposition and purification cycles.

3.4.2.2. Heterocoagulation

Among all the methods for the preparation of structured composite latex particles, the heterocoagulation probably is the simplest. Heterocoagulation is a term used to describe the formation of composite particles from individual particles with dissimilar nature through Brownian motion, which is a spontaneous process. The driving force to adhere one type of particle to the surface of another particle can be based on various interactions, from electrostatic attraction and hydrophobic interaction to secondary molecular interactions like hydrogen bonding and/or specific molecular recognition. The classical heterocoagulation process is usually an assembly process of solid particles driven by non-covalent interactions, especially electrostatic interactions.[69]

In a typical heterocoagulation process, as demonstrated in **Figure 20**, both core and shell particles are synthesized beforehand, which after mixing form self-assembled structures. For

example, Caruso et al. have successfully assembled nano-silica particles on the surface of polyelectrolyte modified polystyrene (PS) latex particles through electrostatic adsorption.[67] Particles with different chemical composition and opposite surface charges have been assembled by Kumacheva et al. also through electrostatic interaction.[70] For successful assembly, the particle size difference between the core and shell particles is the key and needs to be controlled in a proper range [71-73]

The most common morphology of composite latex particles obtained through heterocoagulation is the raspberry-shaped morphology. However, if the shell particles can be fused together through heating, a core-shell morphology is also available.[70, 74] For instance, positively charged poly(butyl methacrylate) particles, a typical low T_g polymer (around 20 ^oC), has been adsorbed onto the negatively charged polystyrene particles, a typical high T_g polymer (around 100 ^oC), to form raspberry-shaped structure first. After heating at 45 ^oC for certain time, soft poly(butyl methacrylate) particles fuse together to form a continuous shell outside polystyrene core particles.

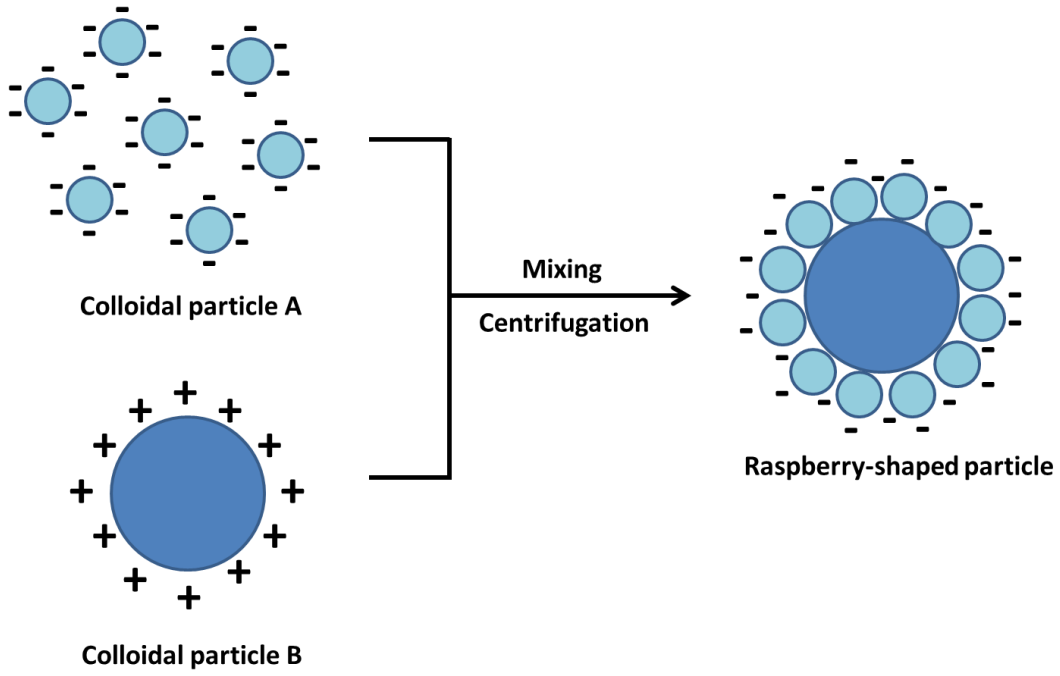

Figure 20. Scheme of a typical preparation route for raspberry-shaped particles through the heterocoagulation method.

3.4.2.3. Block copolymer assembly

Block copolymers are a special type of copolymer, which are made out of two or more chemically distinct, and frequently immiscible polymer blocks that are covalently bound.[75] Due to the incompatibility between different blocks in polymer chains, micro-phase separation takes place automatically. But macro-phase separation is prohibited by entropic forces stemming from the covalent bonds that bind different blocks together.[75] This unique phase behavior endows block copolymers the capability to form materials with well-defined microstructures. The assembly of block copolymers in bulk has been extensively studied since the 1960s for the preparation of bulk composite materials with various structures.[76, 77] When block copolymers are introduced to a solvent or a solvent mixture, the hydrophobicity difference of blocks usually leads to the arrangement of block polymer molecules, which can form a variety of structures inside the solvent or solvent mixtures, which are listed in **Figure 21**. Taken the AB diblock styrene-acrylic acid copolymer for example, various structures from spherical micelles, rod through lamellae, and vesicles to large compound micelles are available depending on the length of two building blocks.[78, 79] In general, the morphologies of the aggregates are strongly influenced by parameters like the block copolymer composition, the block copolymer concentration, and the solvent type based on the competition of these three effects, the stretching of the core-forming blocks, the interfacial tension between blocks and solvent, and the repulsion between corona-forming blocks.[79]

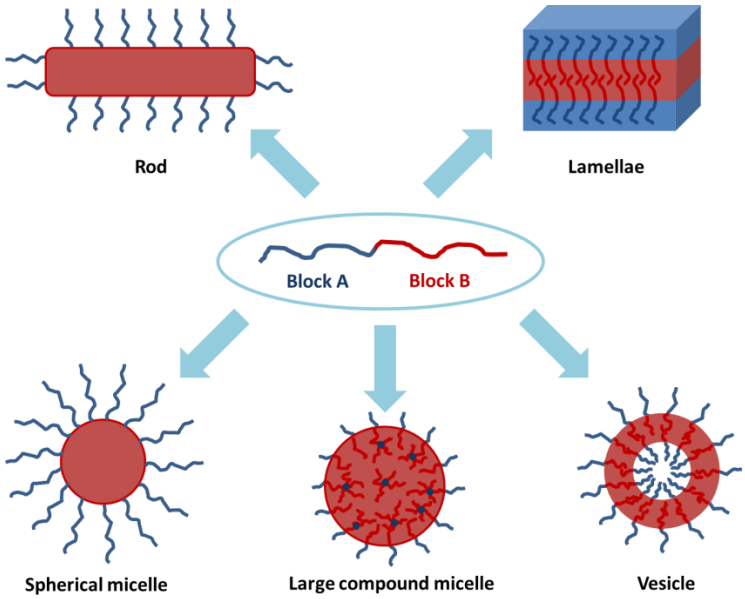

Figure 21. Different morphologies that can be obtained from the self-assembly of AB block copolymers in solvent.

3.4.2.4. Solvent evaporation method

Before the description of the solvent evaporation method, the fundamental consideration of the morphology evolution upon a composition change in a three-phase system should be explained. The pioneer work in this field was done by Torza and Mason over 40 years ago.[80] In their work, there are two immiscible phases (phase 1 and phase 3), which are dispersed in a third phase (phase 2). It is expected that, the final morphology is defined by the equilibrium state of the system, which is dependent on the spreading coefficient S_i, which is described as:

$$S_i = \gamma_{jk} - (\gamma_{ij} + \gamma_{ik})$$

where γ is the interfacial tensions between liquids.

Depending on the differences of S_1, S_2 and S_3, three different morphologies can be generated, as illustrated in Figure **22**. Assuming that the interfacial tension between phase 1 and phase 2 is larger than the one between phase 2 and phase 3 ($\gamma_{12} > \gamma_{23}$), core-shell particles can be generated when $S_1 < 0$, $S_2 < 0$ and $S_3 > 0$, while partial engulfing occurs if S_1, S_2, $S_3 < 0$; and $S_1 < 0$, $S_2 > 0$, $S_3 < 0$ leads to non-engulfing morphologies (separate particles).

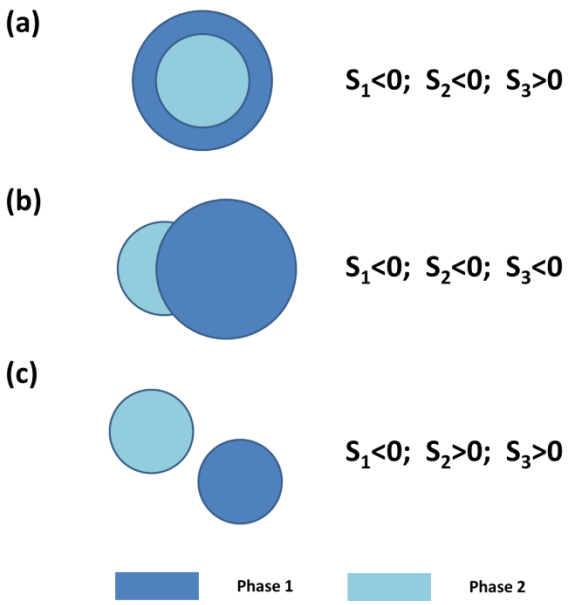

Figure 22. Schematic presentation of different morphologies in a three-phase emulsion system that are dependent on the spreading coefficients for two immiscible phases 1 and 3 dispersed in a continuous phase 2.

The applicable condition for this theoretical prediction is that all three phases are liquid phases with low viscosities, which ensure the achievement of the equilibrium state. When

high molecular weight polymers are utilized as dispersing phases, the high internal viscosity inside the droplets during the solvent evaporation restricts the mobility of polymer chains, which means that the thermodynamically stable morphology may not be obtained. Sundberg et al. demonstrated that the role of the interfacial tensions is importance in controlling the microstructures of hybrid particles.[81] They have found that the morphology of particles can vary from core-shell to hemispherical by simply changing the type of the surfactants. Therefore, the formation of multiphase particles with different morphologies is influenced by various parameters from compatibility between different phases and mobility of polymer chains to internal viscosities.

In a typical production process for the fabrication of core-shell particles through the solvent evaporation method, dissimilar polymers are dissolved together in an appropriate volatile organic solvent or a mixture of solvents, which is emulsified in water to form stable emulsions. For the particles, whose sizes are in the range of nano scale and submicron scale, ultrasound or high pressure homogenization are frequently used to generate miniemulsions rather than conventional emulsions. After the evaporation of the solvents, different polymer species phase separate and generate structured hybrid particles.

3.4.2.5. (Seeded) emulsion polymerization

Multi-stage emulsion polymerization is commonly used in industry to produce compositionally heterogeneously structured polymer particles, due to the flexibility in tailoring polymer latexes. This approach is also referred to as seeded emulsion polymerization technique. Seeded emulsion polymerization is differentiated from conventional emulsion polymerization by the formation of seed particles in the beginning of polymerization as nuclei on which polymer particles can grow.

Figure **23** demonstrates a typical process of seeded emulsion polymerization for the generation of structured particles. Usually seed latex is prepared first by various methods, including conventional emulsion polymerization and miniemulsion polymerization. Moreover, the seed particles can be both organic oligomer/polymer particles and inorganic particles like silica.[23] Afterwards, another monomer or monomer mixture is added and polymerized in the presence of seed particles. If the seed particles can be swollen by the monomer added in the second stage, which is different from the monomeric species inside the seeds, it is possible

that subsequently growing polymer would phase separate from the existing seeds. Various morphologies can be generated based on many physicochemical parameters: the swelling degree, the compatibility between the seed and the polymer formed in the second stage, the reaction kinetics, etc. In principle, the most significant parameter that defines the final morphology of hybrid particles is the compatibility between polymer pairs, which is usually measured by the polarity of polymers.[23, 82] The larger the difference between the polymer pairs in polarity is, the greater is the extent of phase separation during the polymerization. However, even two fully compatible polymers do not necessarily lead to the formation of uniform and homogenous latex particles but rather structured particles, if other factors are adjusted properly, including the distribution of free radicals and monomers, methods of monomer feeding, and so on. If the seed particles cannot be swollen, the subsequent polymerization would be localized at the surface of the seed particles. Therefore, a post-formed polymer tends to form a continuous shell layer or discrete outsides seeds. Hence a variety of morphologies can be obtained, including core-shell, dumbbell-shaped, raspberry-shaped, patchy particles, etc.

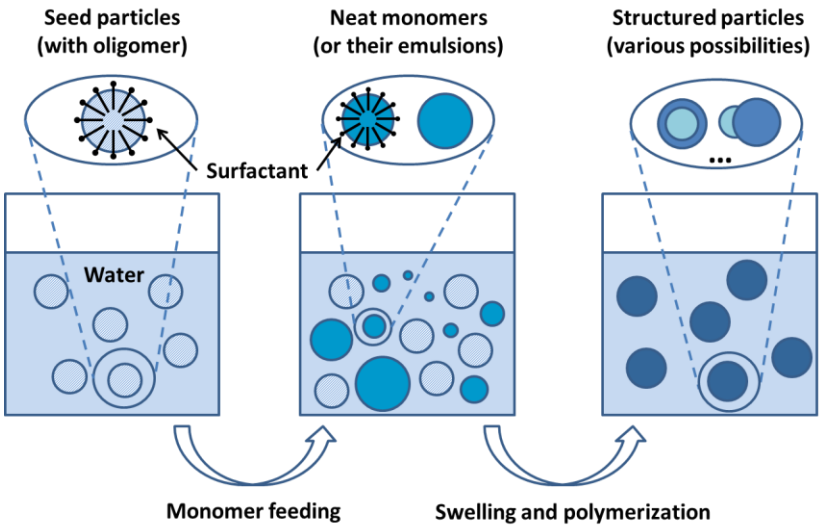

Figure 23. Schematic presentation of the standard seeded emulsion polymerization procedure.

4. Results and Discussion I - The synthesis of structured semi-crystalline composite colloidal particles based on liquid-solid assembly and their applications

This chapter focuses on the preparation of hybrid latexes and films with semi-crystalline features through a novel fabrication approach based on the assembly of liquid droplets and highly semi-crystalline solid particles. Here the liquid droplets are composed of methacrylic monomers, while acrylonitrile has been selected as the monomeric source of semi-crystalline polymer particles. The work presented in this chapter has been accepted by *Macromolecules* as full paper entitled, "*A facile route towards structured hybrid particles based on liquid-solid assembly*" (DOI: 10.1021/ma401893g).

Polyacrylontrile (PAN) and copolymers of PAN have been widely studied and used in various engineering applications.[83-85] Due to its highly semi-crystalline feature, PAN is especially favoured in barrier applications as high barrier polymer.[86] PAN is predominantly white powders till 250 °C, when the degradation starts, which is much lower than crystalline melting point (at 317 °C).[87] In the meantime, the relatively high T_g of PAN makes it almost impossible to obtain continuous PAN films directly from PAN aqueous dispersions.[87] Therefore, copolymers of PAN are much more frequently used compared to the homopolymer, although copolymerization decreases the crystallinity of PAN significantly.[88] It will be shown in this chapter that the conflict between film-formation and high crystallinity can be solved by confining semi-crystalline PAN and film-formable polymers in one colloidal particle.

Among the methods to obtain hybrid latex particles with well-defined microstructures that are described in the section 3.4.2, the heterocoagulation-based method can be considered as the most straightforward approach, which is utilized to generate semi-crystalline hybrid latex particles in this chapter. However, because heterocoagulation is a stochastic process, many parameters need to be controlled carefully to avoid the formation of large aggregates or flocculates.[69, 71-73] For the successful preparation, classic heterocoagulation processes are usually carried out with diluted dispersions (particle concentration < 5 wt%) and exceeding shell particles are employed for better colloidal stability, which requires further separation and purification processes usually through centrifugation.[71]

The major objective of this chapter is to provide a novel, facile method to prepare colloidally stable, structured semi-crystalline hybrid particles, which can be applied to latexes or dispersions with higher solid content (> 15 wt% or even higher). This chapter can be divided into three parts.

In the first part, the synthesis of semi-crystalline PAN dispersions with long-term colloidal stability was presented. Miniemulsion polymerization and dispersion polymerizations approaches have been performed separately. The factors that influence the polymerization process and stability of final latexes have been studied.

In the second part, the fabrication of raspberry-shaped and core-shell shaped semi-crystalline hybrid particles was demonstrated. A schematic demonstration of the detailed synthesis route for structured semi-crystalline hybrid particles is illustrated in **Figure 24**. The most unique part of this method is the utilization of liquid miniemulsion monomer droplets as the precursor of shell materials, rather than solid particles or a soluble precursor. This strategy possesses three major advantages: (1) the synthesis is fast and easy to control, because there is no need for pre-treatment of building blocks before the assembly; (2) it is easier to maintain the colloidal stability during the assembly by using liquid droplets rather than solid particles, because the rearrangement of surfactant molecules on the surface of droplets can take place more easily. This consequently can lead to a decreased surface charge density of droplets adsorbed on PAN and reduce the possibility of further coagulation; (3) the chemical composition of hybrid particles can be easily varied over a wide range and allows a high degree of freedom to tailor the overall hybrid dispersion properties, which is attributed to the use of miniemulsion monomer droplets as nanoreactors[32, 33]. The investigation on the influencing parameters including the ζ-potential and composition of monomer droplets has been performed.

In the last part, the concept was extended to thermoset systems. A two-component PAN/epoxy thermoset composite has been prepared. The oxygen barrier properties of the semi-crystalline thermoset films have been investigated.

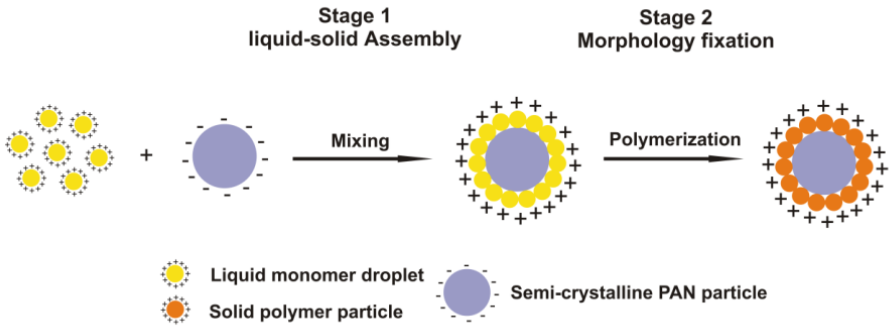

Figure 24. A schematic diagram for the synthesis of raspberry-shaped particles. The preparation can be described as a two stage process. The first step is the assembly of the liquid miniemulsion droplets with solid particles driven by electrostatic interactions. The second step can be considered as morphology fixation due to polymerization.

4.1. Synthesis of colloidally stable semi-crystalline PAN particles

4.1.1. Comparison of different polymerization methods

To synthesize structured semi-crystalline hybrid particles, stable acrylonitrile homopolymer dispersion has to be prepared first. However, due to the strong intermolecular interaction, PAN cannot dissolve in or be swollen by its own monomer, which makes it difficult to obtain colloidally stable homopolymerized acrylonitrile through conventional emulsion polymerization technique relying on the diffusion of monomer/oligomer. In contrast, dispersion and miniemulsion polymerization, which both are not dependent on diffusion, are more commonly used to produce PAN homopolymer dispersions.[83, 84, 88-91] Both methods have been used and compared in this section, which are described in the following paragraphs in detail.

4.1.1.1. Miniemulsion polymerization approach

It was found that miniemulsion polymerization is a direct and convenient method to generate pure PAN particles possessing semi-crystalline properties with SDS as sole surfactant.[88] In this reported work, polyacrylonitrile nanoparticles within the size range between 100 nm and 180 nm were prepared successfully. However, it is found that as-prepared PAN dispersion cannot be stored for long time without sedimentation. In fact, precipitates were observed in the dispersion after placed at room temperature for one day, which has to be re-homogenized before use. It is speculated that the hydrophobic chain length of SDS is not long enough to have a strong interaction with PAN, especially with the semi-crystalline regions, which makes it highly possible that the desorption of SDS molecules takes place during polymerization of AN. Therefore, this thesis focuses on the utilization of polymeric stabilizers for the polymerization of AN. The recipe for polymerization is based on the formulation used in the reported work,[88] however, SDS has been replaced by a polymeric stabilizer, butenediol-vinyl alcohol copolymer (BVOH) with the trade name 'G-polymer OKS-8041', for miniemulsion polymerization of AN in this thesis. The BVOH concentration is fixed to 10 wt% in the miniemulsion formulations based on the weight of oil phase.

The influence of the polymerization temperature

According to the reference article, it is better to initiate the free radical polymerization of AN

at 55 °C rather than 70 °C for a better control during polymerization when SDS is used as stabilizer for the miniemulsion.[88] However, it is found that the conversion of polymerization is only around 50% at 55 °C, which is too low for practical use, when BVOH was used as surfactant. When the polymerization temperature was increased to 70 °C, the conversion increased to 80%. The conversion is roughly calculated based on the ratio between actual solid content and theoretical solid content of latexes. The temperature cannot be increased further because the boiling point of AN is 76 °C. Therefore, the polymerization temperature is fixed as 70 °C for the study described in this chapter, if not specially mentioned.

The influence of SDS

Similar to the case of sole SDS stabilization, the PAN dispersion stabilized by 10 wt% of BVOH solely was still not stable, which appeared to be viscous and phase separated in hours. This indicates that sole electrostatic repulsion or steric hindrance is not strong enough to maintain the long-term colloidal stability of aqueous PAN dispersions. Then it is natural to think whether it is possible to make a stable dispersion by combining two stabilization mechanisms. Considering SDS can be embedded inside the polymer stabilizer layer, SDS has to be added after the formation of miniemulsions, which can provide extra stabilization effect.[92, 93] In this chapter, 0.4 wt% SDS was added after acrylonitrile miniemulsion was generated with 10 wt% BVOH as surfactant. The addition of SDS endowed the BVOH stabilized acrylonitrile miniemulsion droplets with negative surface charges, which is expected to post-stabilize the miniemulsion during free radical polymerization. It has been noticed that the colloidal stability of as-prepared PAN dispersion was improved significantly by using OKS-8041 and SDS together as stabilizers, compared to SDS solely, especially at higher solid contents (> 20 wt%). These dispersions have been stored at room temperature for one year without sedimentation. As-prepared PAN particles possess an average size of 228 nm with a polydispersity index (PDI) of 0.081. SDS is expected to be buried inside the thin polymer layer in water/PAN interface, which led to a comparably low ζ-potential value of -3.15 mV. From the stabilization mechanism point of view, this low ζ-potential value also indicates that as-prepared PAN particles are stabilized by two stabilization mechanisms: electrostatic repulsion and steric hindrance.

The influence of initiator

Besides the oil soluble initiator (V-59), the water soluble initiator (KPS) has also been used to

initiate the polymerization of acrylonitrile. It is found that coagulates were observed shortly after the addition of the KPS aqueous solution. The difference in the oil soluble initiator and the water soluble initiator can be explained by the solubility of acrylonitrile. Acrylonitrile is relatively hydrophilic, the solubility of which is around 7 g/100 ml in water.[89] Therefore, there should be some free acrylonitrile monomer dissolved in water rather than emulsified to form droplets, which are potential loci of secondary nuclei for polymerization. When the oil-soluble initiator is utilized, free radicals generated are hydrophobic, which are thus restricted inside the monomer droplets. Therefore, only the monomers inside the droplets can be polymerized. Free acrylonitrile can diffuse into the droplets upon the consumption of monomer inside the droplets and can be polymerized there. In contrast, radicals generated from KPS dissolve in the aqueous phase, which initiate the polymerization of dissolved acrylonitrile immediately, which form secondary particles or particle nuclei. These particles or particle nuclei will form coagulum due to the lack of stabilizer in the aqueous phase in miniemulsion, which in turn coagulates the whole emulsion system in the end.

4.1.1.2. Dispersion polymerization approach

Dispersion polymerization is commonly used to produce latex particles in the size range from 100 nm to 10 µm, especially for the preparation of monodisperse colloidal particles.[94] Dispersion polymerization is defined as a type of precipitation polymerization in which stabilized polymer particles precipitate out from a homogenous solution of monomer, initiator, and dispersant.[95] Due to the insolubility of PAN in its monomer, dispersion polymerization seems to be a suitable technique for the polymerization of acrylonitrile, which is proved by the amount of reported work in the field of the synthesis of PAN homopolymer colloidal particles. For dispersion polymerization, the choice of solvent is critical, because the precipitation of formed polymer is strongly dependent on the solvent type. Supercritical carbon dioxide,[90] liquid dimethyl ether[91], and water[84] have been reported to be used as solvent for the dispersion polymerization of acrylonitrile. In this chapter, two solvents, ethanol and water, have been used to prepare PAN dispersions.

Polymerization in ethanol

A detailed recipe of the dispersion polymerization of acrylonitrile in ethanol is shown in **Table 1**. It is found that OKS-8041 is not soluble in ethanol-rich aqueous mixture. In DP-PAN-1, OKS-

8041 precipitated out immediately when ethanol was added. When the water concentration in ethanol-water mixture increased to 50 wt%, no precipitation was observed before polymerization. However, the emulsion coagulated after polymerization.

Therefore, another commonly used polymer stabilizer that can be dissolved easily in ethanol, polyvinylpyrrolidone (PVP) with the M_w of 40,000, was used as stabilizer. When the monomer concentration in the formulation is around 20 wt%, both DP-PAN-3 and DP-PAN-4 samples coagulated after polymerization. DP-PAN-5 sample with 10 wt% monomer is slightly better than DP-PAN-3 and DP-PAN-4, which did not coagulate directly but phase separated after placing it at room temperature for 1 day.

Table 1. The colloidal stability of the latexes synthesized through dispersion polymerization of acrylonitrile in water.

	AN [g]	Water [g]	Ethanol [g]	V-59 [g]	BVOH [g]	PVP [g]	Colloidal stability
DP-PAN-1	6	2.4	21.6	0.12	0.9	-	Unstable
DP-PAN-2*	6	12	12	0.12	0.9	-	Unstable
DP-PAN-3	6	12	12	0.12	-	0.9	Unstable
DP-PAN-4	6	2.4	21.6	0.12	-	0.9	Unstable
DP-PAN-5	3	2.4	21.6	0.12	-	0.45	Unstable

*0.9 g of BVOH was pre-dissolved in water

Polymerization in water

For the dispersion polymerization of acrylonitrile in water, there is a limit for the solid content of PAN dispersion, because the solubility of acrylonitrile in water is around 7 g/100 ml at room temperature. Both BVOH and PVP were utilized as stabilizers in the polymerization process, respectively. The detailed formulations are listed in **Table** 2. Unfortunately, coagulations were observed during the polymerization with both recipes.

Table 2. The colloidal stability of the latexes synthesized through dispersion polymerization of acrylonitrile in water.

	AN [g]	Water [g]	AIBA [g]	KPS [g]	OKS-8041 [g]	PVP 40 [g]	Colloidal stability
DP-PAN-6	1.68	24	0.028	-	-	0.252	Unstable
DP-PAN-7	1.68	24	-	0.028	0.252	-	Unstable

In conclusion, compared to the dispersion polymerization approach, miniemulsion polymerization technique is expected to be much easier to handle for the polymerization of acrylonitrile. Therefore, the miniemulsion polymerization approach is selected in this chapter to prepare PAN colloidal particles due to better control in colloidal stability.

4.1.2. The preparation of PAN homopolymer and copolymer dispersions

As mentioned in section 4.1.1, a PAN homopolymer dispersion was synthesized by the miniemulsion polymerization technique with OKS-8041 and SDS as stabilizers. The detailed formulation of the synthesis is listed in section 7.2.1. The resultant PAN is found to crystallize partially (around 25%), as indicated by XRD patterns shown in **Figure 25**. The main crystalline peak is located around 16 - 17 °, which is consistent with a previous reported work.[88] As-produced PAN particles were found to possess crumpled surfaces according to SEM observation, as illustrated in **Figure 26**, which were attributed to the crystalline regions in particles.

The crystallinity of PAN is strongly dependent on the concentration of co-monomers. According to the reported work, the crystallinity of AN-styrene copolymers decreases dramatically with the increase of the amount of styrene.[88] When the content of styrene is over 50 wt%, the copolymer turns to be amorphous. In this chapter, methacrylic monomer is used as co-monomer rather than styrene. It is no surprise that the relationship between the methacrylic monomer concentration and the crystallinity of AN-methacrylic copolymers follows the same trend. As illustrated in Figure 25b, AN-methacrylic copolymer with 50 wt% methacrylic co-monomer shows typical amorphous XRD pattern.

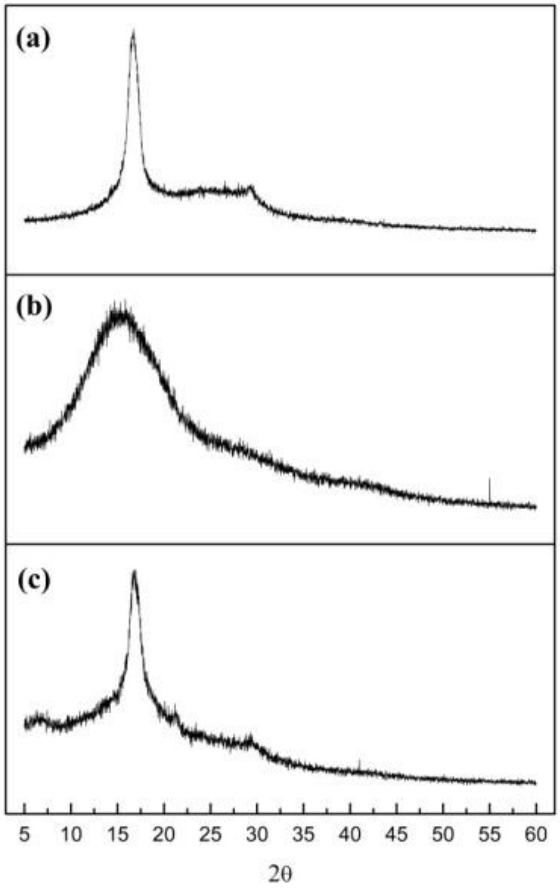

Figure 25. XRD pattern of freeze-dried latexes: (a) pure PAN; (b) AN-methacrylic copolymer (The weight ratio between AN and methacrylic monomer mixture is 1:1) and (c) raspberry-shaped hybrid particles (Sample L-1).

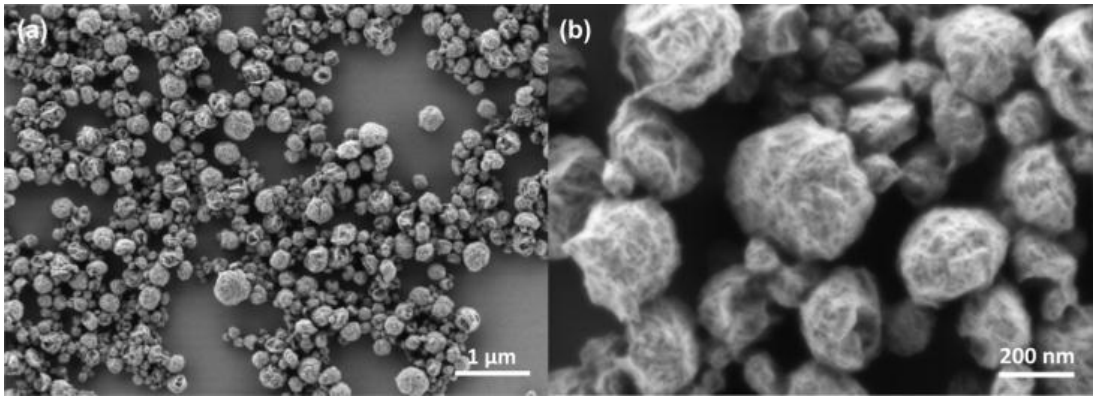

Figure 26. SEM images of semi-crystalline PAN particles with crumpled surfaces due to the emergence of crystalline regions.

4.2. Synthesis of colloidally stable, structured semi-crystalline hybrid particles

4.2.1. Liquid droplets vs solid particles

The basic concept for this chapter is using liquid miniemulsion droplets rather than solid latex particles as building blocks for assembly processes to obtain structured hybrid particles. In detail, CTAB stabilized miniemulsion containing positively charged methacrylic monomer droplets was mixed with negatively charged PAN dispersion at room temperature for 30 min under magnetic stirring. It is expected that raspberry-shaped particles were formed immediately due to electrostatic attraction. The morphology was fixated by subsequent polymerization of droplets at 70 ^{o}C for 4h.

A dramatic improvement in the colloidal stability of the obtained hybrid dispersion was observed and is demonstrated in **Figure 27.** Immediate coagulation was observed after adding a CTAB stabilized methacrylic polymer dispersion into the PAN dispersion (L-15), while a stable hybrid dispersion has been obtained through polymerization of a mixture containing a PAN dispersion and a CTAB stabilized methacrylic monomer miniemulsion. The as-prepared hybrid dispersion has been stored for one year at room temperature without sedimentation.

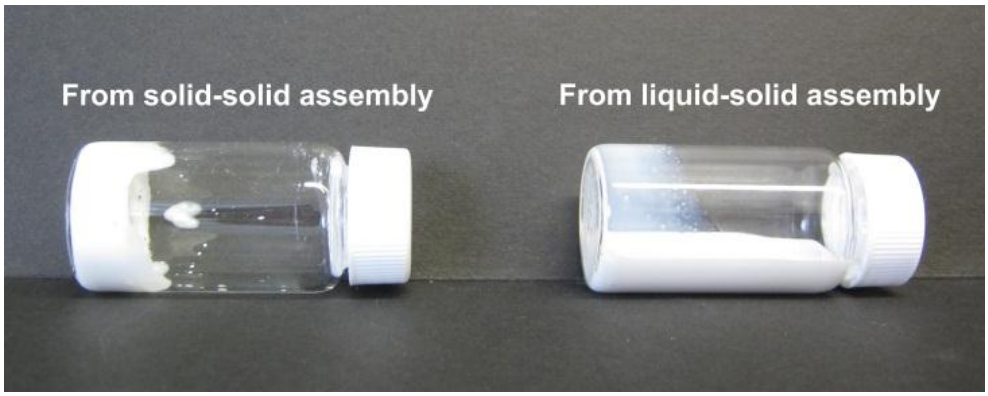

Figure 27. Photographs of hybrid dispersions prepared by different assembly methods (Solid-solid assembly: coagulated; liquid-solid assembly: stable).

The difference in colloidal stability is expected to be related to the mobility difference of CTAB on the surface of solid methacrylic polymer particles and liquid methacrylic monomer droplets.[96, 97] The mobility of CTAB is highly restricted on the surface of solid particles because of the partially embedment of CTAB's hydrophobic tails in the surface. Therefore, when positively charged methacrylic polymer particles are adsorbed onto negatively charged PAN, the surfaces of PAN/methacrylic polymer hybrid particles gain strong positive charges,

which could attract other PAN particles to form coagulum, as shown in **Figure 28**a. In contrast, the mobility of CTAB is much higher on the surface of liquid droplets. Therefore, CTAB could be dragged from the water/droplet interfaces to PAN/droplet interfaces through electrostatic attraction, as schematically shown in Figure 28b. Hence, the CTAB concentration on the water/droplet interface of adsorbed droplets decreases after adsorption, which can avoid "bridging" due to weaker electrostatic attraction.

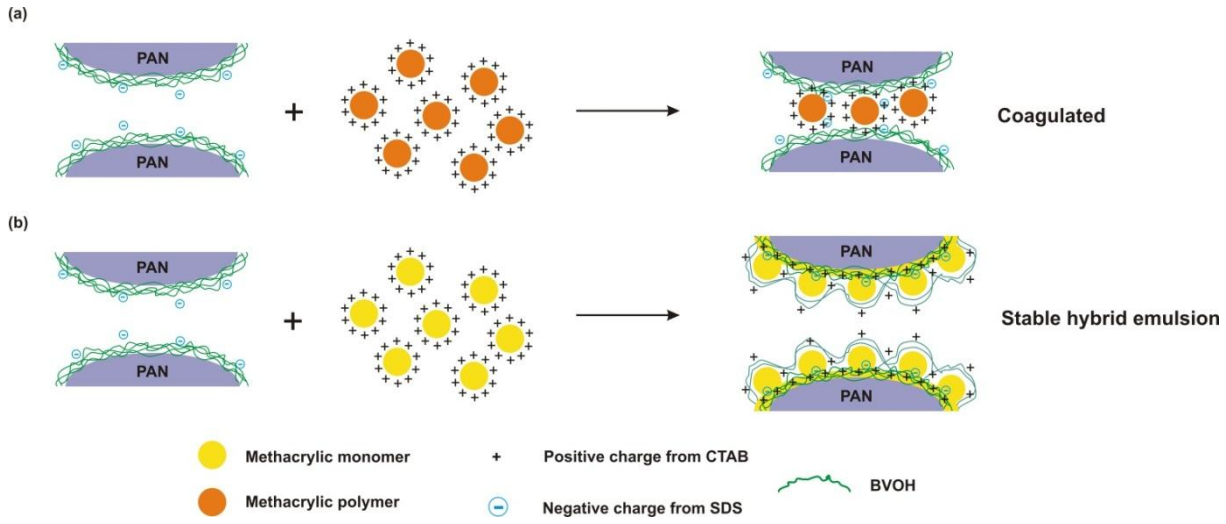

Figure 28. Schematic explanation of the difference between blending methacrylic polymer dispersion (a) and liquid methacrylate miniemulsion (b) with PAN on the stability of derived hybrid emulsion/dispersions.

The decrease of miniemulsion droplets' ζ-potential has been observed after adsorption and polymerization. CTAB-stabilized miniemulsion droplets were strongly positively charged with a ζ-potential of + 69.8 mV. After adsorption onto PAN surfaces and polymerization, the ζ-potential of hybrid particles was found to decrease to only + 12.87 mV. Surprisingly, the hybrid dispersions possessed excellent colloidal stability, because an emulsion/latex usually becomes instable when the ζ-potential is below ± 30 mV.[98] Therefore, there should be an additional stabilization mechanism in our system, which is most likely a steric stabilizing effect. BVOH could provide steric hindrance towards coagulation between particles, which co-stabilize hybrid particles, even when the electrostatic repulsion from CTAB alone is not strong enough.

SEM was used to investigate the morphology of the hybrid particles. It was found that after polymerization of methacrylate miniemulsion/PAN mixture, particles with crumpled surfaces disappeared. Instead, raspberry-shaped particles emerged, as shown in Figure 29a and Figure

29b. Small methacrylic polymer particles have covered the surface of the PAN particles. The z-average particle size of such raspberry-shaped particles is around 249 nm, compared to the 228 nm of pure PAN particles. In addition, methacrylic polymer particles on the surface of PAN were not perfectly spherical, but rather deformed in the interfacial regions between PAN and methacrylic polymer particles. It is probably due to the coalescence between surface particles, as the temperature for polymerization is 70 °C, which is much higher than the calculated T_g of methacrylic copolymer (around 44 °C).

As-prepared raspberry-shaped hybrid particles contain 50 wt% of PAN and 50 wt% of methacrylic polymer. In contrast to AN-methacrylic copolymer with the same chemical composition, raspberry-shaped hybrid particles show typical semi-crystalline featured pattern in XRD, as illustrated in Figure 25c, because AN is homopolymerized before the assembly to retain the highly semi-crystalline feature.

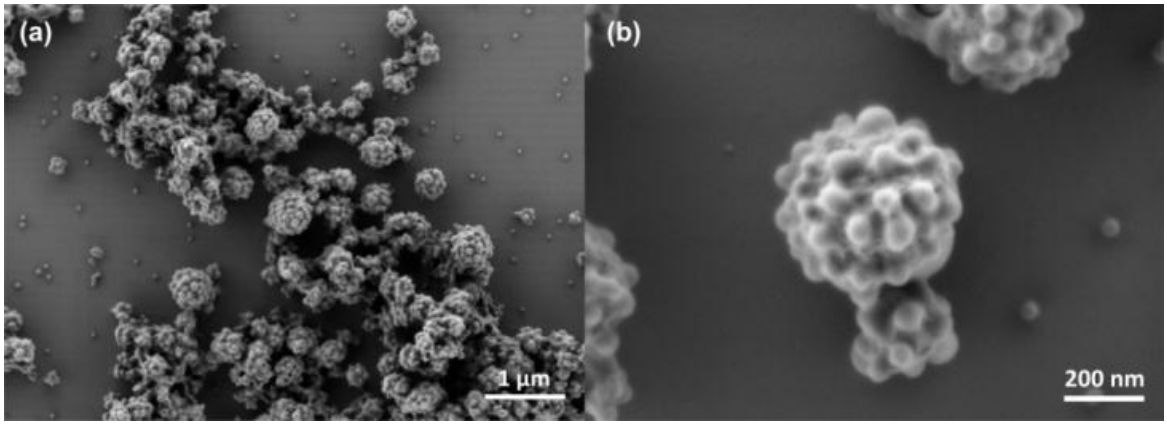

Figure 29. SEM images of raspberry-shaped hybrid particles (Sample L-1): Semi-crystalline PAN as core, methacrylic copolymer as shell particles.

4.2.2. The influence of the ratio between PAN latex and monomer miniemulsion

In principle, the assembly step of solid PAN latex particles and liquid monomer miniemulsion droplets is similar to classic heterocoagulation between solid particles. Therefore, the ratio between latex particles and monomer droplets is important for the colloidal stability and morphology of obtained composite latexes. Three different ratios of the PAN latex and the monomer miniemulsion have been carried out, which are listed in **Table 3**. It is clear that when the weight ratio of PAN latex to monomer miniemulsion is as low as 2 : 1, the emulsions coagulated after mixing and polymerization, while the final hybrid latexes were stable with the ratio higher than 1.33 : 1. This stability difference could be explained by the essence of electrostatic attraction driven heterocoagulation process. Fundamentally heterocoagulation is

a charge reversal process. To maintain the colloidal stability of the system, the core particles should be covered completely by shell particles, which should still possess extra surface charges on the interfacial area with water to keep the assembled structures stable. Therefore, the amount of droplets/particles to be adsorbed on the core particles is critical for the colloidal stability, when the surface charges of core particles and shell droplets/particles are constant. When the quantity of miniemulsion droplets is too small, the charges on the interface with water are not enough to stabilize the assembled structures. **Figure 30** shows that, when the weight ratio between PAN latex and monomer miniemulsion is increased to 1:1, many free polymer particles were observed, which can be attributed to the methacrylic copolymer polymerized from non-adsorbed monomer miniemulsion droplets because of the saturation of adsorption. Therefore, the weight ratio between PAN latex and miniemulsion is fixed as 1.33 to 1 in this chapter, if not mentioned specifically.

Table 3. The relationship between colloidal stability of hybrid dispersions and the weight ratio between PAN latex and methacrylic monomer miniemulsion.

PAN latex [g]	Methacrylic monomer miniemulsion [g]	$m_{PAN\ latex}$:$m_{methacrylic\ monomer\ miniemulsion}$	Colloidal stability
10	5	2 : 1	Coagulated
10	7.5	1.33 : 1	Stable
10	10	1 : 1	Stable

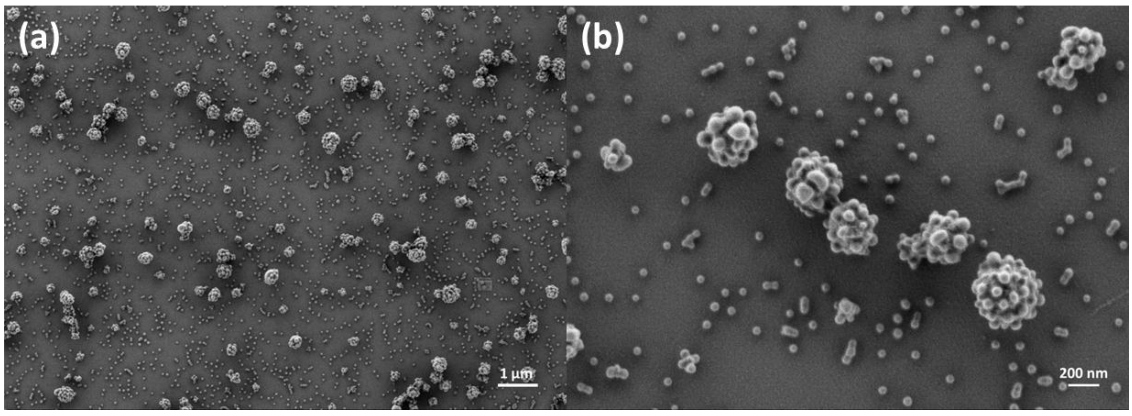

Figure 30. SEM images of raspberry-shaped hybrid particles (Sample L-1): Semi-crystalline PAN as core, methacrylic copolymer as shell particles.

4.2.3. The influence of initiator

It is found that the choice of the initiator for the free radical polymerization of adsorbed miniemulsion droplets is of high importance for the successful preparation of structured

particles in this system. As shown in **Figure 31**, the water-soluble initiator V-50 has led to the formation of raspberry-shaped particles, while the oil-soluble initiator V-59 has induced the formation of agglomerated PAN particles ‘‘glued’’ by soft methacrylic polymer.

The exact cause for this phenomenon is still unclear. We speculate that it is related to the initiation site of polymerization, as illustrated in **Figure 32**. When the polymerization is initiated by a water-soluble initiator, free radicals generate in aqueous phase first and diffuse to the water/monomer interface to initiate the polymerization inside droplets. It means that monomers at the water/monomer interface are initiated earlier than in the PAN/droplet interface. Therefore, monomer has enough time to diffuse into the adsorbed BVOH layer before being polymerized. After the completion of polymerization, polymers formed in the BVOH layer can possibly enhance the fixation of the raspberry-shaped morphology, as illustrated in Figure 32a. On the contrary, when the oil-soluble initiator is utilized to initiate radical polymerization, the polymerization starts inside the droplets, which means that the methacrylic monomer in the PAN/droplet interface also polymerizes much faster than in the case of the water-soluble initiator. The fast build-up of molecular weight can potentially lead to desorption of droplets from the surface of PAN due to a decreased compatibility between the methacrylic polymer and BVOH. In the meantime, the CTAB concentration on the surface of droplets is expected to decrease significantly, because considerable amounts of CTAB can be dragged to the surface of PAN due to electrostatic attraction. Therefore, droplets begin to coalesce and lose spherical shape, as shown in Figure 31a.

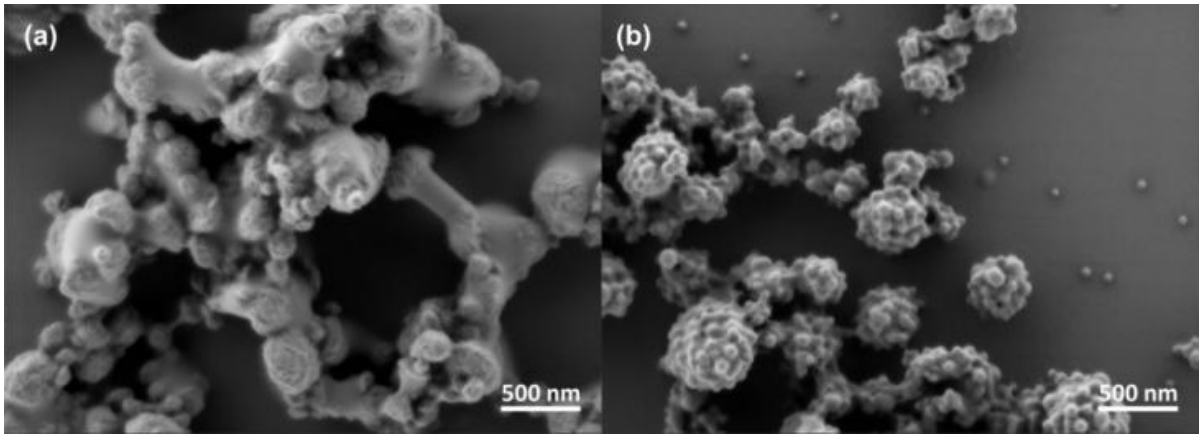

Figure 31. SEM images of hybrid particles polymerized by using (a) the oil-soluble initiator V-59 (Sample L-2) and (b) the water-soluble initiator V-50 (Sample L-1) as initiator.

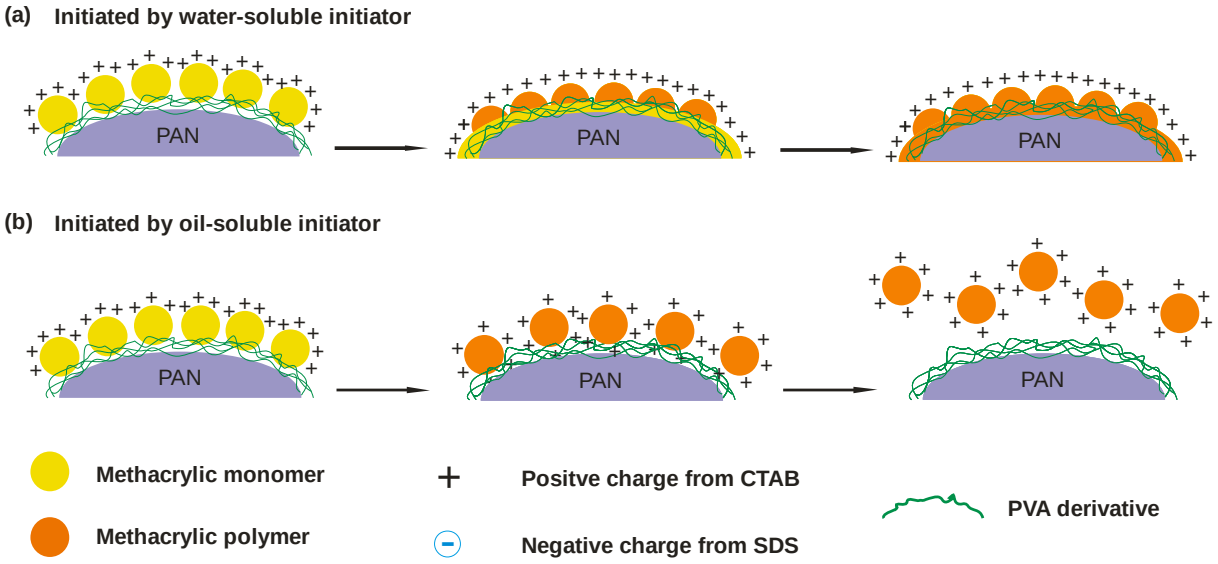

Figure 32. Schematic diagrams comparing the influences of oil-soluble and water-soluble initiators on the morphology of derived PAN-methacrylic copolymer hybrid particles.

4.2.4. The influence of ζ-potential of liquid droplets

As shown in Figure 24, this preparation method is composed of two stages: liquid-solid assembly and morphology fixation. The driving force behind the liquid-solid assembly is the electrostatic attraction between the solid PAN particles and liquid methacrylic monomer miniemulsion droplets which are oppositely charged. Therefore, the influence of the ζ-potential of liquid droplets on hybrid dispersions has been studied. The non-ionic surfactant Lutensol AT25 was used together with CTAB to tune the ζ-potential of miniemulsion droplets without changing the droplet size, as shown in **Table 4**.

Table 4. ζ-potential of miniemulsions with varied CTAB/Lutensol AT25 ratios.

Entry	$m_{CTAB}/m_{Lutensol\ AT25}$	ζ - potential of miniemulsion [mV]	Stability of derived hybrid latex
ME-3	0	- 0.6525	Coagulated
ME-4	1/12.3	+ 12.3	Coagulated
ME-5	1/5.67	+ 16.25	Coagulated
ME-6	1/2	+ 20.5	Stable
ME-1	∞	+ 69.8	Stable

The threshold ζ – potential of the monomer miniemulsion for stable hybrid dispersions is around + 20 mV. When the ζ-potential of the miniemulsion droplets is high, the electrostatic attraction between PAN and droplets is so strong that the PAN/droplets mixture is formed quickly and maintains colloidally stable.[99, 100] Therefore, it is highly possible that the surface

of PAN is coated by droplets in a short time before coagulation takes place, which can be seen as charge reversal process. In contrast, when the ζ-potential of the monomer droplet is too low, the attraction between PAN and droplets is so weak that the completion of the charge reversal process is not fast enough to avoid coagulation. Additionally, SEM images in **Figure 33** have confirmed the formation of raspberry-shaped hybrid particles, even when the ζ-potential of the miniemulsion is only + 20.5 mV.

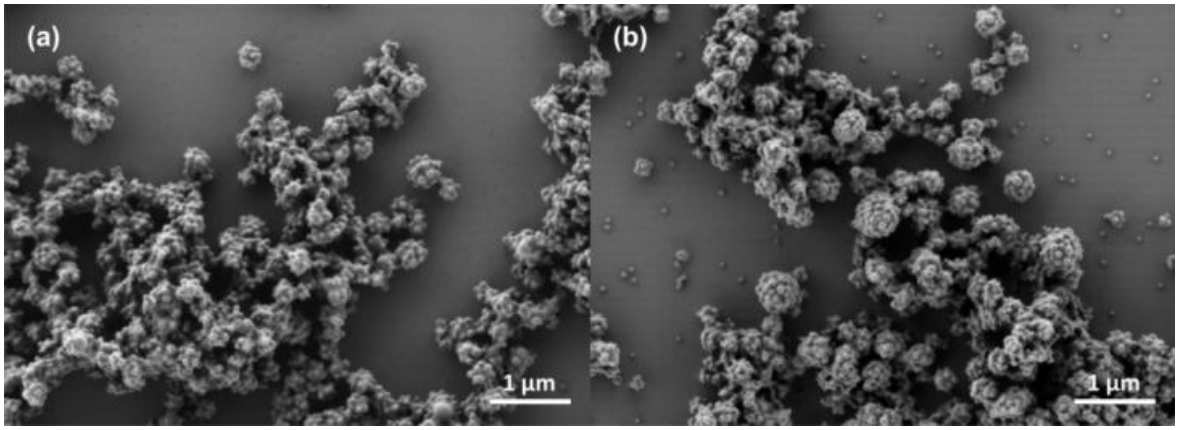

Figure 33. SEM images of raspberry-shaped hybrid particles from miniemulsions with ζ-potential of (a) + 20.5 mV (Sample L-6) and (b) + 69.8 mV (Sample L-1) respectively.

4.2.5. The influence of methacrylic polymer composition

While the assembly process is dominantly controlled by ζ – potential, the morphology fixation is influenced by several other parameters, such as the initiation type as discussed in section 4.2.3. Another important parameter is the composition of the methacrylic polymer, which affects the T_g and the crosslinking densities. MMA, EHMA, and LMA have been mixed at various ratios to achieve different theoretical T_g from about 8 °C to 90 °C, as shown in **Table 5**, based on the Fox equation and with the assumption that all monomers copolymerize ideally. All other parameters were maintained the same.

Table 5. Calculated T_g of shell polymer with different miniemulsion compositions.

Entry	MMA [%][a]	EHMA [%][a]	LMA [%][a]	Calculated T_g [°C][b]
ME-7	95	-	5	90
ME-1	60	35	5	44
ME-8	40	55	5	22
ME-9	25	70	5	8

[a] Percentage is based on total weight of monomers. [b] Based on the Fox equation for ideal copolymerized systems.

It is found that the morphology of hybrid particles changes from raspberry-shaped (**Figure 35**a - Figure 35d) to core/shell-shaped (Figure 35e - Figure 35h) with the decrease of T_g of the methacrylic polymer. Rough PAN surfaces tend to re-appear in Figure 35g - Figure 35h, which is due to the fast spreading of soft shell polymers on the silicon wafer during drying. Meanwhile, ζ-potential of hybrid particles decrease from around + 11 mV to + 7 mV, as illustrated in **Figure 34**.

Both the evolving morphology from raspberry-shaped to core/shell-shaped shaped and the decrease of ζ-potential can be attributed to an increasing coalescence between methacrylic droplets/particles on the surface of PAN with the decrease in T_g of the methacrylic copolymer, which leads to the formation of a continuous shell. Coalescence between droplets/particles on the PAN particle surface is similar to coalescence between latex particles onto the substrate during drying, which is driven by capillary force and is strongly affected by the mobility of polymer chains. However, as the coalescence rate of particles in water is much slower than in air,[12] it is necessary to ensure that the T_g of shell polymers is low enough for sufficient coalescence. For example, a T_g of 44 °C is not low enough to form a continuous layer on PAN till 22 °C, as illustrated in Figure 35c - Figure 35d and Figure 35g - Figure 35h. Improved coalescence compensates the electrostatic repulsion which prevents further adsorption of particles, which leads to the increase of adsorption efficiency for droplets/particles onto the PAN surface. Therefore, the average ζ-potential of hybrid dispersion decreases, because the decrease of free, non-adsorbed methacrylic particles, which possess strong positive charges.

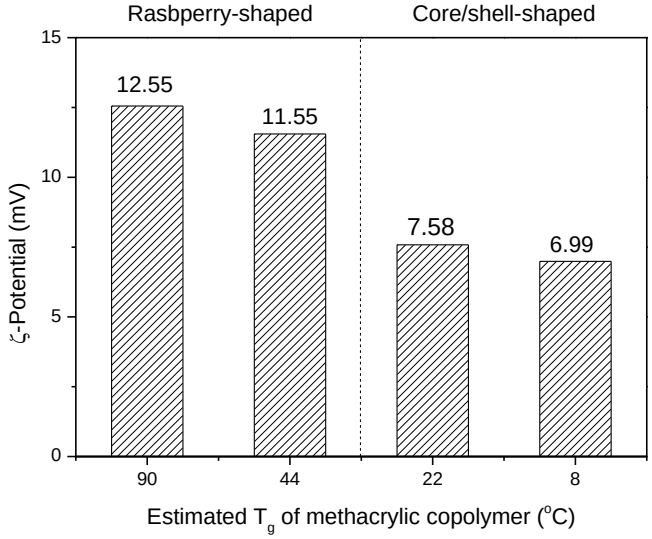

Figure 34. ζ-potentials of hybrid particles containing methacrylic copolymer with varying T_g (Sample L-1 and L-7 ~ L-9).

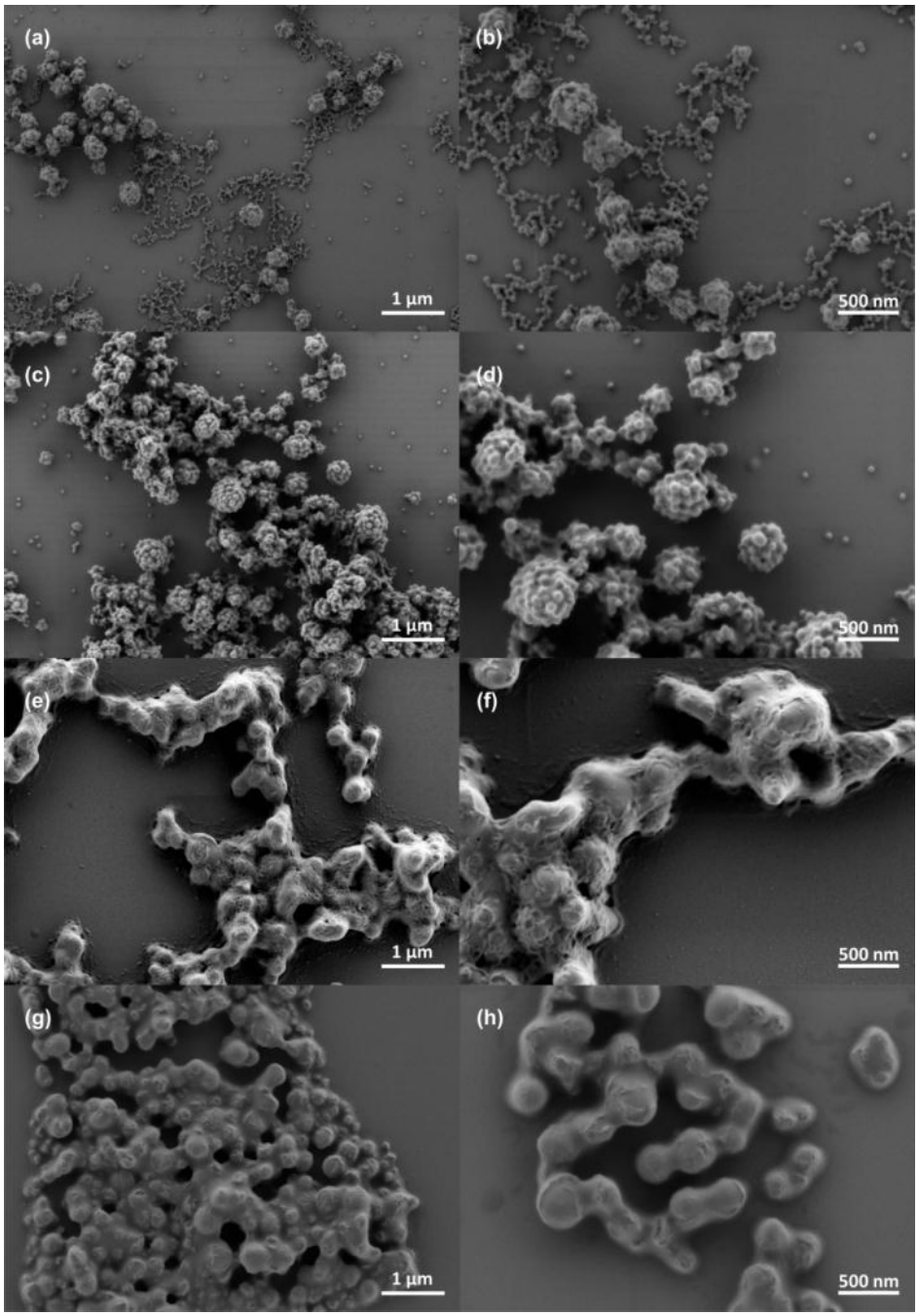

Figure 35. SEM images of hybrid particles possessing shells with different T_g: (a-b) 90 °C; (c-d) 44 °C; (e-f) 22 °C; (g-h) 8 °C (Sample L-1 and L-7 ~ L-9).

4.2.6. The influence of crosslinking

The influence of crosslinking on the morphology and colloidal stability of the hybrid latex has also been investigated. EGDMA has been used as a difunctional monomer to crosslink the shell particles. It is found that with increasing crosslinker concentration from 0.1% to 2%, based on total monomer weight, raspberry-shaped morphology has been retained, as shown

in **Figure 37**. Also, increasing the concentration of crosslinker has the same effect as decreasing the T_g of the methacrylic copolymer on the absorption efficiency. This is due to the counterbalance of the repulsion between adsorbed droplets/particles from the possible interfacial crosslinking reactions between droplets/particles on the surface of PAN. When the crosslinker concentration is as low as 0.1%, free particles are still visible, as shown in Figure 37a, which is further confirmed in **Figure 36** by the similar ζ-potential value as compared to the sample without EGDMA. When more crosslinker is added up to 2%, free particles tend to be absent as detected by SEM. At the same time, the ζ-potential decreases from + 12.55 mV to around + 3 mV. This further confirms the nearly complete absorption of methacrylic polymers onto the surface of PAN particles. Based on the results of SEM observation and ζ-potential measurement, encapsulation saturation takes place when the crosslinker concentration is above 0.25 wt%.

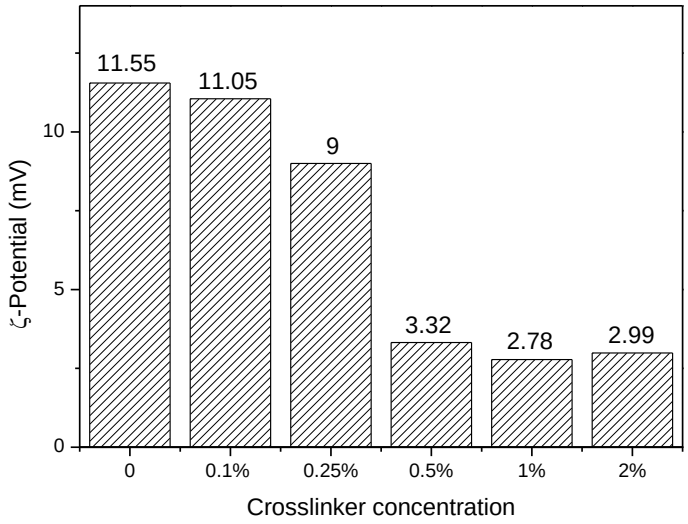

Figure 36. ζ-potential of PAN/methacrylic copolymer hybrid latexes with different crosslinker (EGDMA) concentrations (Sample L-10 - L-14).

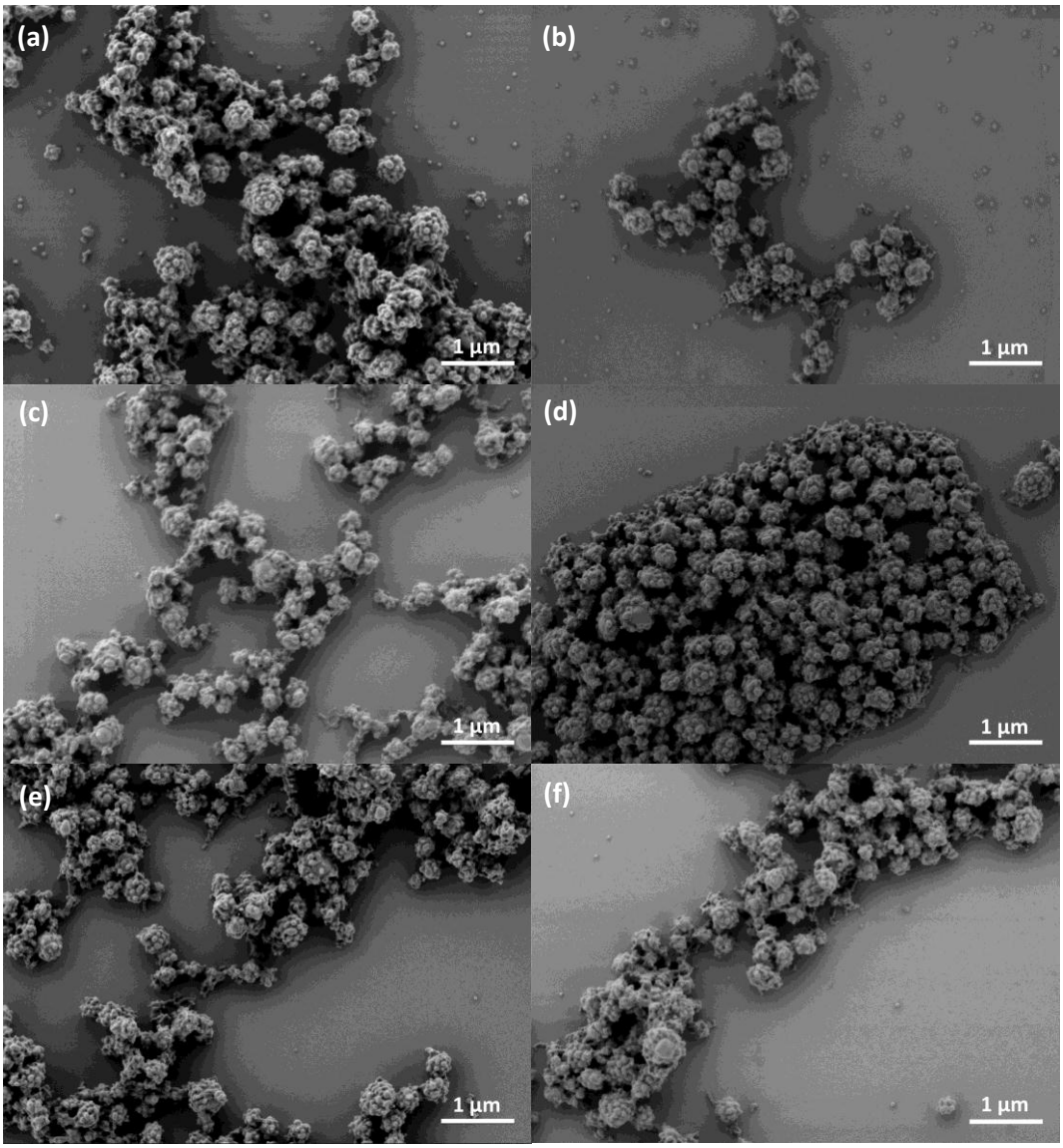

Figure 37. SEM images of PAN/methacrylic copolymer hybrid particles with different EGDMA concentrations: (a) 0%, (b) 0.1%, (c) 0.25%, (d) 0.5%, (e) 1%, (f) 2% (Sample L-10 ~ L-14).

4.2.7. Film formation

Pure PAN particles cannot form a continuous film, due to its semi-crystalline property and high T_g. However, soft methacrylic polymers in structured hybrid particles can bind semi-crystalline PAN particles together to form continuous composite films after drying. As shown in **Figure 38**, pure PAN dispersion leads to the formation of a thin layer of white powder rather than a film, while a continuous coating layer has been generated through the drying of hybrid dispersion (The content of PAN is 30 wt% based on total weight of dry coating). This contrast is more obvious when the films were thick, as illustrated in the right picture in Figure 38. Under the optical microscope, it is even clearer that discrete PAN aggregates, seen as dark

dots, were left on the substrate, while uniform films were derived from PAN/methacrylic polymer hybrids, as shown in **Figure 39**. As-prepared composite films possess semi-crystalline feature, due to the embedment of semi-crystalline PAN particles. The content of crystalline regions can be simply tuned by the ratio of PAN and methacrylic polymer. In addition, the film embedded with 30 wt% PAN still shows certain transparency, which is because of the formation of well-defined microstructure.

Figure 38. Photographs of semi-crystalline films derived from PAN and PAN/methacrylic polymer hybrid dispersions. The films on the left were prepared by rod-coater, while the films on the right were prepared by direct deposition of 1.5 ml dispersions from pipettes. PAN is accounted for 30 % in composite film based on total dry weight.

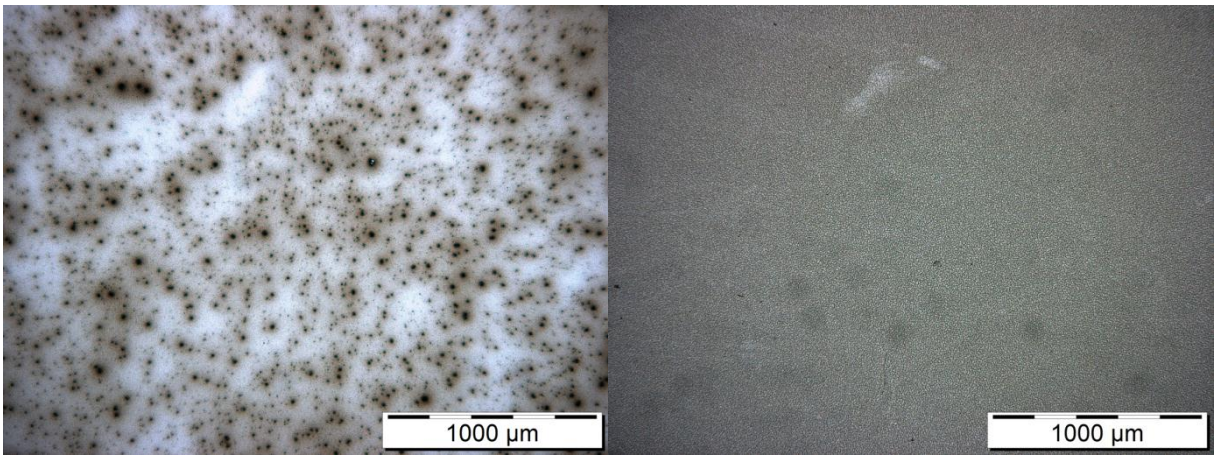

Figure 39. Images of PAN film (left) and PAN/methacrylic polymer (right) with 30 wt% PAN embedded under optical microscope.

4.3. Semi-crystalline PAN/epoxy thermoset composite

In this section, the concept of liquid-solid assembly is extended to the field of thermoset materials. An epoxy thermoset is selected as the model thermoset polymer due to the benefits described in section 3.1.4. The epoxy resin used in this section is a Bisphenol F based epoxy resin with the trade name of D. E. R. 354, while diethylenetriamine (DETA) is used as amine curing agent. A two-component system, which is commonly used in the field of epoxy thermosets due to the high versatility in the selection of the epoxy resin and the curing agent, was designed in this section. The two components are a PAN/epoxy miniemulsion and an epoxy curing agent respectively. The general concept is to prepare a PAN/epoxy hybrid miniemulsion first through the liquid-solid assembly approach demonstrated above, which is subsequently mixed with the water-soluble/dispersible curing agent and is deposited onto the substrate to form a PAN/epoxy thermoset composite film after curing. A schematic demonstration of the concept is demonstrated in **Figure 40**.

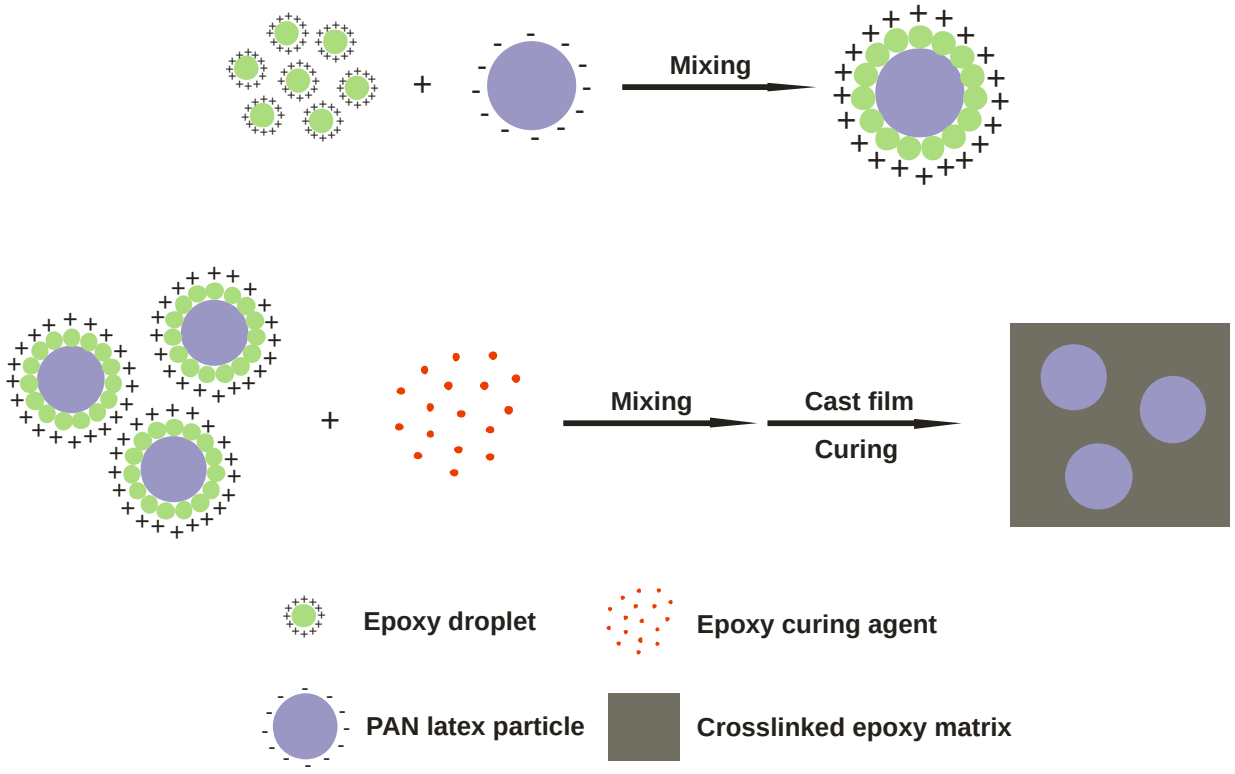

Figure 40. Schematic presentation of the fabrication of a PAN/epoxy thermoset composite film.

4.3.1. Epoxy miniemulsion

The epoxy miniemulsion was prepared using a high-pressure homogenizer at 40 °C, which is

commonly used for the large-scale fabrication of (mini)emulsions. Due to the high viscosity of the epoxy resin used in this work, ethyl acetate (EA) was used to dilute the epoxy resin for a better emulsification process, which was removed by rotary evaporator afterwards. The weight ratio between EA and epoxy resin is 1:1.

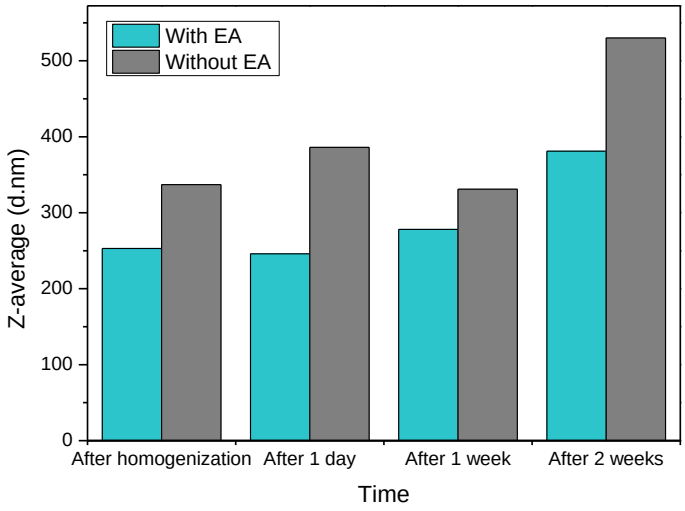

Figure 41. Z-average particle size of epoxy resin miniemulsion after storing at room temperature for various time.

As shown in **Figure 41**, the use of EA has decreased the average particle size of ultimate epoxy droplets in miniemulsions significantly. The average size of the droplets prepared with using EA is around 253 nm after homogenization, while the value for the droplets produced without using EA is around 337 nm. The difference is even larger when the measurement was carried out after storing. However, even the miniemulsion using EA cannot be stored for more than 1 week, which is indicated by the drastic increase of the average particle size from 253 nm to 381 nm. **Figure 42** demonstrates the PDI data of both miniemulsions. The PDI of the sample using EA is around 0.13, which is constant during storing, while the PDI of the sample without using EA is above 0.25, which is fluctuating dynamically. Although the drastic decrease of PDI for the sample without using EA to 0.04 after 2-week storage was observed, the average particle size of the droplets increased to more than 500 nm, which indicates instability of droplets upon storing.

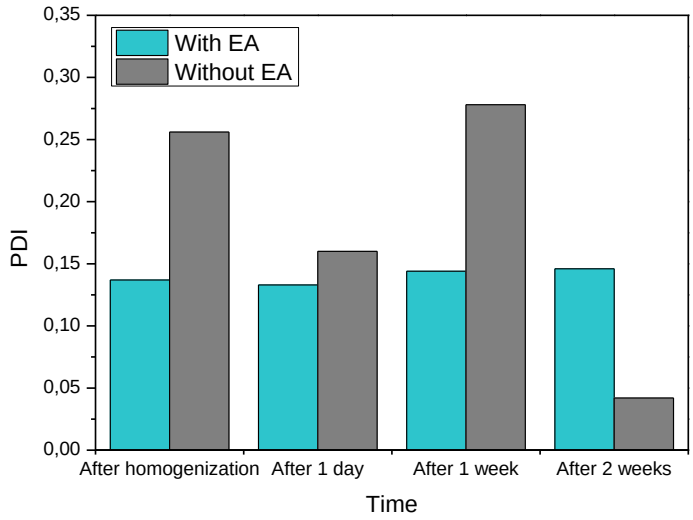

Figure 42. PDI of epoxy resin miniemulsion after storing at room temperature for various time.

4.3.2. PAN/epoxy hybrid miniemulsion

Because of the short storage time of epoxy miniemulsions, a freshly prepared epoxy miniemulsion with a positively charged surface was directly mixed with negatively charged PAN latexes to form a PAN/epoxy composite miniemulsion. By tuning the weight ratio between the PAN dispersion and the epoxy miniemulsion, different amounts of semi-crystalline PAN have been incorporated into the hybrid miniemulsions. The ζ-potential change upon mixing has been investigated and recorded, which is shown in **Figure 43**. Due to the charge neutralization, the ζ-potential of the composite miniemulsion decreased drastically from + 68.1 mV of the fresh epoxy miniemulsion to + 24 mV of the hybrid miniemulsion with 5% PAN. With the increase of PAN amount, the ζ-potential of the hybrid miniemulsion decreased to + 11 mV of the miniemulsion with 10% PAN, then achieved a plateau at around + 5 mV after 20% PAN was introduced into the system. The starting point of the plateau also indicates the saturation of the adsorption of epoxy droplets. Because of the instability of the epoxy droplets, which is discussed in section 4.3.1, also the as-produced PAN/epoxy hybrid miniemulsion lacks of long-term stability as expected.

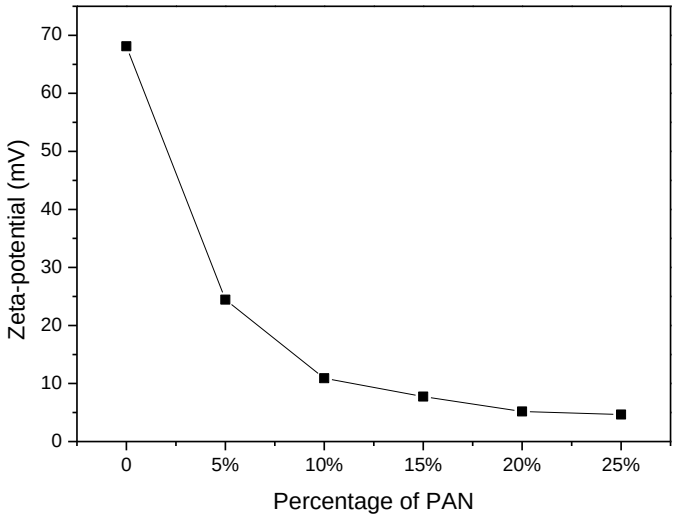

Figure 43. The relationship between the ζ-potential of PAN/epoxy composite miniemulsion and PAN concentration.

4.3.3. PAN/epoxy thermoset composite film

The water-soluble amine curing agent, diethylenetriamine (DETA), was mixed with the PAN/epoxy miniemulsion and deposited onto flexible PET substrates by a rod coater to form continuous films. The molar ratio between the epoxide group and the active hydrogen atom from amine is fixed as 1 : 1.6. After curing, a continuous PAN/epoxy thermoset composite film was obtained, as shown in **Figure 44**.

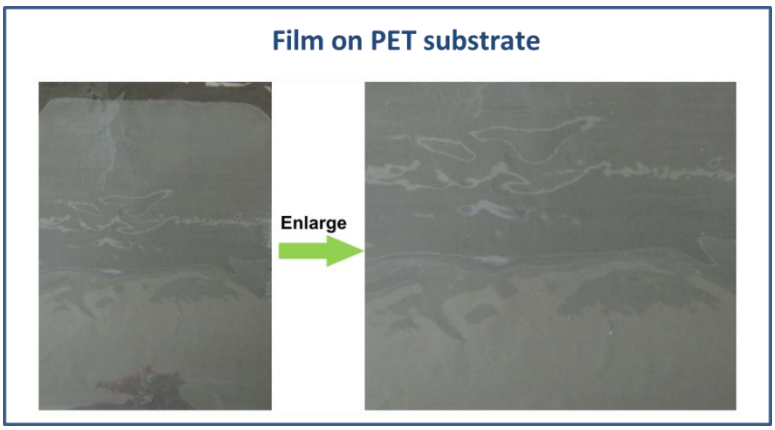

Figure 44. Appearance of PAN/epoxy thermoset composite film.

The oxygen barrier property of as-obtained films has been evaluated by measuring the oxygen transmission rate (OTR) of the films. The lower the OTR value is, the better is the oxygen barrier property. The results are listed in **Table 6**. The mixture of CTAB stabilized epoxy miniemulsion and DETA cannot form a continuous film on the surface of PET due to wetting

problems. So there is no OTR value for the pure epoxy thermoset film. The control sample is uncoated PET films, which has a OTR value of around 116 $cm^3/(cm^2$-24h-ND). When a layer of PAN/epoxy thermoset composite film is deposited onto the PET substrate, the lowest OTR value obtained was 75 $cm^3/(cm^2$-24h-ND). The general trend of the relationship between PAN concentration and OTR value is that it increases from around 80 to 116 $cm^3/(cm^2$-24h-ND), which indicates a significant decrease of barrier property, when the PAN concentration increases from 5 - 10 % to 15 - 20%. Then the OTR value decreased again to around 90 with the increase of PAN to 25%.

Table 6. Oxygen transmittance rates of the composite films with various PAN concentrations.

PAN concentration (%)	OTR @ 50% relative humidity [$cm^3/(cm^2$-24h-ND)]
0	-
5	75
10	80
15	116
20	115
25	90

To understand the origin of the observed relationship between PAN concentration and composite films' oxygen barrier properties, the morphologies of the films have been investigated by SEM and are shown in **Figure 45** and **Figure 46**. Figure 45 indicates that the distribution of PAN particles in the cured composite films is not uniform, which is independent of how much PAN is incorporated. This is probably because the curing of the epoxy resin was started from the surface of PAN/epoxy hybrid miniemulsion droplets by the water-soluble amine curing agent, which makes it easy to bind epoxy resin on two different PAN particles. Therefore, the distance between discrete PAN particles in the cured thermoset matrix is expected to be in the range of the size of epoxy miniemulsion droplets. Figure 46 roughly shows that the distance between PAN particles are around 200 - 300 nm averagely, which is in consistence with the assumption.

Besides, slight differences can be noticed in the morphology of PAN rich regions in Figure 46. When the PAN concentration is 5%, there is no obvious crack in the film. With the increase of the PAN concentration to 10%, visible cracks start to appear, which turns more and more obvious when the PAN concentration reaches 15% and 20%. Afterwards, the cracks start to

disappear again. This morphological change upon the increase of PAN concentration can be connected with the changes in oxygen barrier property. It is known that, the transport of gas through a material follows two basic mechanisms: (1) bulk diffusive flow via the solubility-diffusion mechanism; and (2) flow through defects in the materials due to inhomogeneity such as microcracks.[101] The influence of the flow from defects can be many times higher than the diffusion flow. Based on this principle, it is reasonable that the OTR value is strongly correlated to the number and width of cracks in the composite films. When 5% of PAN is embedded in the epoxy composite film, there is no crack, which corresponds to the lowest OTR value. With the increase of PAN concentration to 15%, 20% and 25%, the formation of more cracks during curing increased the possibility for oxygen flow to pass through, which is shown by increased OTR values.

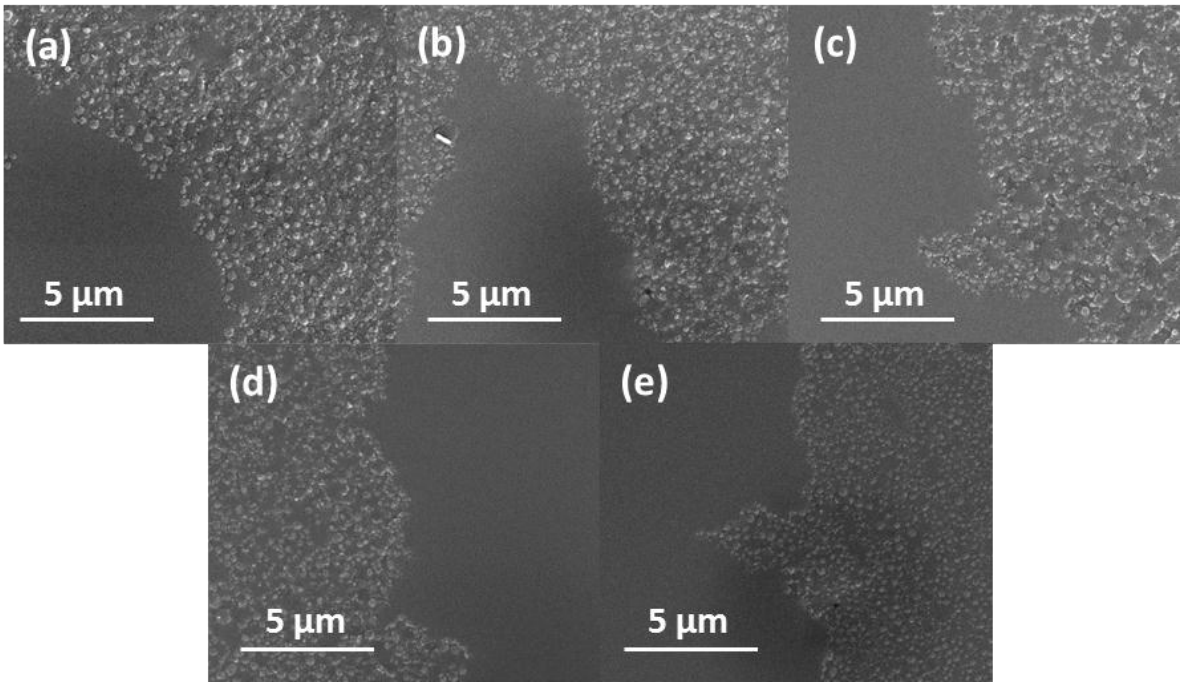

Figure 45. SEM images of PAN/epoxy thermoset composite films with various amount of PAN embedded: (a) 5 %; (b) 10 %; (c) 15 %; (d) 20 %; (e) 25 %.

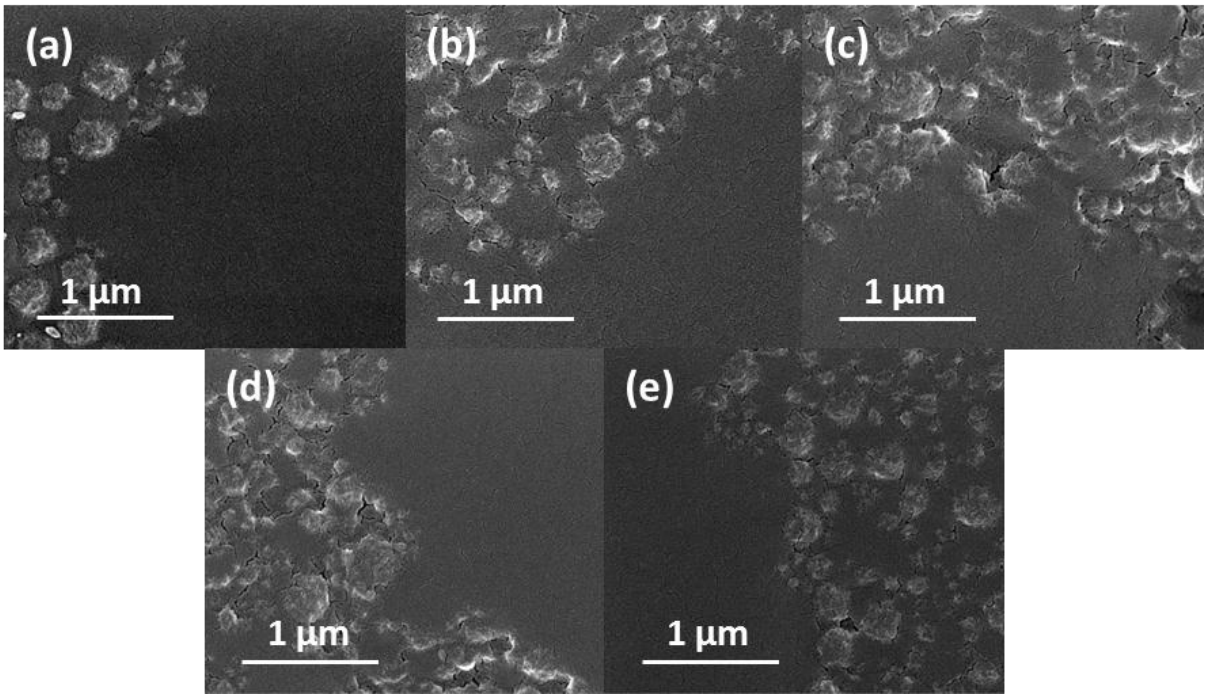

Figure 46. SEM images of PAN/epoxy thermoset composite films with various amount of PAN embedded: (a) 5%; (b) 10%; (c) 15%; (d) 20%; (e) 25%.

4.4. Conclusion

In this chapter, a novel fabrication method for structured hybrid particles was presented which is based on the assembly of liquid droplets and solid particles. In the first part, semi-crystalline polyacrylonitrile (PAN) dispersions with long-term colloidal stability have been fabricated through miniemulsion polymerization technique. It is found that post-addition of SDS as co-stabilizer in vinyl alcohol copolymer stabilized miniemulsion enhanced the colloidal stability of final hybrid dispersions significantly. As-prepared dispersions possess solid content higher than 15 wt% and can be stored for one year without visible sedimentation.

In the second part of this chapter, raspberry-shaped and core-shell shaped semi-crystalline hybrid particles have been prepared based on a modified hetercoagulation process. Compared to classic heterocoagulation method, liquid methacrylic monomer droplets, rather than solid methacrylic polymer particles were assembled with solid semi-crystalline PAN particles first through electrostatic attraction, which were polymerized afterwards to form structured hybrid particles. The advantage of this process is the better colloidal stability of the obtained hybrid latexes and the versatility of reactions inside the droplets. It has been found that, if two dispersions containing methacrylic polymer particles and PAN particles respectively were mixed directly, the mixture coagulated immediately. In contrast, the latexes prepared by this novel assembly method were stable for months without sedimentation observed. The improved stability is expected to be derived from the increased mobility of surfactant on the surface of liquid droplets compared to solid particles. Depending on the composition of the vinyl monomer mixture in the droplets, it is possible to obtain raspberry-shaped and core-shell shaped respectively. The soft polymer particles or layer on the surface of semi-crystalline PAN particles make it possible to obtain continuous semi-crystalline films at relatively low temperature.

In the third part of this section, the concept of liquid-solid assembly was extended to thermoset polymers. Difunctional epoxy resin has replaced the vinyl monomers in the miniemulsion droplets for the assembly. Due to the high viscosity of epoxy resin at room temperature, ethyl acetate has to be used to dilute epoxy resin in the oil phase, which decreased the size of epoxy miniemulsion droplets to around 250 nm. Even so, it is unfortunate that as-prepared epoxy miniemulsion cannot be stored for more than 1 week. A

two component curing system has been designed to obtain semi-crystalline epoxy thermoset films. One component is PAN-epoxy hybrid latex, while the other component is the amine curing agent, which is diethylenetriamine. Hybrid films with various amounts of PAN embedded has been casted on flexible PET substrates. The oxygen transmittance rate of the films has been measured, which is an indicator for the oxygen barrier property of the coatings. A decreased OTR value compared with uncoated PET substrates indicates that as-prepared hybrid films have potentials to be used in barrier applications.

5. Results and Discussion II - The preparation of structured thermoset-thermoplastic composite colloidal particles and derived thermoset reinforced thermoplastic films

This chapter focus on the preparation of structured thermoset-thermoplastic composite particles based on chemically induced phase separation (CIPS) process and seeded emulsion polymerization technique. The work presented in this chapter has been submitted to *Polymer* as full paper, entitled "*Thermoset-thermoplastic hybrid nanoparticles and composite coatings*".

As described in section 3.4, structured composite particles have attracted tremendous academic and industrial interest. A variety of materials, such as noble metal, metal oxide nanoparticles and different polymers, have been incorporated into single particles with different morphologies.[63, 102-106] For coating and adhesive industry, polymer-based core-shell particles with soft shell and hard core are widely used in water-borne latexes for the production of films with comprehensive properties.[107] During drying, hard materials in the core form isolated domains that provide mechanical, thermal and barrier properties, while the soft polymer can fuse together and form continuous films. There is no need to use environmentally unfriendly volatile additives and organic solvents to assist the film-formation process of rigid latex particles through softening. Commonly used rigid materials are various inorganic fillers, i. e. silica,[47] and rigid polymers like polystyrene.[108, 109] Generally speaking, inorganic fillers are more efficient than rigid polymers, especially for the improvement of mechanical and thermal properties, because they are much harder and more stable. However, substantial time and amount of dispersants are needed to disperse inorganic fillers in an organic phase without phase separation. In contrast, it is much easier to create hybrid particles with rigid polymers as hard domains through continuous processes. In addition, large refractive index difference between polymer matrices and inorganic fillers makes it much more difficult to obtain transparent hybrid films, especially with higher filler concentration and fillers with relatively large size. It is because the transparency of multiphase systems is determined by two major factors: the refractive index difference between the disperse phase and the matrix, and the size of disperse phase[110]. When the refractive index difference is large, the dispersing phase has to be sufficiently small (the top limit is usually around 50 nm) to avoid affecting the transparency of the hybrid materials. In comparison, although there are

differences in refractive index between various polymer species, the gap is much smaller than the one between inorganic fillers and polymers. Therefore, it is much easier to use suitable polymers as “fillers” especially in transparent systems.

Currently, mostly used rigid polymers are thermoplastic polymers with high T_g. Another important category of polymer materials – a thermoset polymer is rarely reported as functional domains in hybrid latex particle, especially as core materials, based on our knowledge. However, thermoset polymers are supposed to be more suitable as rigid domains or cores than thermoplastic polymers because they are highly crosslinked and therefore possess superior mechanical properties like higher stiffness in combination with thermal and chemical stability. A possible reason for this phenomenon is that it is difficult to obtain stable aqueous dispersions with cured thermoset polymer as disperse phase through conventional emulsion techniques. Fortunately, there is one technical solution for this problem which is miniemulsion polymerization[29, 32, 33]. As describe in section 3.3.2, miniemulsion droplets can be seen as independent nanoreactors, in which various reactions from free radical polymerization to polyaddition can be carried out as in-bulk [34]. Furthermore, hybrid particles can be generated through a one-pot approach even with various reactions involved. For instance, different polymerizations, such as free radical polymerization and polyaddition, have been carried out either simultaneously [111] or subsequently in miniemulsion droplets[38]. An earlier work from our group has reported the successful synthesis of high molecular weight polyurethane (PU)/ polystyrene (PS) and PU/ polybutylacrylate (PBA) hybrid nanoparticles with the size in the range from 90 nm to 130 nm by subsequent polymerizations.[112]. However, most of the reported work on the combination of various polymerization mechanisms is still focused on the incorporation of soft polymers like PU rather than highly crosslinked, rigid thermosets.

In this chapter, structured thermoset-thermoplastic composite particles embedded with highly crosslinked thermoset domains have been fabricated easily by seeded emulsion polymerization, in which thermoset seed emulsions are prepared by miniemulsion polymerization. Bisphenol F diglycidyl epoxide resin with the trade name of D. E. R. 354 and a hydrophobic amine curing agent with the trade name of Cardolite NX 5454 have been selected as model thermoset materials. In the first part of this chapter, the compatibility between various vinyl monomer/polymer and epoxy resin/thermoset has been studied in

bulk. In the second part, structured thermoset-thermoplastic composite particles were prepared. A schematic presentation of the fabrication process is illustrated in **Figure 47**, a miniemulsion containing epoxy resin, amine curing agent and 1st vinyl monomer is first obtained through ultrasonication, which is cured subsequently to form thermoset containing seed emulsion. Afterwards a 2nd vinyl monomer is fed and polymerized by the free radical polymerization mechanism and structured thermoset-thermoplastic hybrid particles are generated. After drying, hybrid films can be obtained from as prepared hybrid latexes on various substrates. The influence of various factors, including the amount and composition of 1st and 2nd monomer, the type of the epoxy resin on the morphologies of the hybrid latexes has been studied in detail. A mechanism based on the compatibility between vinyl monomer/polymer and epoxy thermoset has been proposed to explain the different morphologies of hybrid latexes and films. In the third part, four model latexes, poly(St-*co*-MA), poly(St-*co*-MA)/epoxy thermoset, poly(EHMA-*co*-MA) and poly(EHMA-*co*-MA)/epoxy thermoset, have been designed, the morphologies and mechanical properties of which have been investigated comprehensively.

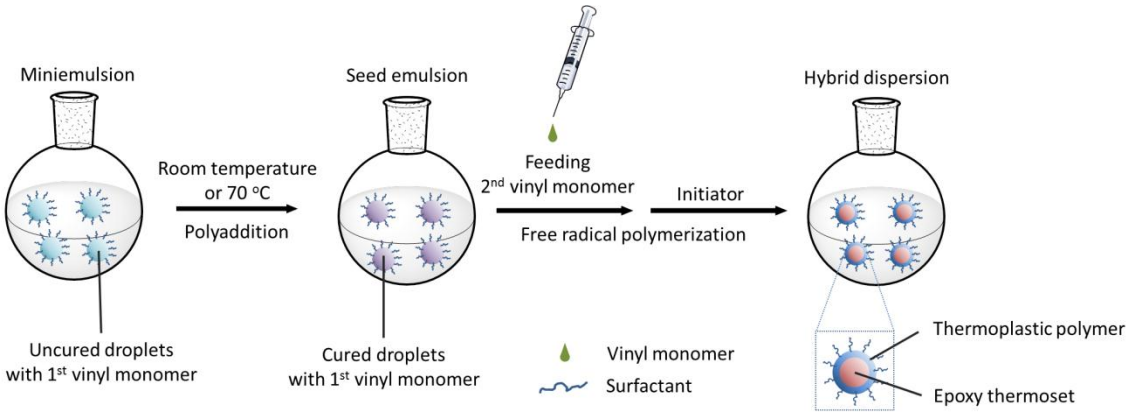

Figure 47. A schematic diagram for the synthesis of thermoset-thermoplastic hybrid core-shell nanoparticles is presented, which includes two steps: (1) epoxy curing in miniemulsion droplets at room temperature or 70 °C, and (2) feeding and polymerization of vinyl monomer.

5.1. In-bulk study of the compatibility between thermoset phase and thermoplastic phase

As described in section 3.1.5, chemically induced phase separation (CIPS) is an important method to create well-defined morphologies in thermoset-thermoplastic hybrids, in which thermoplastic phase is usually the dispersing phase [113-115]. In a typical process, a solvent or thermoplastic polymer of low T_g is mixed uniformly with an uncured thermoset resin first, which then can separate out automatically into defined soft domains upon curing. Such phase separation process can be considered as spinodal decomposition as a result of the rapid increase of molecular weight of thermoset resin upon curing as quench, based on Flory-Huggins lattice theory[116]. This is the most commonly used method to incorporate well distributed thermoplastic domains into thermoset matrices for toughening purpose. Here in this work, we demonstrate that the principle of CIPS can also be utilized to introduce thermoset domains in thermoplastic matrices by creating structured thermoset-thermoplastic hybrid particles.

In multiphase materials, the compatibility between different phases is of key significance to the morphology, structure of materials, and derived properties. Therefore, the compatibility between the vinyl monomer/polymer and the epoxy resin/thermoset has been studied in bulk first. The compatibility is indicated by the transparency of the mixture. The in-bulk study is divided into three parts: (a) the vinyl monomer-epoxy thermoset, in which the curing of epoxy resin takes place in the monomer; (b) the vinyl polymer-epoxy resin, in which vinyl monomers polymerize in the epoxy resin; (c) the vinyl polymer-epoxy thermoset, where both the free radical polymerization of vinyl monomer and curing of epoxy resin take place. Due to the high versatility in the properties, methacrylic and acrylic polymers are selected as the major source of vinyl species in this chapter.

5.1.1. Vinyl monomer-epoxy thermoset

Influence of Michael addition

The amine curing agent used in this chapter contains primary and secondary amine groups. If a vinyl monomer has to be incorporated into the epoxy curing system, it is speculated that an acrylic monomer should have negative effect on epoxy curing reaction by reacting with amine groups through Michael addition mechanism, as shown in **Figure 48**.

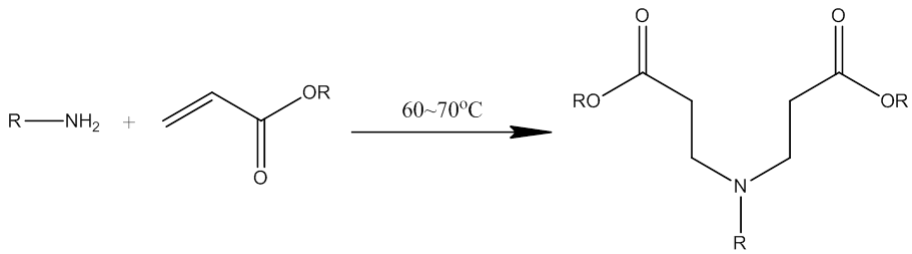

Figure 48. Michael addition reactions between primary amine and acrylates.

This hypothesis is proved by the results shown in **Table 7.** Pure epoxy resin and amine curing agent cured and solidified in less than half an hour. When the curing reaction takes place in MMA, the solidification time is 135 min due to dilution effect. But the solidification of the mixture takes one week, if the curing takes place in MA, which cannot be simply attributed to the dilution effect. At 70 ^{o}C, primary and secondary amine groups in the curing agent react with acrylate first, which consumes part of the curing agent that slows down the curing reaction.

Table 7. Comparison of the curing of epoxy resin in acrylic and methacrylic monomers.

Monomer	Solidification time	Appearance
-	less than 30 min	Transparent
MA	1 week	Transparent
MMA	135 min	Transparent
EHMA	30 min	Opaque
LMA	30 min	Opaque

* The molar ratio between epoxide group in D. E. R. 354 and active hydrogen atom on amine (NX 5454) is stoichiometric;
* The weight ratio between monomer and D. E. R. 354 is fixed as 2 : 1;
* Solidification time is defined as the time needed for samples to lose visible mobility.

Influence of monomer type

Table 7 has also shown that the type of methacrylic monomer has significant influence on the curing rate of epoxy resin and the compatibility between vinyl and epoxy phase. A general trend is that the solidification rate is negatively correlated to the transparency of the mixture. The faster the solidification is, the more opaque is the mixture. The solidification process took only 30 min in hydrophobic monomers, EHMA and LMA, which led to the formation of an opaque solid. Meanwhile, the solidification in MMA is much slower, which did not affect the transparency at all. This phenomenon can be explained from the perspective of compatibility between the vinyl and epoxy phases. When the compatibility is poor, as it is the case for EHMA and LMA, severe phase-separation takes place fast, which generates separated vinyl

and epoxy phases after curing starts. Inside epoxy rich regions, the curing rate of the epoxy is fast due to higher concentration of the epoxy resin and the epoxy curing agent. On the contrary, good compatibility weakens the interaction between reactive groups, which slows down the curing reaction by dilution.

Influence of the ratio between vinyl phase and epoxy phase

Besides the monomer type, the influence of the ratio between the vinyl phase and the epoxy phase has also been investigated by using a monomer mixture as vinyl phase.

Table 8. The relationship of epoxy phase concentration to the compatibility between vinyl monomer and epoxy thermoset.

Vinyl monomer [g]	D.E.R. 354 [g]	NX 5454 [g]	Epoxy phase [wt %]	Vinyl phase [wt %]	Appearance
5.75	0.25	0.20	7	93	Liquid with many precipitates
5.50	0.50	0.39	14	86	Liquid with many precipitates
5.25	0.75	0.59	20	80	Solid (very soft), white
5.00	1.00	0.78	26	74	Solid, white
4.00	2.00	1.56	47	53	Solid, transparent
3.00	3.00	2.34	64	36	Solid, transparent
2.00	4.00	3.12	78	22	Solid, transparent

* The vinyl monomer is composed of MMA, EHMA and LMA with the weight percentage of 60 %, 35 % and 5 % respectively;
* Epoxy phase includes both epoxy resin and amine curing agent;
* The molar ratio between epoxide group in D. E. R. 354 and active hydrogen atom on amine (NX 5454) is stoichiometric.

It is found that, the epoxy thermoset precipitated out from the liquid vinyl monomer when the weight ratio of epoxy phase (including epoxy resin and amine curing agent) is below 20 %, as shown in **Table 8**. With the increase of the epoxy phase, the mixture can be solidified. However, the transparency of the mixture is dependent on the concentration of the epoxy phase. The more epoxy phase is present, the higher is the transparency. This can be explained from the perspective of phase separation kinetics. Even the thermodynamics predicts the occurrence of phase separation in the multiphase system. This process can be prohibited or hindered, if it is not favored in kinetics. Here the kinetic parameter is the viscosity of the mixture. Upon the curing of the epoxy resin, the viscosity of the mixture increases drastically that has a negative effect on the phase separation process by restricting mobility of

components. When there is enough monomer, like in the samples with 80 wt% and 74 wt% of monomer added, the gradually forming, viscous epoxy thermoset networks are diluted by monomer, which makes it much easier for incompatible phases to separate thoroughly. With the decrease of the monomer amount, the fast build-up of the internal viscosity restricts the phase separation due to the limited mobility of components. Therefore, a transparent solid was generated after solidification.

5.1.2. Vinyl polymer-epoxy resin

The epoxy resin acts as a solvent when vinyl monomer is polymerized in it. The general trend of the change in the compatibility between phases is similar to the case of vinyl monomer-epoxy thermoset. The transparency of the mixture decreases upon the decrease of epoxy resin due to the fast build-up of viscosity, as illustrated in **Table 9**.

Table 9. The relationship of epoxy phase concentration to the compatibility between vinyl polymer and epoxy resin.

Vinyl monomer [g]	D.E.R. 354 [g]	V-59 [g]	Appearance
2.00	4.00	0.033	Opaque
3.00	3.00	0.050	Opaque
4.00	2.00	0.066	Transparent
5.00	1.00	0.083	Transparent
5.50	0.50	0.092	Transparent
5.75	0.25	0.096	Transparent

* The vinyl monomer is composed of MMA, EHMA and LMA with the weight percentage of 60 %, 35 % and 5 % respectively.

5.1.3. Vinyl polymer-epoxy thermoset

If the curing of the epoxy resin and the free radical polymerization of the vinyl monomer took place simultaneously, all the mixtures turned opaque, which indicates strong phase separation, as demonstrated in **Table 10**. This is a typical example of the incompatibility between different polymer species, which is an inherent feature of polymers as described in the section of 3.1.5. Both the epoxy curing and the free radical polymerization lead to a fast build-up of the molecular weight, which strengthen the tendency of phase separation by providing a stronger thermodynamic driving force.

Table 10. The compatibility between vinyl polymer and epoxy thermoset.

Vinyl monomer [g]	D. E. R. 354 [g]	NX 5454 [g]	V-59 [g]	Appearance
2	4	3.12	0.033	Opaque
3	3	2.34	0.050	Opaque
4	2	1.56	0.066	Opaque
5	1	0.78	0.083	Opaque
5.5	0.5	0.39	0.092	Opaque

* The vinyl monomer is composed of MMA, EHMA and LMA with the weight percentage of 60 %, 35 % and 5 % respectively;
* The molar ratio between epoxide group in D. E. R. 354 and active hydrogen atom on amine (NX 5454) is stoichiometric.

5.1.4. The vinyl monomers for thermoset-thermoplastic composite particles

Three commonly used vinyl monomers, MMA, St and EHMA, are selected as model monomers according to hydrophobicity differences (the hydrophobicity increases from MMA, St to EHMA) for the preparation of thermoset-thermoplastic composite particles. As described above, the hydrophobicity of the vinyl monomers dominates the compatibility between vinyl monomers and the epoxy thermoset. The more hydrophobic the vinyl monomer is, the worse is the compatibility. First, the epoxy resin and the amine curing agent was mixed with these monomers separately. It has been noticed that MMA and St are fully compatible/soluble with/in the epoxy resin, while EHMA is incompatible/insoluble with/in epoxy resin due to relatively high hydrophobicity, as illustrated in **Figure 49**a. However, the hydrophobic amine curing agent used in this work has shown a “compatibilizing” effect for EHMA, which leads to the formation of uniform transparent mixtures, as seen in Figure 2b. When the epoxy resin and the amine curing agent were mixed together, polyaddition reaction took place and started to create a cured epoxy thermoset network. Similar to the standard CIPS process, the molecular weight build-up of the epoxy thermoset led to phase separation between the epoxy phase and the vinyl monomers in the case of EHMA, which turned the transparent liquid monomer mixture into an opaque solid polymer mixture, as shown in **Figure 50**a and Figure 50b. Solidification time and transparency has been recorded to indicate the phase separation process of all three model monomers from continuously forming epoxy network, as listed in **Table 11**. Both the solidification time and the transparency can be used as indicators for the compatibility between different phases. The higher the transparency is, the better is the

compatibility. The longer the solidification time is, the better is the compatibility, because a good solvent with a high compatibility between the epoxy and the amine can decrease the curing rate dramatically due to the dilution effect. At both room temperature and 70 ^{o}C, the epoxy resin cures fastest in EHMA, and slowest in MMA, which means that the compatibility between three vinyl monomers and epoxy thermoset can be ordered as: MMA>St>EHMA. When MMA and St are used as solvent for the epoxy curing reaction, the final solid materials obtained are transparent and soft, while utilizing EHMA leads to the formation of an opaque, hard solid. In terms of curing kinetics, when the epoxy is cured in EHMA, it can be speculated that the strong phase separation derived from a poor compatibility leads to the formation of a separated epoxy-rich phase, where the epoxy curing reaction can progress faster. In contrast, when the epoxy is cured in MMA and St, the higher compatibility obviously slows down the epoxide-amine curing reaction because of restricted phase separation accompanied by the dilution of the reactive groups for the polyaddition reaction. Attributing to the continuous formation of the thermoset network, the diffusion of the epoxy and the amine turns to be more and more difficult. As a result, the epoxy curing reaction is terminated in the early stage, which leads to soft and elastic gels with respective vinyl monomers trapped inside.

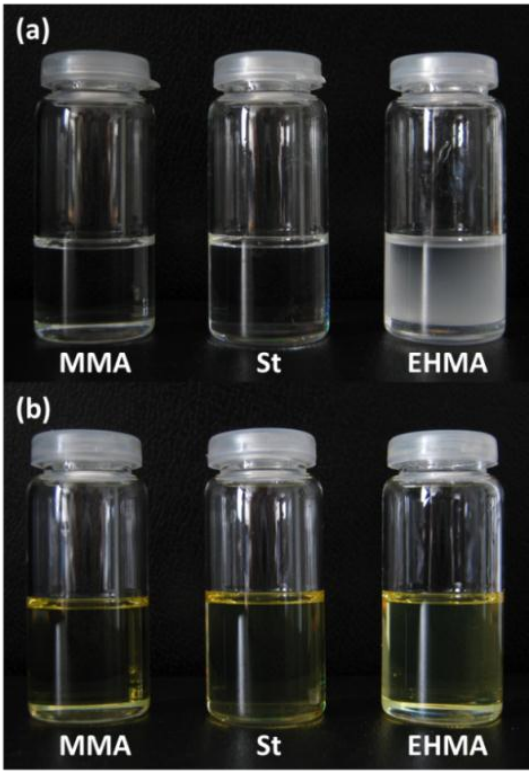

Figure 49. Appearance of the mixture of the epoxy resin and different vinyl monomers (a) before the addition of the amine curing agent; (b) after the addition of the amine curing agent.

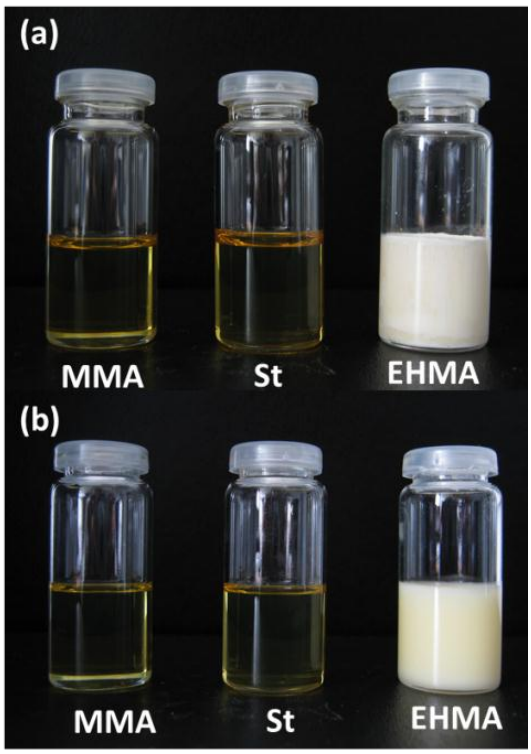

Figure 50. Appearance of epoxy/vinyl monomer hybrids cured at different temperatures: (a) 70 ^{o}C; (b) Room temperature.

Table 11. Solidification and appearance of epoxy in various vinyl monomers.

Vinyl monomer	Solidification time (room temperature)	Solidification time (70 ^{o}C)	Appearance
MMA	30 h	135 min	transparent
St	24 h	90 min	transparent
EHMA	8 h	30 min	opaque

* Solidification time is defined as the time needed for samples to lose visible mobility.

5.2. Structured thermoset-thermoplastic composite particles

There are two approaches to prepare composite particles through the combination of free radical polymerization and polyaddition, which are: (1) simultaneous polymerizations and (2) subsequent polymerizations. Because the existence of amine curing agents prevents the achievement of high conversion of free radical polymerization due to the capture of free radicals by amine, these two polymerizations have to be conducted subsequently. In this chapter, polyaddition reaction between epoxy and amine was carried out first in miniemulsion droplets with the existence of a 1st monomer as solvent, which can be seen as seeds. Afterwards, a 2nd monomer was fed into the seed emulsion and polymerized to form thermoset-thermoplastic hybrid particles.

Similarly to the in-bulk study, the epoxy and the amine curing agent have been cured in miniemulsion droplets at both room temperature and 70 ^{o}C. In such seed emulsions, the stability of the droplets is determined by two competing processes: (1) the formation of the epoxy thermosetting polymer inside droplets, which is beneficial for the stability of droplets and (2) the destabilization of droplets that can be accelerated at high temperature. With EHMA in the droplets, the epoxy resin is cured extremely fast at 70 ^{o}C due to strong phase separation, which turns liquid droplets to solid particles within 2 h, as shown in **Figure 51**c. Monomers are either trapped inside epoxy thermoset particles or expelled out during epoxy curing, which evaporated during the preparation of TEM sample. On the contrary, epoxy curing rate is much slower in MMA and St even at 70 ^{o}C. Therefore the formation of the thermoset polymer inside droplets is not fast enough to counterbalance the destabilization of droplets that is accelerated by high temperature, as shown in Figure 51a and Figure 51b. When the epoxy resin is cured at room temperature, the epoxy curing reaction is expected to be terminated in very early stage because the diffusion of the epoxy and the amine decreases dramatically along curing due to the fast build-up of internal viscosity. Therefore, all miniemulsion droplets are stable in all three samples with different vinyl monomer inside, as shown in **Figure 52**.

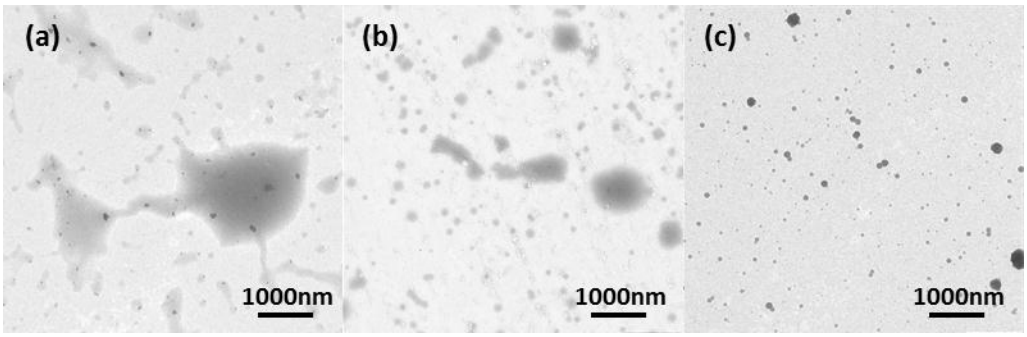

Figure 51. TEM image of seed particles prepared at 70 °C with MMA (a), St (b) and EHMA (c) inside miniemulsion droplets.

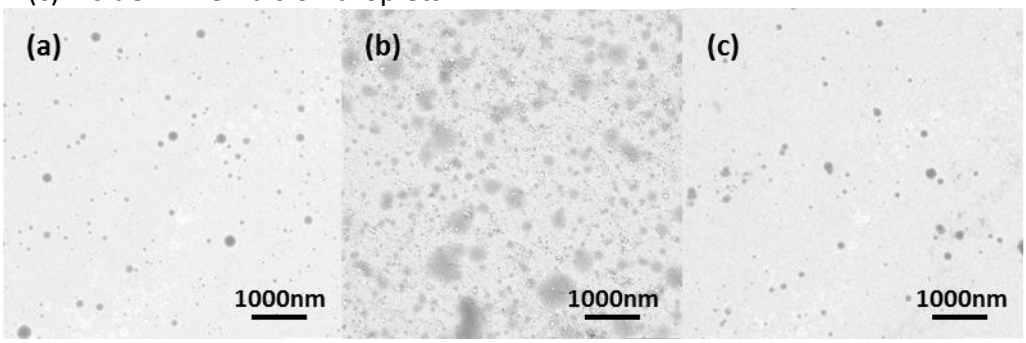

Figure 52. TEM image of seed particles prepared at room temperature with MMA (a), St (b) and EHMA (c) inside miniemulsion droplets.

5.2.1. The influence of the 1st monomer

It has been found that the morphology of derived hybrid particles differs according to the type of the 1st monomer in the seed emulsions. As illustrated in **Figure 4**a-b and 4d-e, well-defined core-shell particles can only be generated when St is utilized as 1st monomer, while more homogenous particles were obtained with MMA as 1st monomer. In contrast, Figure 4c and 4f demonstrate that two types of particles exist at the same time when EHMA is used as 1st monomer. The large, dark particles can be attributed to epoxy thermoset containing particles, while the blurry, "fused" particles should be EHMA/MMA copolymer particles, which possess low T_g and are vulnerable under the electron beam.

The explanation for the observed results can be related to the compatibility between vinyl species and the epoxy thermoset. The compatibility between the vinyl phase and the epoxy phase in the 1st step (formation of seed emulsions by polyaddition) and 2nd step (monomer feeding and free radical polymerization) is determined by the 1st monomer and the mixture of the 1st and 2nd monomer respectively. According to the results from in-bulk studies, MMA has the highest compatibility with the epoxy thermoset, which leads to the formation of homogenous seeds and derived hybrid particles. When St is used as the 1st monomer, epoxy

thermoset seeds from 1st step are still homogenous. But, after the initiation of free radical polymerization, the fast build-up of molecular weight starts the phase separation between vinyl polymer and epoxy thermoset. Continuously forming vinyl polymers are expelled out from the thermoset network to the water/seed interface and stabilized by the surfactant, which generates a core-shell shaped morphology. On the contrary, EHMA is extremely incompatible with the epoxy thermoset, which leads to the strong phase separation between EHMA and epoxy species during the curing of the seeds. It is highly possible that some EHMA is expelled out of the seeds into the aqueous phase to form separate droplets. So two types of particles are expected after polymerization: epoxy thermoset-rich particles, which are larger, are stable and have a higher contrast under TEM, and EHMA/MMA copolymer particles, which coalescence and fuse during drying on the copper grid due to a low T_g, which are smaller and blurry under TEM.

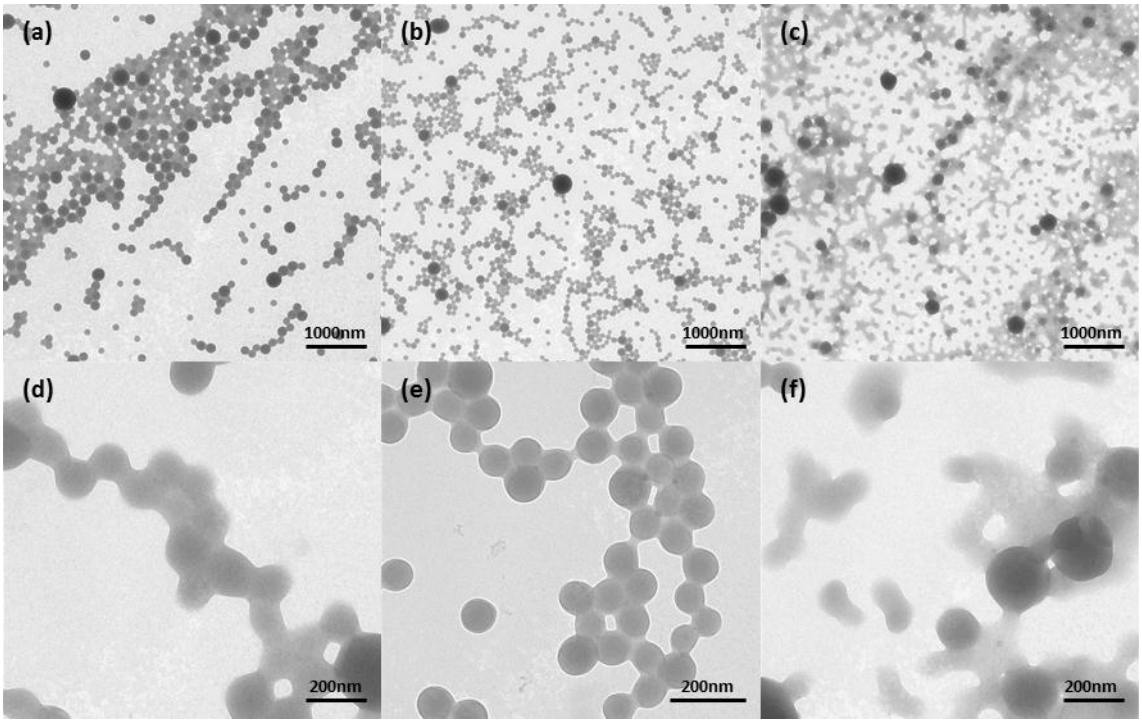

Figure 53. TEM images of thermoset-thermoplastic hybrid nanoparticles with different 1st monomers in seeds and MMA as 2nd monomer: (a, d) CS-4, MMA as 1st monomer; (b, e) CS-1, St as 1st monomer; (c, f) CS-5, EHMA as 1st monomer.

5.2.2. Influence of the surfactant concentration

The influence of the surfactant concentration on the property of the composite latexes has been studied. To maintain the colloidal stability, at least 3 wt% of Lutensol AT 50 (based on the weight of the oil phase in miniemulsion) has to be used. The difference in surfactant

concentration did not change the morphology of the composite particles, which are always core-shell shaped, as demonstrated in **Figure 54**. However, a difference in the particle size of composite particles has been noticed, which is obviously shown in both TEM images in Figure 54 and the DLS data in **Table 12**. It is not surprising that the particle size decreased from 213 nm to 170 nm, when the surfactant concentration increased from 3% to 5%, which suppresses the coalescence between miniemulsion droplets during epoxy curing.

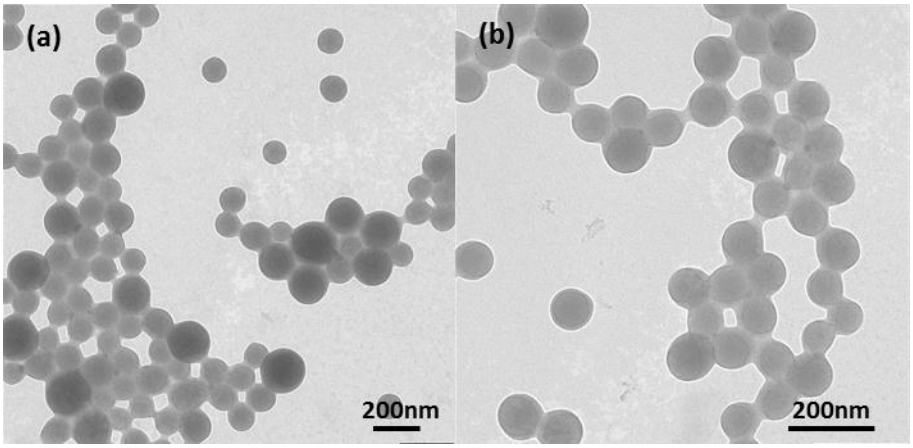

Figure 54. TEM images of thermoset-thermoplastic composite particles with different Lutensol AT 50 concentrations, (a) 3 wt% and (b) 5 wt% based on the weight of oil phase in miniemulsion (St as 1st monomer, MMA as 2nd monomer).

Table 12. The relationship between surfactant concentration and particle size of composite particles.

Surfactant concentration	Average particle size [nm]
3 %	213
5 %	170

5.2.3. Influence of the composition of epoxy resin

As described in the section 3.1.4, the functionality of the epoxy resin, which defines the EEW, determines the crosslinking density of the thermoset domains. Therefore, a trifunctional epoxy resin (ED-505) and a tetrafunctional epoxy resin (GA-240) have been used to replace a part of the difunctional epoxy resin, D. E. R. 354, to produce styrene-epoxy thermoset seed particles, the chemical structures of which are demonstrated in **Figure 55**.

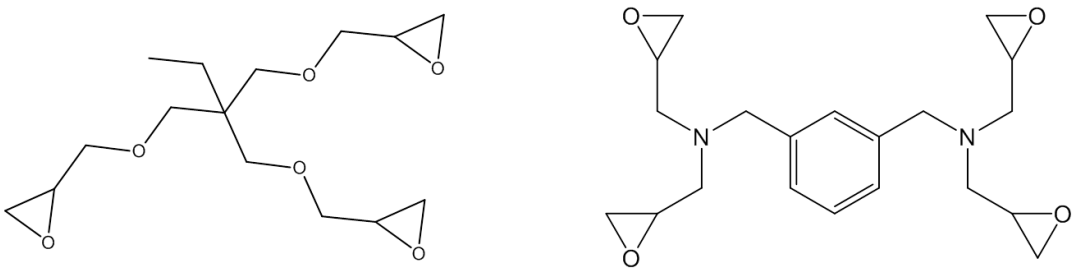

Trifunctional epoxy resin **Tetrafunctional epoxy resin**

Figure 55. Chemical structure of trifunctional and tetrafunctional epoxy resin.

With the increase of the number of epoxide groups in the structure, the polarity of the epoxy resin becomes higher, which is not favorable for the stability of miniemulsion droplets due to diffusion. Therefore, the average size of miniemulsion droplets increases from 190 nm to 296 nm with the increase of functionality of the epoxy resin, as demonstrated in **Table 13**.

Table 13. The relationship between the functionality of the epoxy resin and the size of miniemulsion droplets and composite particles.

The composition of epoxy resin	size of miniemulsion droplet *d* [nm]	size of composite particle *d* [nm]
Difunctional	190	170
Difunctional + Trifunctional	223	211
Difunctional + Tetrafunctional	296	234

After epoxy curing and free radical polymerization, the size of the composite particles from various epoxy resins follows the same trend as miniemulsion droplets. The average size of the composite particles increases from 170 nm to 234 nm with the increase of the functionality of the second epoxy resin. It has to be mentioned that the size difference between droplets and final composite particles is due to the inherent difference between droplets and particles. In this thesis, the average particle size of emulsions and latexes was measured by dynamic light scattering. Before the measurement, emulsions and latexes have to be diluted strongly (1:2500) in order to avoid multiscattering. Upon dilution, it is highly possible that droplets could change due to dissolving of hydrophilic ingredients and surfactant molecules during dilution.

The morphologies of as-prepared composite particles have been investigated by TEM, which are illustrated in **Figure 56**. The size change detected by DLS is confirmed by the TEM observation also. It is obvious that the average size of composite particles derived from

difunctional epoxy is much smaller than the ones from the mixtures of difunctional and trifunctional epoxy or difunctional and tetrafunctional epoxy, if comparing Figure 56a, Figure 56c and Figure 56e. Another observed trend is that the particles prepared from the sample containing only difunctional epoxy are discrete (Figure 56 a and Figure 56b), while particles derived from the sample containing tetrafunctional epoxy stick together (Figure 56 e and Figure 56f) after drying on the copper grids. This can be attributed to the polarity difference of epoxy resin also. It is a common phenomenon in the TEM investigation of polymer particles that hydrophilic polymer particles turn to stick together due to stronger interactions between particle surfaces. Besides, it seems that the contrast between the epoxy thermoset and the thermoplastic polymer is stronger under TEM when tri- and tetra-functional epoxy resin was used as the co-source of epoxide groups, as shown in Figure 56 c-Figure 56 f. This is probably because of the higher crosslinking density brought by the decreased EEW of the epoxy resin due to increased epoxide functionality.

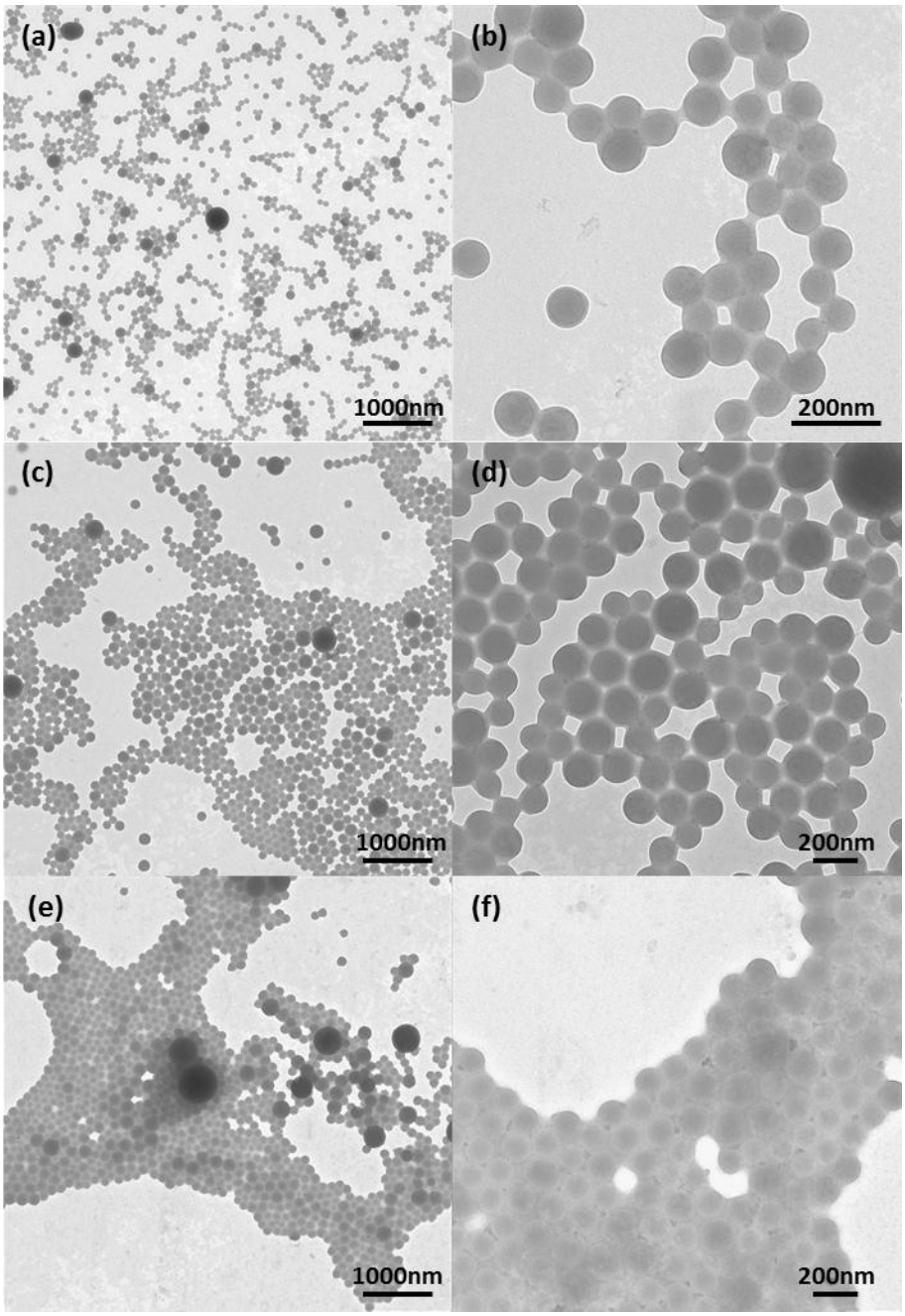

Figure 56. TEM images of thermoset-thermoplastic composite particles with epoxy thermoset derived from epoxy resins with different functionality: (a, b) difunctional; (c, d) difunctional + trifunctional; (e, f) difuncitional + tetrafunctional.

5.2.4. The influence of 2nd monomer

Based on the discussion in Section 5.2.1, St has been chosen as the 1st monomer for the study on the influence of the 2nd monomer on the preparation of structured thermoset-thermoplastic particles. According to the principle of seeded emulsion polymerization, the feature of the 2nd monomer that fed after the formation of a seed emulsion is critical for the properties of final hybrid latexes. In our work, neat monomer rather than emulsified

monomer emulsion was fed as 2nd monomer into seed emulsions to restrict the formation of secondary nuclei. [117, 118] So the hydrophobicity of the 2nd monomer is of key importance to the fabrication of structured hybrid particles, which defines both the capability of the 2nd monomer to diffuse from monomer droplets to epoxy thermoset seeds through the aqueous phase and the compatibility between the 1st, the 2nd monomer/polymer and the epoxy thermoset. It is found that, the sample with EHMA and MAA as 2nd monomer (CS-3 and CS-4) coagulated during polymerization, while stable latexes (CS-1 and CS-2) were obtained with St and MMA as 2nd monomer. This result indicates that neither an extreme hydrophobic monomer nor hydrophilic monomer is suitable as the 2nd monomer. EHMA is so hydrophobic that it is difficult for them to diffuse through the aqueous phase to seeds. Also, the incompatibility between EHMA and the epoxy thermoset makes it difficult for EHMA to be captured by the epoxy thermoset seeds due to weak interactions. MAA is so hydrophilic that it dissolves partially in the aqueous phase. Therefore, both EHMA and MAA form secondary nuclei in seed emulsions, which are polymerized separately. Due to the lack of surfactant in the aqueous phase, the newly formed polymers outside the seeds form agglomerates and destabilize the colloidal system.

As commonly used monomers for emulsion polymerization, it is easy for St and MMA to diffuse from large monomer droplets through the aqueous phase to the epoxy thermoset seeds. Mixtures of St and MMA blended with different ratios have been used as 2nd monomer to investigate the influence of 2nd monomer composition on the morphology of final hybrid particles. **Figure 57**a indicates that hybrid thermoset-thermoplastic particles are “sticky” and coalescence during drying on the copper grids, when only St is used as the 2nd monomer (sample CS-2). Meanwhile, the conversion of free radical polymerization of this sample is low (less than 40%, based on solid content measurement). In contrast, well-defined core-shell shaped morphology has been generated, when at least 20 wt% MMA is blended with St as 2nd monomer, as shown in Figure 57c-Figure 57f. A possible explanation is that MMA is more hydrophilic and compatible with the epoxy thermoset than St. Therefore it is easier for MMA to diffuse and penetrate into the seeds sufficiently to avoid the formation of free droplets composed of the 2nd monomer before polymerization, which is beneficial for a more controlled phase separation during free radical polymerization.

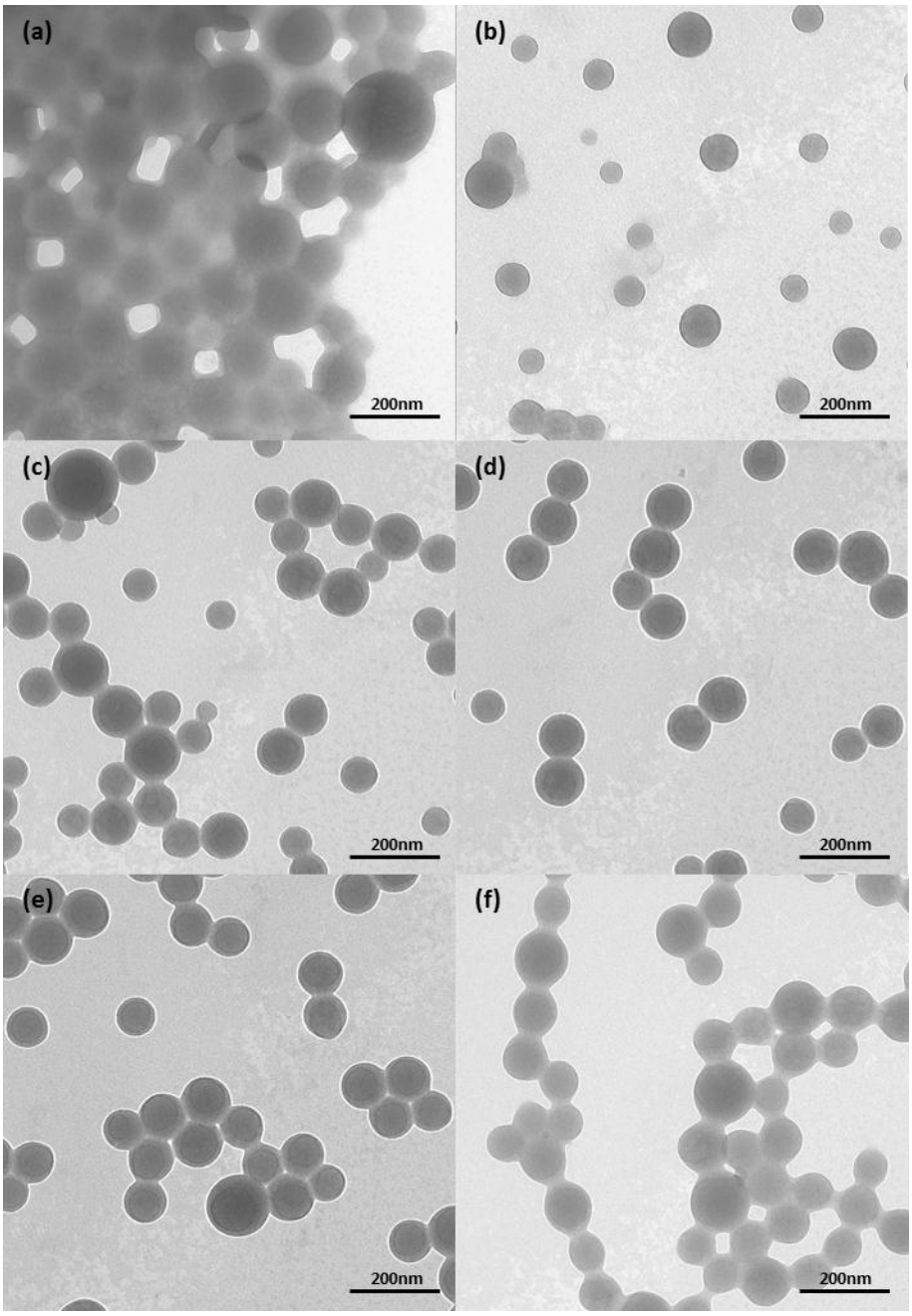

Figure 57. TEM images of thermoset-thermoplastic hybrid particles with various St/MMA ratios (weight ratio) in 2nd monomer (a) 1 : 0 (b) 9 : 1 (c) 4 : 1 (d) 1 : 1 (e) 1 : 4 (f) 0 : 1.

5.2.5. The influence of the amount of 2nd monomer

Besides the type, the amount of the 2nd monomer also affects the properties of final thermoset-thermoplastic composite particles, which is investigated in this section. Based on the results from section 5.2.4, MMA was used as the 2nd monomer, the concentration of which differed from 50 wt% to 333 wt% based on the weight of the 1st monomer with other parameters fixed. **Table 14** demonstrates the change in the average particle size of composite particles upon the increase of the usage of MMA. When the concentration of the 2nd

monomer is below 100 wt%, the average size of composite particles maintains constant around 170 nm. Then the average size increases to 245 nm and 318 nm with 200 wt% and 333 wt% of MMA added as the 2nd monomer respectively.

Table 14. The relationship between the amount of MMA and the average particle size of composite particles.

Amount of MMA [g]	Concentration of MMA based on the weight of the 1st monomer [%]	Average size of composite particles *d* [nm]
1.50	50	168
3.00	100	170
6.00	200	245
10.00	333	318

The morphological changes have been recorded and are shown in **Figure 58**. The tendency in the size change of composite particles is in consistence with the founding from DLS data in Table 14. When the amount of the 2nd monomer is as small as 50% based on the weight of 1st monomer, the core-shell structure is not clear and well-defined as shown in Figure 58a. With the increase of the amount of 2nd monomer, the particle size of the composite particles increased gradually and started to possess well-defined core-shell structures as illustrated in Figure 58b and Figure 58c. Then secondary particles, which are much smaller than core-shell shaped composite particles, are observed in Figure 58d when 333 wt% of MMA was added as 2nd monomer, which is 2.3 times more than the amount of the 1st monomer inside the seeds. It can be attributed to the secondary nucleus formed by free MMA, due to the saturation of "swelling" of epoxy thermoset seeds.

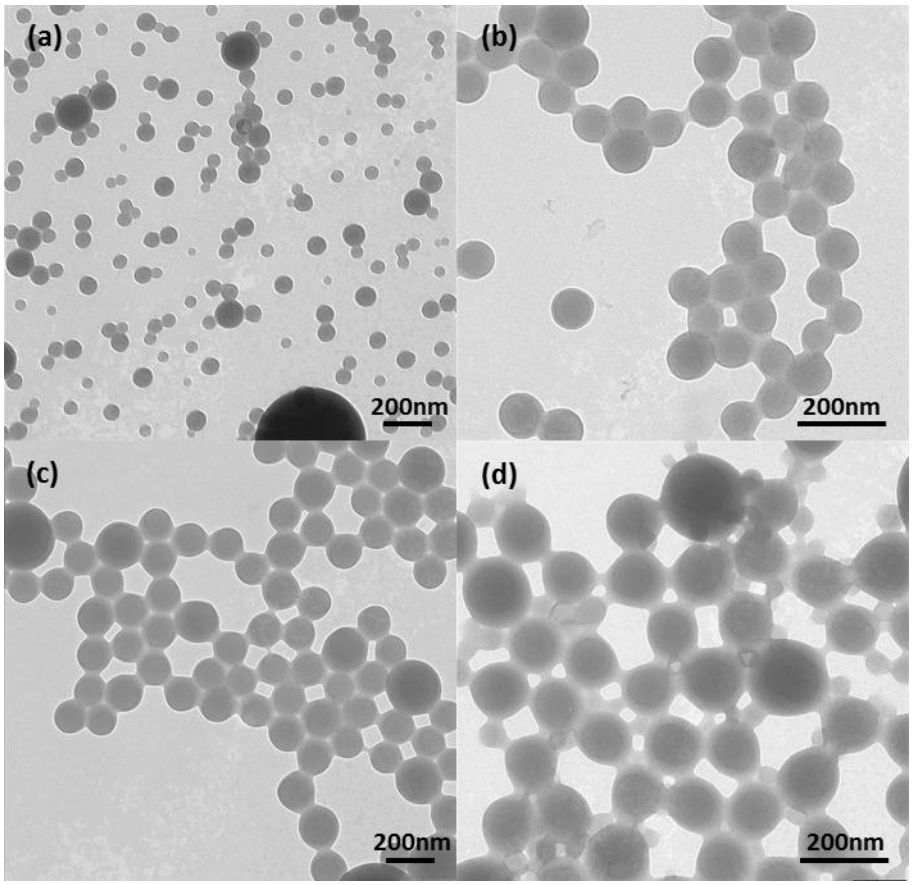

Figure 58. TEM images of composite particles with various concentrations of MMA as the 2nd monomer (a) 50%; (b) 100%; (c) 200%; (d) 333% based on the weight of the 1st monomer.

5.2.6. The influence of crosslinker concentration in 2nd monomer

In this section, a crosslinker, divinyl benzene (DVB) was added in the 2nd monomer to crosslink the thermoplastic polymer shell in the thermoset-thermoplastic composite particles. First, the average particle size of the thermoset-thermoplastic composite particles has been measured, which is shown in **Figure 59**.

It is found that the crosslinking density of the thermoplastic polymer in shell has no influence on the average particle size of the composite particle, which is not surprising. The influence of cross linker concentration on the morphology of the composite particles was studied and is demonstrated in **Figure 60**.

When the crosslinker concentration is below 6 wt%, there is no significant difference in morphology of core-shell shaped composite particles. But the particles start to lose their spherical shape with the increase of crosslinker concentration to 12 wt%, which is probably

due to the deformation induced by the internal elastic stress from increased crosslinking density of the shell polymer.

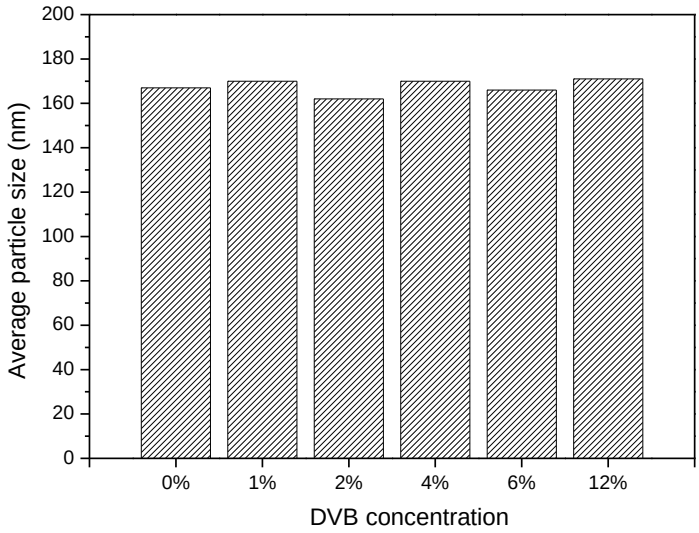

Figure 59. The relationship between average particle size of composite particles and DVB concentration (The DVB concentration is based on the weight of 2nd monomer).

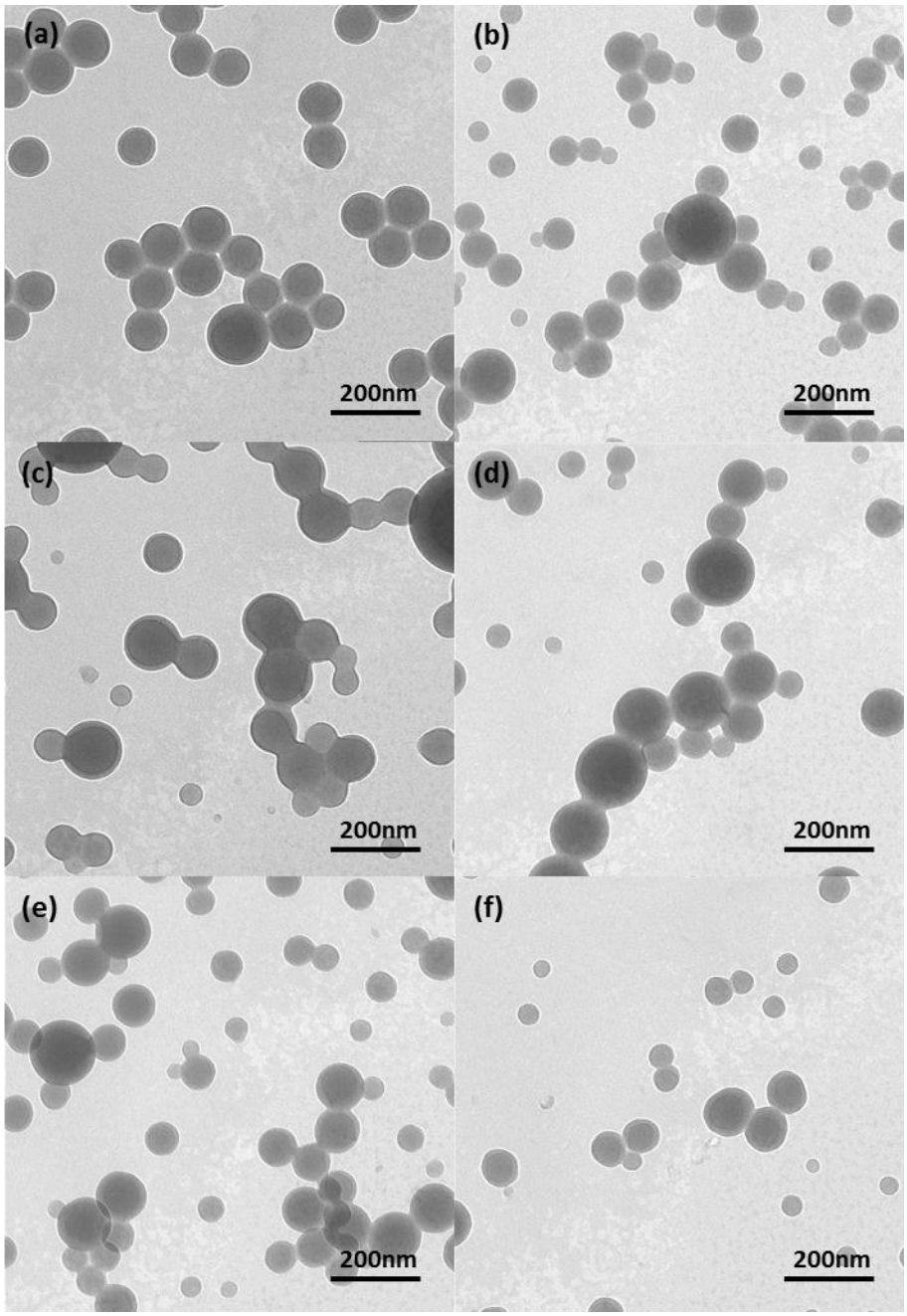

Figure 60. TEM images of thermoset-thermoplastic hybrid particles with various DVB concentrations based on the amount of 2nd monomer (a) 0 (b) 1% (c) 2% (d) 4% (e) 6% (f) 12%. The 1st monomer is St, while the 2nd monomer is composed of 20 wt% of MMA and 80 wt% of St.

5.3. Model systems

5.3.1. Thermoset-thermoplastic hybrid latexes

To further investigate the property of the film materials derived from thermoset-thermoplastic hybrid latex particles, four model latexes have been designed based on the consideration of the T_g of copolymers, which are poly(St-co-MA) (CS-13), poly(St-co-MA)/epoxy thermoset (CS-11), poly (EHMA-co-MA) (CS-14), and poly (EHMA-co-MA)/epoxy thermoset (CS-12). MA has been utilized as the 2nd monomer because of the relatively low T_g (around 10 ^{o}C) of its homopolymer compared with PMMA (around 105 ^{o}C).

The influence of the incorporation of the epoxy thermoset on the average particle size of hybrid latex particles has been studied. As illustrated in **Table** 15, the incorporation of epoxy thermoset domains led to the decrease of the average particle size. The z-average particle size of poly(EHMA-*co*-MA) and poly(St-*co*-MA) is 214 nm and 277 nm respectively, while this value of poly(EHMA-*co*-MA)/epoxy thermoset and poly(St-*co*-MA)/epoxy thermoset is 181 nm and 162 nm. The decreased particle size upon the incorporation of epoxy phase can be explained by the additional stabilizing force from the epoxy resin and the hydrophobic amine curing agent in miniemulsion droplets. It is known that, miniemulsions are not thermodynamically stable, the stability of which relies on the hindrance of two destabilization processes: coalescence and Ostwald ripening. While the coalescence can be suppressed by the addition of surfactant, Ostwald ripening requires the use of ultrahydrophobes like hexadecane, which can build up osmotic pressure inside miniemulsion droplets to counterbalance the Laplace pressure. However, an ultrahydrophobe has not been used in both poly(St-*co*-MA) and poly(EHMA-*co*-MA) latexes. Hence Ostwald ripening led to the formation of relatively large particles after polymerization. For poly(EHMA-*co*-MA)/epoxy thermoset and poly(St-*co*-MA)/epoxy thermoset latexes, the epoxy resin, the hydrophobic amine and the instantly formed thermosetting polymer act as ultraphydrophobe for the miniemulsion droplets.[32] As result, poly(EHMA-*co*-MA)/epoxy thermoset and poly(St-*co*-MA)/epoxy thermoset latexes possess smaller particles compared to poly(St-*co*-MA) and poly(EHMA-*co*-MA) latexes. Meanwhile due to the higher hydrophobicity of EHMA, poly(EHMA-*co*-MA) and poly(EHMA-*co*-MA)/epoxy thermoset show smaller particle size values than poly(St-*co*-MA) and poly(St-*co*-MA)/epoxy thermoset latexes.

Table 15. Particle size and polydispersity (PDI) results of obtained latexes.

	Poly (EHMA-*co*-MA)	Poly (EHMA-*co*-MA)/epoxy thermoset	poly (St-*co*-MA)	Poly (St-*co*-MA)/epoxy thermoset
Z-average particle size [nm]	214	181	277	162
PDI	0.030	0.107	0.072	0.049

The morphology of poly(St-*co*-MA)/epoxy thermoset latex particles is in consistence with poly(St-*co*-MMA)/epoxy thermoset particles, as shown in **Figure 61**a and Figure 61b. In all the formulations, the weight ratio between the epoxy phase (epoxy resin and amine curing agent) and the thermoplastic polymer is 1 : 2. Under the assumption that the densities of the epoxy thermoset and the thermoplastic polymer are the same, epoxy thermoset takes 1/3 of the total volume of the composite particle (the diameter of the epoxy core is around 70 % of the diameter of whole particle), which basically fits the information from TEM images. The morphology of poly(EHMA-*co*-MA)/epoxy thermoset latex particles is different from poly(EHMA-*co*-MMA)/epoxy particles. Figure 61c and Figure 61d demonstrated the existence of large, spherical shaped agglomerates, probably due to the extreme low T_g of the EHMA/MA copolymer that led to the fusion between hard, small particles.

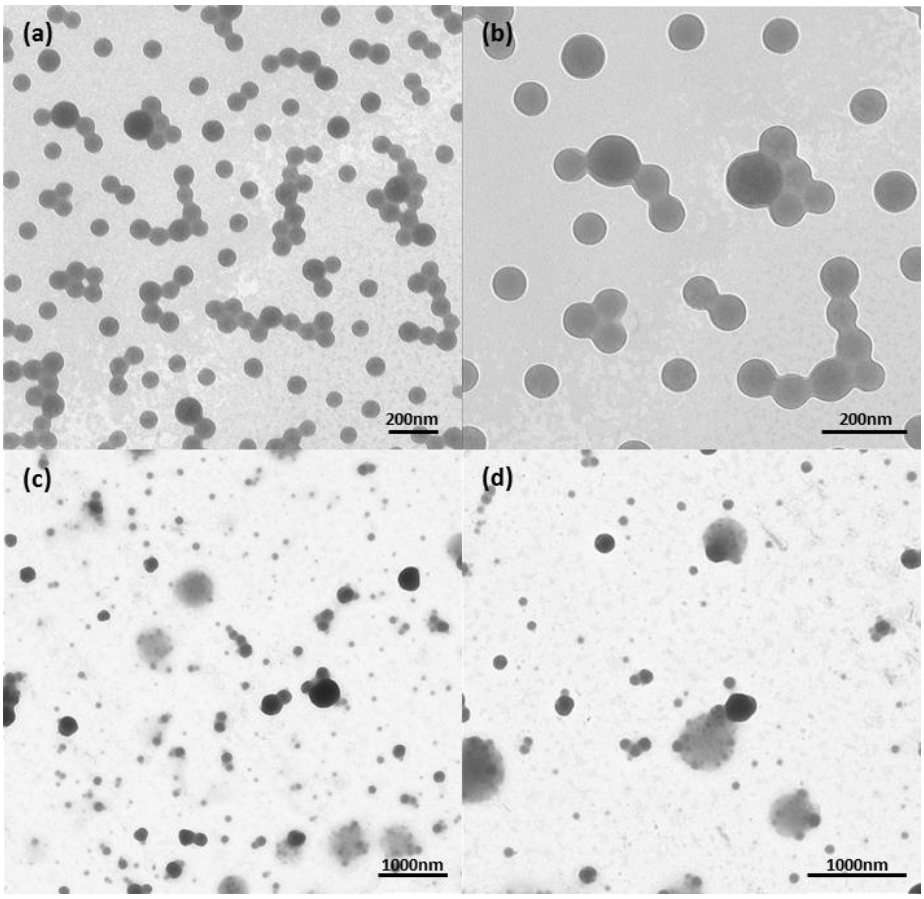

Figure 61. TEM images of poly(St-*co*-MA)/epoxy thermoset (a, b) and poly(EHMA-co-MA)/epoxy thermoset (c-e) hybrid particles.

To further confirm the size of epoxy thermoset domains, hybrid latexes were diluted by THF to dissolve thermoplastic phase before TEM observation. It is found that, the size of thermoset domains in both poly (St-*co*-MA)/epoxy and poly (EHMA-*co*-MA)/epoxy latexes is around 100 - 150 nm, as illustrated in **Figure 62**.

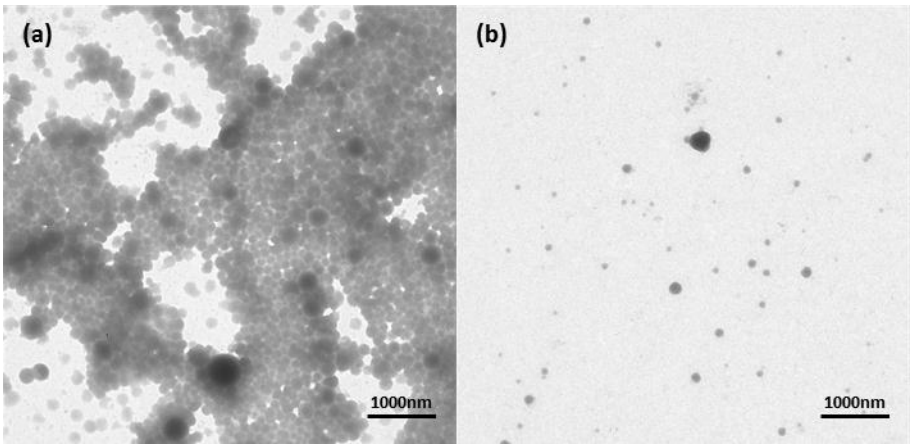

Figure 62. TEM images of poly (St-co-MA)/epoxy (a) and poly (EHMA-co-MA)/epoxy (b) hybrid particles diluted by THF.

The thermal property of as-prepared model particles has been measured by DSC, as illustrated in **Figure 63**. There are two observed T_g in poly (EHMA-*co*-MA) particles, which are around -3 ^oC and 32 ^oC, while no accurate T_g value can be identified in poly(EHMA-*co*-MA)/epoxy thermoset particles. The temperature regime for glass transition in poly (EHMA-*co*-MA)/epoxy thermoset is around -30 ^oC ~ 50 ^oC. Because St is more rigid than EHMA, poly(St-*co*-MA) and poly(St-*co*-MA)/epoxy thermoset possess higher T_g compared with EHMA containing samples. Similar to poly(EHMA-*co*-MA), poly(St-*co*-MA) has also two different T_g, which are about 24 ^oC and 63 ^oC, while poly(St-co-MA)/epoxy thermoset has only single T_g around 43 ^oC.

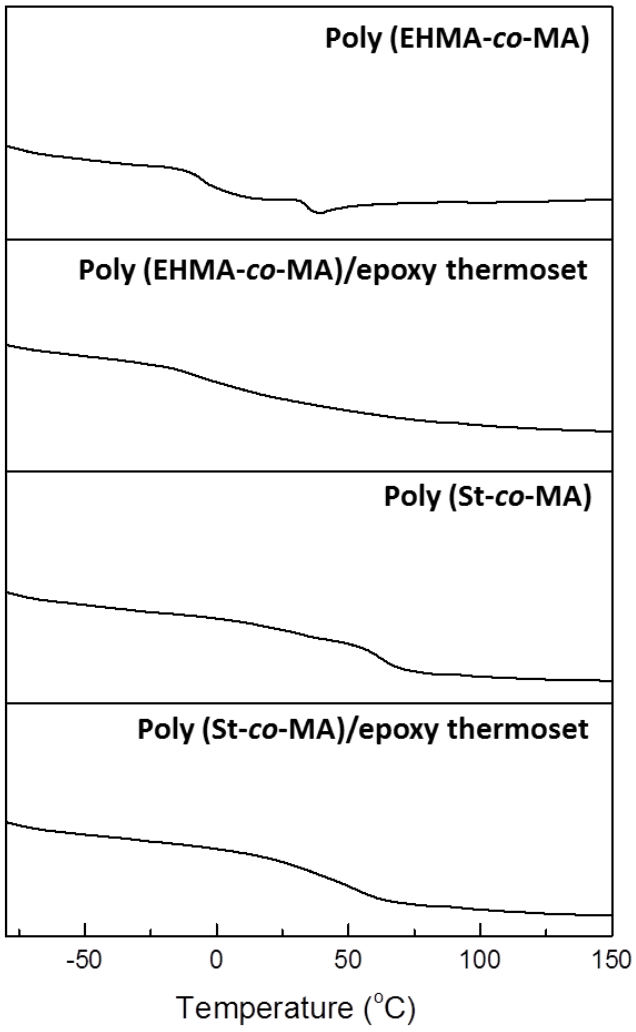

Figure 63. DSC curves of freeze-dried model polymer particles.

5.3.2. Thermoset-thermoplastic hybrid films

Appearance

Films from all latexes were dried at 100 °C to make sure that coalescence between colloidal particles during drying is enough. It is because one important parameter for the film formation of water-based polymer dispersion is the evaporation rate of water. If the coalescence between particles is slower than the evaporation of water, there is not enough time for the polymer to spread uniformly on the substrate to form a continuous film, which also affects the transparency of dried films. As discussed above, poly(EHMA-*co*-MA) and poly(EHMA-*co*-MA)/epoxy thermoset particles have low T_g that makes them form continuous films at 100 °C easily. A commonly used coalescence agent, 2,2,4-trimethyl-1,3-pentanediol monoisobutyrate (Texanol) has to be added into the latexes of poly (St-*co*-MA) and poly (St-*co*-MA)/epoxy thermoset to soften the particle for better coalescence. The concentration of Texanol in the latex is 10 wt% based on dry polymer weight. Otherwise continuous films cannot be generated from these two samples at 100 °C. **Figure 64** shows the transparency of dried films with and without epoxy thermoset domains, which is visualized by placing the coated glass slides on the logos of the Max Planck Institute for Polymer Research and the Henkel Company. All four films are transparent, which indicates that the incorporation of epoxy thermoset domains has not affected the transparency of polymer films.

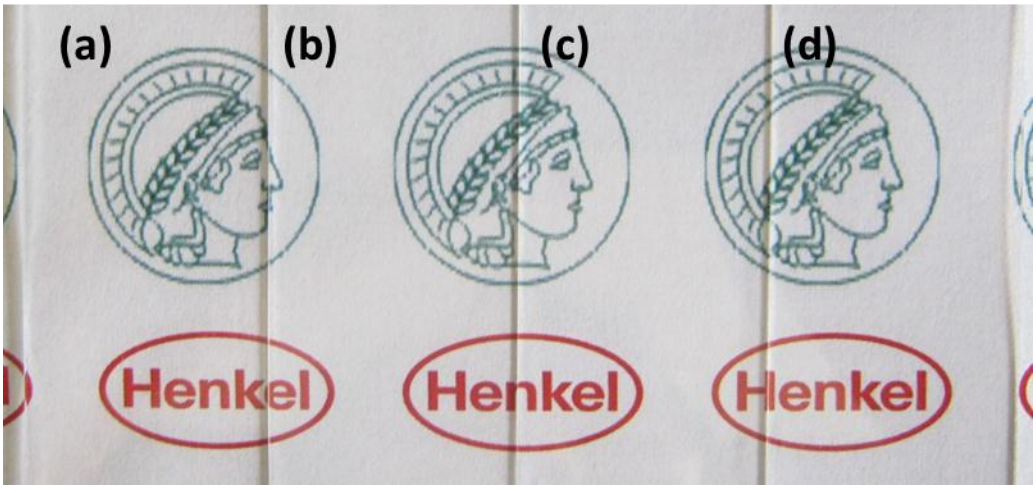

Figure 64. Appearance of the films derived from model latexes: (a) poly(EHMA-co-MA); (b) poly(EHMA-co-MA)/epoxy thermoset; (c) poly(St-co-MA); (d) poly (St-co-MA)/epoxy thermoset.

Mechanical properties

The reinforcement of poly(St-co-MA) and poly(EHMA-co-MA) films in hardness after incorporating epoxy thermoset domains has been investigated through the pencil hardness test and the cross cut test.

The pencil hardness test results are illustrated in **Figure 65** and **Figure 66**. Different forces ranging from 1 N to 10 N have been applied on the surfaces of films to create scratches. If the resistance of the film to the scratch is not strong enough, the cut can go through the film and expose the steel panel underneath, which will be corroded by acidic $CuSO_4$ solution. Figure 65a and Figure 66a indicate that a force of only 1 N can cut through poly(St-*co*-MA) and poly(EHMA-*co*-MA) films. On the contrary, poly(St-*co*-MA)/epoxy thermoset can stand a force as high as 9 N, while poly (EHMA-*co*-MA)/epoxy thermoset can only be cut through with forces over 5 N, as shown in Figure 65b and Figure 66b.

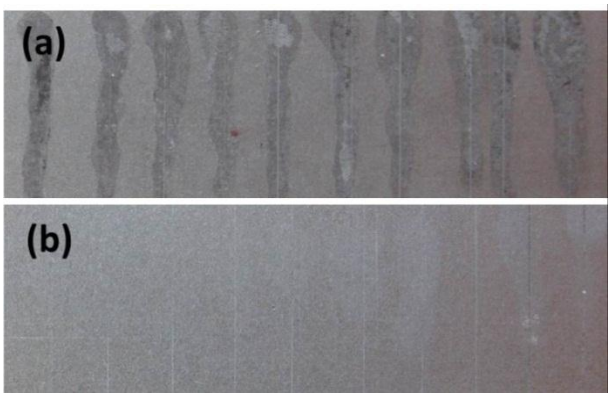

Figure 65. Pencil hardness test results of the films derived from model latexes: (a) poly(St-co-MA); (b) poly(St-co-MA)/epoxy thermoset (The forces applied on the films differ from 1 N to 10 N with the increment of 1 N, which cause the scratch lines on the surfaces).

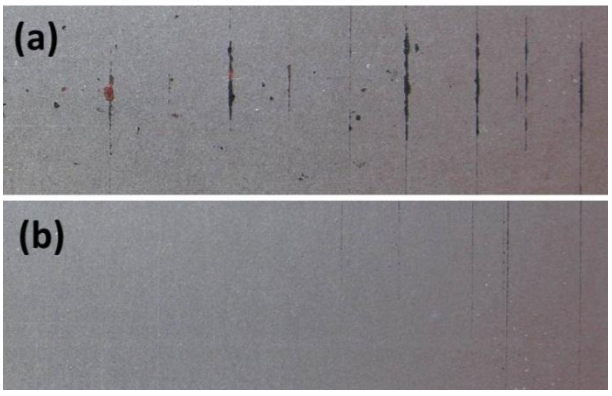

Figure 66. Pencil hardness test results of the films derived from model latexes: (a) poly(EHMA-co-MA); (b) poly(EHMA-co-MA)/epoxy thermoset (The forces applied on the films differ from 1 N to 10 N with the increment of 1 N, which cause the scratch lines on the surfaces).

In the cross cut test, as shown in **Figure 67**a, the poly(EHMA-*co*-MA) film was completely removed after the cross cut test. In contrast, poly(EHMA-*co*-MA)/epoxy thermoset still stays on the surface of steel panels after the removal of adhesive tapes, as demonstrated in Figure 13b. Poly(St-*co*-MA) and poly(St-*co*-MA)/epoxy thermoset films were not peeled off the panel after the test. However, the depth of the cut is much deeper in the poly(St-*co*-MA) film than the poly(St-*co*-MA)/epoxy thermoset film, which is indicated by darker colored grids due to the reaction between acidic $CuSO_4$ solution and steel panel underneath. The adhesion test result from the cross cut test is affected by both the adhesion force in substrate/film interface and the hardness of the films. In our case, it can be speculated that the significant improvement of the films with epoxy thermoset domains is derived from the increase of film hardness, because epoxy thermoset domains cannot bring in any extra intermolecular interactions in the substrate/film interface compared with the samples without epoxy.

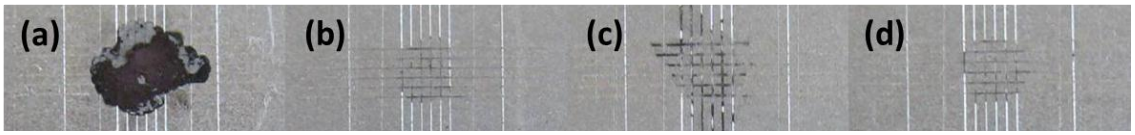

Figure 67. Cross cut test results of the films derived from model latexes: (a) poly(EHMA-co-MA); (b) poly(EHMA-co-MA)/epoxy thermoset; (c) poly(St-co-MA); (d) poly(St-co-MA)/epoxy thermoset.

5.4. Conclusion

In this chapter, the synthesis of structured thermoset-thermoplastic composite particles based on chemically induced phase separation process and seeded emulsion polymerization technique has been described. In the first part, detailed investigations on the compatibility between various vinyl monomers/polymers and epoxy resin/thermoset have been performed in bulk. In vinyl monomer-epoxy thermoset and vinyl polymer-epoxy resin systems, the compatibility is dependent on the hydrophobicity of monomer/polymer and ratios between different phases. On one hand, the more hydrophobic the vinyl monomer is, the worse is the compatibility between vinyl phase and epoxy phase. On the other hand, the more the less viscous phase, the stronger is the phase separation. Nevertheless, if both the vinyl phase and the epoxy phase were polymerized, the fast build-up of molecule weight of both phases induced a strong phase separation immediately, which is irrelevant to the hydrophobicity of vinyl phase and ratios between two phases.

In the second part of this section, structured thermoset-thermoplastic composite particles have been produced by the combination of the chemically induced phase separation process and the seeded emulsion polymerization technique. The curing of epoxy resin was performed inside miniemulsion droplets with the existence of various vinyl monomers, which is regarded as 1^{st} monomer. After the addition of a 2^{nd} monomer and the initiation of free radical polymerization, core-shell shaped thermoset-thermoplastic particles have been generated. Styrene has been selected as the standard 1^{st} monomer for the investigation of different parameters that affect the morphologies of composite particles. It has been found that the size and morphology of final composite particles is strongly dependent on the amount and composition of the seed and feed. In detail, these factors include the surfactant concentration, the amount of the 1^{st} monomer, the composition of the 1^{st} monomer, the composition of epoxy resin, the amount of the 2^{nd} monomer and the composition of the 2^{nd} monomer.

In the third part of this section, MA has replaced MMA as the 2^{nd} monomer due to its lower T_g after polymerization. Four model latexes, poly(St-*co*-MA)/epoxy thermoset, poly(EHMA-*co*-MA)/epoxy thermoset, poly(St-*co*-MA) and poly(EHMA-*co*-MA), have been prepared following the method described in the second part of this chapter. Transparent composite films have been obtained by drying the films at 100 ^{o}C. The results from the cross-cut tape test and

pencil hardness test have indicated that the incorporation of epoxy thermoset domains can improve the mechanical properties of the thermoplastic films significantly.

6. Chacterization methods

6.1. Size measurement

The size of the latex particles was determined by dynamic light scattering using a Nano-Zetasizer from Malvern Instruments at 25 ^{o}C. Before measurement the latexes were diluted around 2500 times by D. I. water

6.2. Zeta potential measurement

Zeta potential of the latex particles were measured on a Nano-Zetasizer from Malvern Instruments at 25 ^{o}C. Before measurement, the latexes were diluted around 2500 times by aqueous KCl solution (10^{-2} M).

6.3. Transmission Electron Microscopy (TEM)

The morphologies of latex particles were investigated with transmission electron microscopy (TEM, Philips Tecnai 10). Diluted latex samples in water (or THF) were deposited on 400-mesh carbon-coated copper grids and left to dry prior to analysis with operating at 100 kV.

6.4. Scanning Electron Microscopy (SEM)

The morphologies of latex particles were also investigated with scanning electron microscopy (SEM) Zeiss Gemini 1530 (Carl Zeiss, Germany). Before measurement, latexes were highly diluted and dried on silicon wafer. The surface morphologies of PAN/epoxy thermoset films were obtained from Nova NanoSEM 450 (FEI, USA).

6.5. Optical microscopy

The morphologies of the semi-crystalline films derived from PAN latex and PAN/methacrylic polymer hybrid latex were studied with an optical microscope, the model of which is BX 60 (Olympus, Japan).

6.6. Mechanical Testing

The mechanical properties of the film materials obtained from the hybrid latexes were evaluated by cross cut tape test and pencil hardness test, which indicate the adhesion of films to the substrates and film hardness.

Cross cut tape test

The adhesion between the film layer and hot-dip galvanized (HDG) panel was assessed by cross-cut tape test according to ASTM D3359-02. In a typical procedure, a lattice pattern, as shown in **Figure 68**, was made on the substrate by a scratch hardness tester (Model 430, Erichsen) equipped with cross hatch cutter (Model 295, Erichsen). Then a Permacel tape was taped on the top of the film and peeled off. The adhesion was evaluated by how many grids remain on the substrate. 17 wt% $CuSO_4$ aqueous solutions with pH adjusted to 1 by HCl was spread on the films and dried by tissue papers after cross cut tap test to visualize the scratch lines and the areas where films were peeled off. Films with good adhesion are more difficult to be removed from the substrate, which means more grids remain on the substrate. On the other hand, the hardness of the film plays a role here, because it is more difficult to cause damages in the films with higher hardness, thus more difficult to peel off less damaged films.

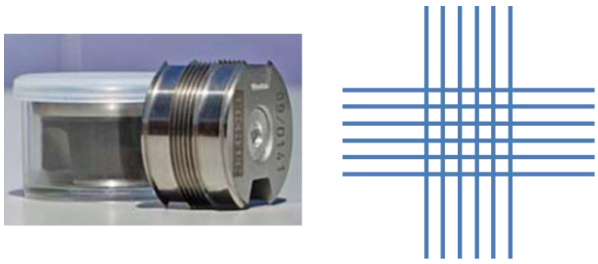

Figure 68. Cross hatch cutter (left, picture taken from Erichsen website) and the Lattice pattern on the film for tape test (right).

Pencil hardness test

The hardness of the films was characterized by pencil hardness test. The test was carried out by applying different vertical forces from 1 N to 10 N with hardness test pencil (Model 318 S, Erichsen) to the horizontal film surfaces in a way as illustrated in **Figure 69**. 17 wt% $CuSO_4$ aqueous solutions with pH adjusted to 1 by HCl was spread on the films and dried by tissue papers after pencil hardness test to visualize the scratch lines. Films with higher hardness are more resistant to scratch, which means it is more difficult to cut the films to expose steel substrate. Therefore, acidic $CuSO_4$ aqueous solutions cannot penetrate into the film and react with the steel surface, which means the scratch lines are less visible.

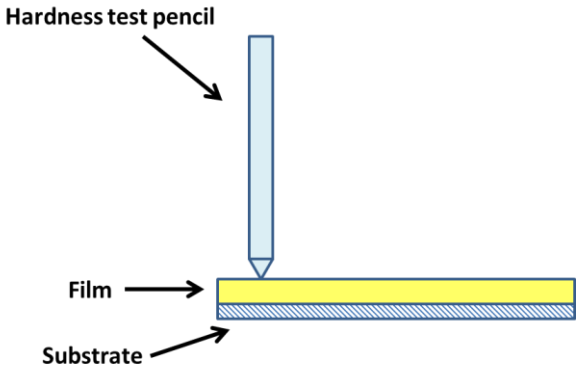

Figure 69. Schematic presentation of pencil hardness test of a film.

6.7. Thermal Analysis

Differential scanning calorimetry (DSC) was measured on a TA instrument Q1000 analyzer. Free dried latex samples were heated from -90 ^{o}C to 150 ^{o}C at a heating rate of 10 ^{o}C/min under nitrogen.

6.8. X-ray diffraction (XRD)

Crystallization of the polymers was investigated by X-ray diffraction (XRD) with a Philips Goniometer PW 1820 at a wavelength of 1.5418 Å (Cu-Kα) on freeze-dried latex samples.

6.9. Oxygen barrier measurement

Oxygen transmission rate (OTR) of the films was measured on OX-TRAN Model 2/21 (Mocon, USA) in this thesis to evaluate the oxygen barrier property of the films. In this method, the amount of oxygen gas that passes through a substance over a given period of time was measured. A schematic presentation of the internal structure of the Mocon equipment is shown in **Figure 70**. A flat test film sample with the size larger than 50 cm x 50 cm was clamped into the diffusion cell between inside chamber and outside chamber first. Then nitrogen was purged into the diffusion cell to remove residual oxygen. Subsequently pure oxygen was introduced into the outsider chamber. The amount of oxygen molecules that diffuse through the film into the inside chamber is detected by the sensor. In this dissertation, the film test sample is a coated polyethylene terephthalate (PET) film. The measurement was lasted for 24h, which was carried out with the humidity of 50%. The coatings were casted from freshly made latexes on PET substrate by a 20 µm rod-coater and cured at 60 ^{o}C for 24 h.

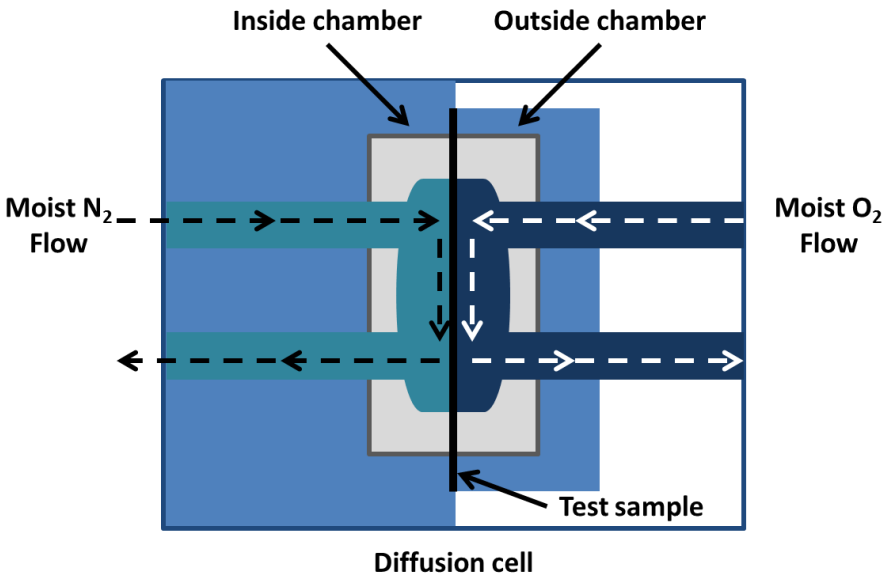

Figure 70. Schematic presentation of internal structure of the oxygen permeability test chamber in Mocon equipment.

7. Experimental Details

7.1. Raw materials

Name	Abbreviation	Supplier
2,2,4-trimethyl-1,3-pentanediol monoisobutyrate	Texanol	Alfa Aesar
2,2'-Azobis (2-methylbutylonitrile)	V-59	Wako Chemicals
2,2'-Azobis (2-methylpropinamidine)	V-50	Wako Chemicals
2-Ethylhexyl methacrylate	EHMA	Sigma-Aldrich
Acrylonitrile	AN	Sigma-Aldrich
Bisphenol F based epoxy resin [epoxy equivalent weight (EEW) is around 170 g/eq]	D. E. R. 354	Dow Chemical
Butenediol-vinyl alcohol copolymer (Trade name G-Polymer OKS-8041)	BVOH	Nippon Gohsei
Cetyltrimethylammonium bromide	CTAB	Sigma-Aldrich
Cooper (II) sulfate	$CuSO_4$	Sigma-Aldrich
Divinylbenzene	DVB	Sigma-Aldrich
Diethylenetriamine	DETA	Merck
Ethylene glycol dimethacrylate	EGDMA	Sigma-Aldrich
Hexadecane	HD	Merck
Hydrogen chloride	HCl	Sigma-Aldrich
Lauryl Methacrylate	LMA	Sigma-Aldrich
Lutensol AT 25 [Chemical formula $RO(CH_2CH_2O)_{25}H$, R is linear,		BASF

saturated C16~C18 fatty alcohol]		
Lutentsol AT 50 (Non-ionic surfactant, alkylpolyethylene glycol ethers made from a linear, saturated C_{16}~C_{18} fatty alcohol)		BASF
Methyl acrylate	MA	Sigma-Aldrich
Methyl acrylic acid	MAA	Sigma-Aldrich
Methyl methacrylate	MMA	Sigma-Aldrich
Phenalkamine based amine curing agent [amine hydrogen equivalent weight (AHEW) is around 133 g/eq]	NX 5454	Cardolite
Polyvinylpyrrolidone ($\mathbf{M}_w$ 40,000)	PVP 40	Sigma-aldrich
Potassium chloride	KCl	Sigma-aldrich
Potassium peroxide sulfate	KPS	Acros
Sodium dodecyl sulfate	SDS	BASF
Styrene	St	Sigma-Aldrich
Tetrahydrofuran	THF	Sigma-Aldrich
Trimethylolpropane triglycidyl ether	ED-505	Adeka
Tetraglycidyl meta-xylenediamine	GA-240	Emerald

All chemicals were of reagent grade and used as received unless otherwise stated. Demineralized water was used throughout the work. The chemical structures of Bisphenol F based epoxy resin and phenalkamine based amine curing agent are shown in **Table 16**.

Table 16. Chemical structures of bisphenol F based epoxy resin and phenalkamine based amine curing agent.

	Chemical Structure
Bisphenol F based epoxide resin (D. E. R. 354)	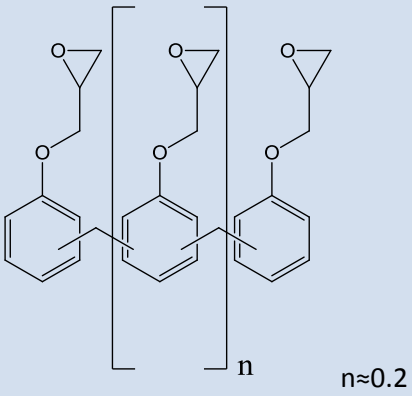 n≈0.2
Phenalkamine based amine curing agent (NX 5454)	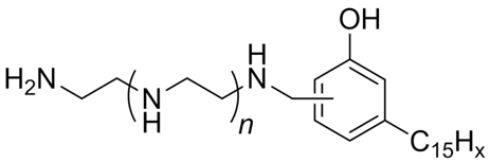

7.2. Synthesis of structured semi-crystalline hybrid latex particles through the assembly of liquid droplets and solid particles

7.2.1. Preparation of semi-crystalline PAN dispersion

Miniemulsion polymerization approach

A typical procedure for the preparation of semi-crystalline PAN dispersion through miniemulsion polymerization approach is described. 18 g of acrylonitrile, 750 mg of hexadecane and 450 mg of V-59 were mixed uniformly and added into an aqueous solution containing 1.8 g of BVOH in 91 g of water. After 2 min of magnetic stirring at 300 rpm, the mixture was sonicated under ice cooling for 2 min at 90% amplitude using a Branson 450 W sonifer and a 1/2" tip. Subsequently, 72 mg of SDS dissolved in 8 g of water were added into the as-prepared miniemulsion, which was then transferred to a round-bottom flask and placed in a 70 ^{o}C oil-bath under magnetic stirring with the speed of 400 rpm to initiate polymerization. The polymerization was completed in 4 h. To investigate the influence of methacrylic co-monomer on the crystallinity of PAN, 50 % of the acrylonitrile in the standard recipe has been replaced by a mixture of MMA, EHMA and LMA (The weight ratio between MMA, EHMA and LMA is 60:35:5). Other parameters were maintained the same.

Dispersion polymerization approach

In a typical dispersion polymerization produce of acrylonitrile, certain amount of polymer stabilizer, acrylonitrile, and initiator was first weighed into a three-neck round-bottom flask containing solvent. After the dissolving of all ingredients, N_2 was purged into the mixture for 10 min. Then the temperature of the mixture was increased to 70 ^{o}C to initiate the free radical polymerization. The mixture was maintained at 70 ^{o}C for 24h under magnetic stirring. For the polymerization in ethanol, V-59 was used the initiator. For the polymerization in water, V-50 or KPS was used as the initiator. The detailed recipes for the polymerization in ethanol and in water are illustrated in **Table 17** and **Table 18**.

Table 17. Recipe for the dispersion polymerization of acrylonitrile in ethanol.

	AN [g]	Water [g]	Ethanol [g]	V-59 [g]	BVOH [g]	PVP [g]
DP-PAN-1	6	2.4	21.6	0.12	0.9	-
DP-PAN-2*	6	12	12	0.12	0.9	-
DP-PAN-3	6	12	12	0.12	-	0.9
DP-PAN-4	6	2.4	21.6	0.12	-	0.9
DP-PAN-5	3	2.4	21.6	0.12	-	0.45

*0.9 g of BVOH was pre-dissolved in water

Table 18. Recipe for the dispersion polymerization of acrylonitrile in water.

	AN [g]	Water [g]	V-50 [g]	KPS [g]	BVOH [g]	PVP [g]
DP-PAN-6	1.68	24	0.028	-	-	0.252
DP-PAN-7	1.68	24	-	0.028	0.252	-

7.2.2. Preparation of methacrylic monomer miniemulsions

Methacrylic miniemulsions with different compositions and surface properties have been synthesized, the details of which are listed in **Table 19** and **Table 20**. A typical synthesis process is as follows: 6 g of methacrylic monomer were added into an aqueous surfactant solution containing certain amounts of CTAB and/or Lutensol AT25 and 24 g of water under magnetic stirring. The mixture was kept stirring for 2 min at 300 rpm. Subsequently, the miniemulsion was prepared through 2 min ultrasonication with 90% amplitude. All miniemulsions were used directly after preparation for subsequent procedures.

Table 19. Formulations of methacrylic miniemulsions without crosslinker.

	CTAB [g]	Lutensol AT 25 [g]	MMA [g]	EHMA [g]	LMA [g]	V-59 [g]
ME-1	0.24	-	3.6	2.1	0.3	-
ME-2	0.24	-	3.6	2.1	0.3	0.1
ME-3	-	0.24	3.6	2.1	0.3	-
ME-4	0.018	0.222	3.6	2.1	0.3	-
ME-5	0.036	0.204	3.6	2.1	0.3	-
ME-6	0.080	0.160	3.6	2.1	0.3	-
ME-7	0.24	-	5.7	-	0.3	-
ME-8	0.24	-	2.4	3.3	0.3	-
ME-9	0.24	-	1.5	4.2	0.3	-

Table 20. Formulations of methacrylic miniemulsions with crosslinker.

	CTAB [g]	Monofunctional monomer* [g]	EGDMA [g]
ME-10	0.24	5.9940	0.006
ME-11	0.24	5.9985	0.015
ME-12	0.24	5.9700	0.030
ME-13	0.24	5.9400	0.060
ME-14	0.24	5.8800	0.120

* MMA, EHMA and LMA has been pre-mixed with the ratio of 60 : 35 : 5 (in weight) before use; The estimated Tg of non-crosslinked methacrylic copolymer is around 44 °C.

7.2.3. Preparation of structured semi-crystalline hybrid particles

In a typical procedure to prepare semi-crystalline hybrid particles, 7.5 g of methacrylic miniemulsion were weighed into a flask equipped with a magnetic stirrer. 10 g of PAN dispersion were added slowly into the flask at 300 rpm magnetic stirring and kept stirring for 30 min. Subsequently, the flask was placed in a 70 °C oil bath. Initiator solution (0.025 g of V-50 dissolved in 1 g of water) was added to initiate free radical polymerization and the reaction mixture was maintained at 70 °C for 4 h. If the oil-soluble initiator V-59 was used instead of water-soluble V-50, it was directly dissolved in the monomer mixture before sonication. The nomenclature of as-prepared hybrid dispersion follows that of the miniemulsions, but with 'L' as initial rather than 'ME' (for example, hybrid dispersion derived from ME-1 is named as L-1, etc). In addition, L-15 has been prepared by blending 7.5 g of latex derived from ME-1 (polymerization condition same as described above for hybrid latex) with 10 g of PAN dispersion at room temperature, which was designed to compare liquid (methacrylic monomer droplet)-solid (PAN particle) and solid (methacrylic polymer particle)-solid (PAN particle) assembly.

7.2.4. The preparation of semi-crystalline films

For better film quality, more concentrated PAN dispersion was synthesized following the same method described above, but with solid content of 22.3%. Hybrid dispersion with 30 wt% PAN (based on total weight of PAN and methacrylic polymer) has been synthesized with the procedure mentioned above with ME-1 as miniemulsion. Films were cast from as-prepared PAN and PAN/methacrylic hybrid dispersions on glass slides by 20 µm rod-coater and dried in an oven at 60 °C. Before film casting, glass slides were cleaned thoroughly with acetone.

7.2.5. The preparation of epoxy miniemulsion

To prepare epoxy miniemulsion, 40 g of D. E. R. 354 was dissolved first in 40 g of Ethylacetate, which was mixed with an aqueous CTAB solution at 40 ^{o}C (1.6 g of CTAB dissolved in 160 g of water). The mixture was pre-emulsified by a rotary homogenizer at 11,000 rpm for 3 min. Then the coarse emulsion was transferred to a high-pressure homogenizer, which was homogenized at 40 ^{o}C with the pressure set as 11,000 psi for 2 cycles and cooled with ice for the 3rd cycle. Ethylacetate was removed by rotary evaporator at 70 ^{o}C under the pressure of 350 mbar. For the control sample without using ethylacetate, all other parameters and procedures were maintained the same.

High-pressure homogenizer

The high-pressure homogenizer used in this dissertation is a Microfluidic® M-100Y Microfluidizer processor. The general working principle is that coarse emulsion is powered by a high-pressure pump through the chamber which possesses microchannels with well-defined geometry at speeds up to 400 m/s to generate fine emulsions. The resulting shear forces can create narrowly distributed emulsions. Different geometries are available for the microfluidizer. In this thesis, a chamber composed of two "Z"-type interaction chambers (as shown in **Figure 71**) with diameter of 400 and 200 µm has been used.

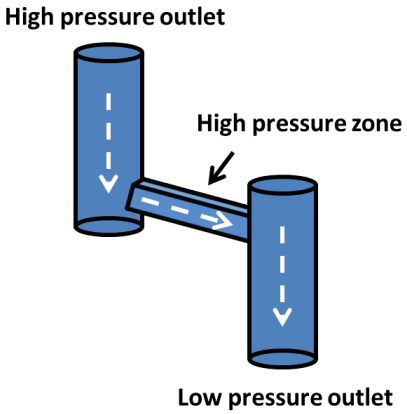

Figure 71. Schematic illustration of "Z"-type interaction chamber.

7.2.6. The preparation of PAN/epoxy hybrid miniemulsion and PAN/epoxy thermoset composite films

PAN/epoxy hybrid miniemulsion was obtained by mixing certain amount of the epoxy miniemulsion with the PAN dispersion under magnetic stirring for 30 min. To obtain

PAN/epoxy thermoset composite films, a certain amount of DETA (the molar ratio between the epoxide group and the active hydrogen atom from DETA is 1 : 1.6) was first added into the PAN/epoxy hybrid miniemulsion and mixed for 10 min. Then the hybrid miniemulsion was deposited onto flexible PET films by a 20 μm rod coater, which was dried and cured at 60 ^{o}C for 24h. Before film casting, PET films were cleaned thoroughly with ethanol.

7.3. Structured thermoset-thermoplastic hybrid particles and derived thermoset reinforced thermoplastic films

7.3.1. In-bulk study

The compatibility between the vinyl phase (vinyl monomer or vinyl polymer) and epoxy phase (epoxy resin, amine curing agent or cured epoxy thermoset) has been investigated through in-bulk study. In a typical procedure, certain amount of Bisphenol F based epoxide resin D. E. R. 354, amine curing agent, Cardolite NX 5454, (0.8 of amine hydrogen atom to 1 epoxy stoichiometric ratio) were mixed uniformly with certain amount of vinyl monomers and oil-soluble initiator V-59 in glass bottles at room temperature. Subsequently, these mixtures were placed in 70 ^{o}C oven and room temperature separately for curing. The compatibility between the epoxy phase and the vinyl phase was indicated by the transparency of the obtained solids.

7.3.2. Synthesis of thermoset-thermoplastic hybrid nanoparticles

A typical synthesis procedure for thermoset-thermoplastic hybrid particles is described below. First, a certain amount (see **Table 21** to **Table 25**) of vinyl monomer (named as 1st monomer), epoxy resin, and amine curing agent, Cardolite NX 5454, were weighted in a glass beaker and mixed uniformly. Then, the mixture was added into Lutensol AT 50 aqueous solution (0.3 g Lutensol AT 50 dissolved in 23 g of water). After 2 min magnetic stirring, a stable miniemulsion was obtained by 2 min ultrasonication by Branson W450 sonifer with a 1/2"tip. The amplitude was set to 90%. During homogenization, the mixture was cooled with an ice-bath to suppress polymerization. Subsequently, as-prepared miniemulsion was transferred into a round-bottom flask and cured at different temperatures (70 ^{o}C or room temperature) equipped with magnetic stirring. The cured miniemulsions are called seed emulsions in this work. After curing (24 h at room temperature or 2h at 70 ^{o}C), a certain amount (see Table 21 to Table 25) of vinyl monomers (named as 2nd monomer) were fed into the seed emulsions and mixed for 30 min at room temperature under vigorous stirring. Then the mixture was transferred to 70 ^{o}C oil-bath and fed with V-50 aqueous solution (V-50 was pre-dissolved in 1 g of water) to initiate free radical polymerization. The reaction mixture was maintained stirring at 70 ^{o}C for 24 h. In this thesis, the order of monomer in the nomenclature defines the 1st and 2nd monomer in the thermoset-thermoplastic nanoparticles. Take poly(St-*co*-MA)/epoxy thermoset for example, St is the 1st monomer, and MA is the 2nd monomer. If a mixture of monomers is used for the 2nd monomer, such as St and MMA, the latex sample is named as

poly (St-*co*-St/MMA)/epoxy thermoset. For the investigation of the influence of surfactant concentration on the physicochemical property of composite latexes, one control sample with 0.18 g of Lutensol AT 50 was synthesized. In this sample, 3 g of St and 3 g of MMA was used as the 1st and 2nd monomer respectively, while the epoxy phase is composed of 1.85 g of D. E. R. 354 and 1.18 g of NX 5454. All other parameters were kept the same as described in the typical synthesis procedure. All other formulations for the synthesis of thermoset-thermoplastic hybrid particles are listed in the following tables from Table 21 to Table 25.

Table 21. Formulations for the investigation on the influence of the 1st monomer.

Sample name	1st monomer [g]			Epoxy phase [g]	2nd monomer [g]
	St	MMA	EHMA		MMA
CS-1	3	-	-	3	3
CS-9	-	3	-	3	3
CS-10	-	-	3	3	3

* Epoxy phase is composed of 1.85 g of D. E. R. 354 and 1.15 g of NX 5454;
* The amount of water and Lutensol AT 50 in seed emulsion is 23 g and 0.3 g respectively;
* The initiator solution contains 0.1 g of V-50 and 1 g of water.

Table 22. Formulations for the investigation on the influence of the functionality of epoxy resin.

Sample name	Epoxy phase [g]				1st monomer [g]	2nd monomer [g]
	D. E. R. 354	ED-505	GA-240	NX 5454	St	MMA
CS-1	1.85	-	-	1.15	3	3
CS-15	1.57	0.28	-	1.15	3	3
CS-16	1.64	-	0.21	1.15	3	3

* The amount of water and Lutensol AT 50 in seed emulsion is 23 g and 0.3 g respectively;
* The initiator solution contains 0.1 g of V-50 and 1 g of water.

Table 23. Formulations for the investigation on the influence of the 2nd monomer.

Sample name	1st monomer [g]	Epoxy phase [g]	2nd monomer [g]			
	St		EHMA	St	MMA	MAA
CS-3	3	3	3	-	-	-
CS-2	3	3	-	3	-	-
CS-5	3	3	-	2.7	0.3	-
CS-6	3	3	-	2.4	0.6	-
CS-7	3	3	-	1.5	1.5	-
CS-8	3	3	-	0.6	2.4	-
CS-1	3	3	-	-	3	-
CS-4	3	3	-	-	-	3

* Epoxy phase is composed of 1.85 g of D. E. R. 354 and 1.15 g of NX 5454;

* The amount of water and Lutensol AT 50 in seed emulsion is 23 g and 0.3 g respectively;

* The initiator solution contains 0.1 g of V-50 and 1 g of water.

Table 24. Formulations for the investigation on the amount of the 2nd monomer.

Sample name	1st monomer [g]	Epoxy phase [g]		2nd monomer [g]
	St	D. E. R. 354	NX 5454	MMA
CS-17	3	1.85	1.15	1.5
CS-1	3	1.85	1.15	3
CS-18	3	1.85	1.15	6
CS-19	3	1.85	1.15	10

* The amount of water and Lutensol AT 50 in seed emulsion is 23 g and 0.3 g respectively;

* The initiator solution contains 0.1 g of V-50 and 1 g of water.

Table 25. Formulations for the investigation on the amount of vinyl crosslinker.

Sample name	1st monomer [g]	Epoxy phase [g]		2nd monomer [g]		
	St	D. E. R. 354	NX 5454	St	MMA	DVB
CS-5	3	1.85	1.15	2.7	0.3	0
CS-20	3	1.85	1.15	2.7	0.3	0.03
CS-21	3	1.85	1.15	2.7	0.3	0.06
CS-22	3	1.85	1.15	2.7	0.3	0.12
CS-23	3	1.85	1.15	2.7	0.3	0.18
CS-24	3	1.85	1.15	2.7	0.3	0.36

* The amount of water and Lutensol AT 50 in seed emulsion is 23 g and 0.3 g respectively;

* The initiator solution contains 0.1 g of V-50 and 1 g of water.

7.3.3. The preparation of thermoset-thermoplastic films

To obtain thermoset-thermoplastic films, two model thermoset-thermoplastic latexes (CS-11 and CS-12) have been prepared using the procedure described in section 7.3.2. For comparison, two control samples (CS-13 and CS-14) without epoxy thermoset inside have been synthesized. 3 g of MA was mixed with 3 g of St and EHMA respectively as oil phase before miniemulsification, which was polymerized directly afterwards without extra monomer feeding step. All other parameters were kept the same as described in the typical synthesis procedure of thermoset-thermoplastic latexes. Detailed formulations are illustrated in Table **26**.

Table 26. Formulations of four model latexes for film property investigation.

Sample name	Composition of seed				Composition of feed
	St [g]	EHMA [g]	MA [g]	Epoxy phase [g]	MA [g]
CS-11	3	-	-	3	3
CS-12	-	3	-	3	3
CS-13	3	-	3	-	-
CS-14	-	3	3	-	-

* Epoxy phase is composed of 1.85 g of D. E. R. 354 and 1.15 g of NX 5454;
* The amount of water and Lutensol AT 50 in seed emulsion is 23 g and 0.3 g respectively;
* The initiator solution contains 0.1 g of V-50 and 1 g of water.

Films were casted on pre-treated glass slides and hot-dip galvanized (HDG) steel panels from sample CS-11, CS-12, CS-13 and CS-14 by a 13 µm rod-coater. 2,2,4-trimethyl-1,3-pentanediol monoisobutyrate (Texanol) was added into CS-11 and CS-13 latexes before film-casting to soften the colloidal particles for better film-formation. The amount of Texanol applied is 10 wt% based on the solid content of latexes. Before film-casting, glass slides were cleaned thoroughly by aceton. The surface of HDG steel panels was cleaned by two Henkel cleaners, Ridoline 1340 and Emalan 570, at 75 ^{o}C for 60 s with subsequent twice rinsing by D. I. Water. The panels were dried at 70 ^{o}C in an oven and cooled down to room temperature before use.

8. Conclusion

In this work, composite colloidal particles with different microstructures and properties have been fabricated. Two basic concepts have been proposed: (1) creating structured semi-crystalline hybrid particles based on a novel liquid-solid heterocoagulation approach, and (2) creating structured thermoset-thermoplastic composite particles from homogeneous droplets. In both cases, composite films have been obtained directly after the evaporation of water. Benefitting from the controlled microstructure of colloidal particles, functional domains such as semi-crystalline polymers or highly crosslinked thermosets have been incorporated successfully into the films. The preliminary studies on oxygen barrier and mechanical properties indicate that as-prepared functional colloidal particles have great application potential in the coating and adhesive industry.

In detail, the first concept is a new approach to produce raspberry-shaped or core/shell-shaped hybrid particles with high colloidal stability based on the assembly of semi-crystalline polyacrylonitrile particles and liquid methacrylic monomer droplets. In this case, the heterogeneous structure of the colloidal particles is generated from heterogeneous sources, namely semi-crystalline polyacrylonitrile dispersion and methacrylic monomer miniemulsions. In the first part of this work, highly semi-crystalline polyacrylonitrile particles with long-term storage stability and relatively high solid content have been successfully synthesized by miniemulsion polymerization with a polymeric surfactant, butenediol-vinyl alcohol copolymer, and an anionic surfactant, sodium dodecyl sulfate. In the second part, a liquid-solid assembly of strongly positive charged methacrylic monomer miniemulsion droplets and weakly negative charged polyacrylonitrile particles has been carried out at high particle concentration. After free radical polymerization of the droplets, structured hybrid semi-crystalline particles have been obtained. Compared to classic heterocoagulation between solid particles, this method possesses two major advantages: (1) stable hybrid latexes can be obtained easily even at high solid content; (2) the discrete miniemulsion droplets offers high versatility in the chemistry of shell particles. For the first advantage, it has been found that direct solid-solid assembly of methacrylic polymer particles and polyacrylonitrile particles has led to immediate coagulation. The morphology of as-obtained hybrid particles can be easily changed from raspberry-shaped to core-shell shaped by tuning the T_g of the methacrylic copolymers. Based on the results from the study on different parameters that affect the morphology and other physicochemical

properties of hybrid latexes, an explanatory model based on the mobility of surfactant in droplet/particle interface is proposed and partially proved by experimental results. In the third part, methacrylic monomers inside the miniemulsion droplets have been replaced by an epoxy resin and cured by a water-soluble amine curing agent, diethylenetriamine. Semi-crystalline thermoset films have been obtained by simply casting the hybrid dispersion on flexible substrates with subsequent drying and curing. The concentration of semi-crystalline polymer inside the film has been tuned by changing the ratio between polyacrylonitrile latex and epoxy miniemulsion. The measurement results of oxygen transmittance rates of the films indicate that this material can be potentially used as flexible barrier materials for moisture and oxygen.

The second concept represents a new approach to produce structured thermoset-thermoplastic composite particles based on the combination of chemically induced phase separation process and seeded emulsion polymerization technique. Unlike the first concept, the in here reported heterogeneous structures are created from homogenous mixtures in confined space, namely the miniemulsion droplets. In this concept, thermoset domains act as reinforcement like fillers in the film derived from such composite particles. In the first part, simple in-bulk study has directly illustrated the compatibility between various vinyl phases (vinyl monomer or polymer) and epoxy phases (uncured and cured). It has been found that the compatibility is majorly determined by the ratio between different phases and the hydrophobicity of the vinyl phase. In general, the more hydrophobic the vinyl phase is, the lower is the compatibility. In the second part, structured thermoset-thermoplastic composite particles have been prepared by a two-step approach, which includes the curing of epoxy resin in vinyl monomer (1^{st} monomer) and the subsequent free radical polymerization after the feeding of 2^{nd} monomer. The successful fabrication of core-shell shaped particles is determined by the hydrophobicity of monomer added to the seed emulsions. While the addition of hydrophobic monomers, including EHMA and St, destabilize the emulsion, MMA and MA with suitable hydrophobicity leads to the formation of colloidally stable, structured hybrid particles. The influences of various factors, including the amount and composition of seed and feed, on the physicochemical properties of the composite latexes have been investigated. In the third part, four model systems, poly(St-*co*-MA), poly(St-*co*-MA)/epoxy thermoset, poly(EHMA-*co*-MA) and poly(EHMA-*co*-MA)/epoxy thermoset, have been designed and fabricated to investigate the film properties from structured thermoset-thermoplastic

composite particles. It has been found that the mechanical properties, such as film hardness and adhesion, have been improved significantly by the tailored incorporation of epoxy thermoset domains. Moreover, the transparency of the composite film has not been affected by the incorporation of thermoset domains even at high concentration, which is a major advantage compared with traditional inorganic fillers.

The main aspects of the two preparation routes for different composite colloidal particles described in this thesis are summarized in **Table 27**.

Table 27. Summary of the two preparation routes for composite colloidal particles.

Origin of well-defined heterogeneous structure	Type of colloidal particles	Method	Morphology
Heterogeneity (liquid droplet + solid particle)	semi-crystalline composite particle	- liquid-solid assembly - miniemulsion polymerization	- raspberry shaped - core-shell Shaped
Homogeneity (liquid droplet containing homogenous mixture)	thermoset-thermoplastic composite particle	- chemically induced phase separation - seeded emulsion polymerization	- homogeneous - core-shell Shaped

As mentioned in the beginning, well-defined heterogeneous structures have been created in colloids from both heterogeneous and homogeneous sources based on the utilization of miniemulsion droplets. It has been demonstrated that the microstructures of the colloidal particles can be controlled easily by applying different approaches (e.g. liquid-solid assembly or chemically induced phase separation) and/or tuning of various parameters. Due to the versatility of the chemistry in the droplets, it is expected that the methods demonstrated in this thesis can be extended to the fabrication of composite colloidal particles with different physicochemical properties. In addition, from the perspective of industrial potentials, both methods can be performed easily with the solid content in the level of common industrial standard and generate composite latexes with long term storage stability, which makes it promising also for the large-scale production of different functional composite colloids in coating and adhesive industry.

Abbreviations and Characters

Abbreviations

AHEW	Amine hydrogen equivalent weight
AN	Acrylonitrile
ASTM	American Society for Testing and Materials
BVOH	Butenediol-vinyl alcohol copolymer
CIPS	Chemically induced phase separation
CMC	Critical micelle concentration
CTAB	Cetyltrimethylammonium bromide
DETA	Diethylenetriamine
DLS	Dynamic light scattering
DLVO	Derjaguin-Landau-Vervey-Overbeek
DSC	Dynamic scanning calorimetry
DVB	Divinylbenzene
EA	Ethyl acetate
EEW	Epoxy equivalent weight
EGDMA	Ethylene glycol dimethacrylate
EHMA	2-ethylhexyl methacrylate
HD	Hexadecane
HDG	Hot-dip galvanized
LCST	Lower critical solution temperature
LMA	Lauryl methacrylate
MA	Methyl acrylate
MAA	Methyl acrylic acid
MFFT	Minimum film formation temperature
MMA	Methyl methacrylate
MPI-P	Max Planck Institute for Polymer Research
OTR	Oxygen transmittance rate

o/w	Oil-in-water
PAN	Polyacrylonitrile
PBA	Polybutylacrylate
PDI	Polydispersity index
PS	Polystyrene
PU	Polyurethane
PVP	Polyvinylpyrrolidone
SEM	Scanning electron microscopy
St	Styrene
TEM	Transmission electron microscopy
THF	Tetrahydrofuran
TIPS	Thermally induced phase separation
UCST	Upper critical solution temperature
XRD	X-ray diffraction
w/o	Water-in-oil

Characters and Symbols

Greek

ε	Dielectric constant
ε_r	Dielectric constant of the dispersion phase
κ	The inverse of the Debye length
η	Viscosity
ϕ	Volume fraction
χ_{12}	Flory-Huggins interaction parameter
ψ	Surface potential of the particle

Latin/ Roman

A	Hamaker constant
a	Radius of particle

f(κa)	Henry's function
G_{mix}	Gibbs energy of mixing
H	Shortest interparticle distance
H_{mix}	Enthalpy of mixing
M_w	Weight averaged molecular weight
R	Molar gas constant
S_{mix}	Entropy of mixing
T_g	Glass transition temperature
T	Temperature
U_E	Velocity of the particle or droplet
V_T	Total potential energy of interactions
V_A	Attraction part in the total potential energy of interactions
V_R	Repulsion part in the total potential energy of interactions
wt	Weight
$X_{1,2}$	Degree of polymerization

References

[1] A. B. Strong, "Fundamentals of Composites Manufacturing: Materials, Methods and Applications", SME, 2008.

[2] A. Kelly, C. H. Zweben, "Comprehesive composite materials, volume 1", Elsevier, 2000.

[3] D. D. L. Chung, "Composite Materials: Science and Applications", Springer, New York, 2010.

[4] J. Y. Sheikh-Ahmad, "Machining of Polymer Composites", Springer, New York, 2009.

[5] J. W. Nicholson, "The Chemistry of Polymers", The Royal Society of Chemistry, 2006.

[6] D. Ratna, "Handbook of Thermoset Resins", Smithers Rapra Technology, 2009.

[7] M. P. Stevens, "Polymer Chemistry: An introduction ", Oxford University Press, New York, 1999.

[8] J. R. Ebdon, "Synthetic Polymers: Technology, Properties, Applications", Springer, New York, 1996.

[9] "Epoxy Polymers", J.-P. Pascault; and R.J.J. Williams, Eds., Wiley-VCH, 2010.

[10] H. Q. Pham, M. J. Marks, "Epoxy Resins", in *Ullmann's Encyclopedia of Industrial Chemistry*, Wiley-VCH Verlag GmbH & Co. KGaA, 2000.

[11] Z. Dai, A. Constantinescu, A. Dalal, C. Ford, "Phenalkamine: Multipurpose epoxy resin curing agents", in *SPI-ERF Conference*, Cardolite Corporation, 1994.

[12] D. I. Bower, "An Introduction to Polymer Physics", Cambridge University Press, New York, 2002.

[13] J. Kiefer, J. Hedrick, J. Hilborn, "Macroporous Thermosets by Chemically Induced Phase Separation", in *Macromolecular Architectures*, J. Hilborn, P. Dubois, C.J. Hawker, J.L. Hedrick, J.G. Hilborn, R. Jérôme, J. Kiefer, J.W. Labadie, D. Mecerreyes, and W. Volksen, Eds., Springer Berlin Heidelberg, 1999, p. 161.

[14] K. Holmberg, B. Jönsson, B. Kronberg, B. Lindman, "Surfactants and polymers in aqueous solution", John Wiley & Sons, 2002.

[15] D. Mayers, "Surfaces, Interfaces, and Colloids: Principles and Applications", Wiley-VCH, 1999.

[16] D. J. Shaw, "Introduction to Colloid and Surface Chemistry", Elsevier Science, 1992.

[17] P. Debye, E. Hückel, *Physikalische Zeitschrift* **1923**, 22.

[18] S. Levine, *Proceedings of the Royal Society of London A* **1939**.

[19] S. Levine, G. P. Dube, *Transactions of the Faraday Society* **1940**, 16.

[20] B. Derjaguin, L. Landau, *Acta Physico Chemica URSS* **1941**.

[21] E. J. W. Verwey, J. T. G. Overbeek, "Theory of the stability of lyophobic colloids", Elsevier, Amsterdam, 1948.

[22] "Colloid Science: Principles, Methods and Applications", second edition, T. Cosgrove, Ed., John Wiley & Sons Ltd., Chichester, 2010.

[23] C. Chorung-Shyan, "Principles and applications of emulsion polymerization", Wiley, 2008.

[24] M. Antonietti, K. Tauer, *Macromolecular Chemistry and Physics* **2003**, *204*, 207.

[25] Z. Pan, "Polymer Chemistry", Chemical Industry, 2003.

[26] J. Ugelstad, M. S. El-Aasser, J. W. Vanderhoff, *Journal of Polymer Science: Polymer Letters Edition* **1973**, *11*, 503.

[27] Y. J. Chou, M. S. El-Aasser, J. W. Vanderhoff, *Journal of Dispersion Science and Technology* **1980**, *1*, 129.

[28] K. Landfester, N. Bechthold, S. Förster, M. Antonietti, *Macromolecular Rapid Communications* **1999**, *20*, 81.

[29] J. M. Asua, *Progress in Polymer Science* **2002**, *27*, 1283.

[30] K. Landfester, N. Bechthold, F. Tiarks, M. Antonietti, *Macromolecules* **1999**, *32*, 5222.

[31] K. Landfester, *Macromolecular Rapid Communications* **2001**, *22*, 896.

[32] K. Landfester, M. Antonietti, *Progress in Polymer Science* **2002**, *27*, 689.

[33] K. Landfester, *Angew Chem Int Ed Engl* **2009**, *48*, 4488.

[34] K. Landfester, F. Tiarks, H.-P. Hentze, M. Antonietti, *Macromolecular Chemistry and Physics* **2000**, *201*, 1.

[35] F. Tiarks, K. Landfester, M. Antonietti, *Journal of Polymer Science Part A: Polymer Chemistry* **2001**, *39*, 2520.

[36] M. Barrère, K. Landfester, *Polymer* **2003**, *44*, 2833.

[37] W. Qun, F. Shoukuan, Y. Tongyin, *Progress in Polymer Science* **1994**, *19*, 703.

[38] A. Guyot, K. Landfester, F. J. Schork, C. Wang, *Progress in Polymer Science* **2007**, *32*, 1439.

[39] A. Musyanovych, K. Landfester, "Macromolecular Engineering. Precise Synthesis, Materials Properties, Applications", K. Matyjaszweski, Y. Gnanou, and L. Leibler, Eds., Wiley-VCH, 2007.

[40] W. Ming, D. Wu, R. van Benthem, G. de With, *Nano Letters* **2005**, *5*, 2298.

[41] S.-H. Kim, G.-R. Yi, K. H. Kim, S.-M. Yang, *Langmuir* **2008**, *24*, 2365.

[42] D. Xu, M. Wang, X. Ge, M. Hon-Wah Lam, X. Ge, *Journal of Materials Chemistry* **2012**, *22*, 5784.

[43] F. Tiarks, K. Landfester, M. Antonietti, *Langmuir* **2001**, *17*, 5775.

[44] S. Fortuna, C. A. L. Colard, A. Troisi, S. A. F. Bon, *Langmuir* **2009**, *25*, 12399.

[45] M. J. Percy, C. Barthet, J. C. Lobb, M. A. Khan, S. F. Lascelles, M. Vamvakaki, S. P. Armes, *Langmuir* **2000**, *16*, 6913.

[46] M. J. Percy, V. Michailidou, S. P. Armes, C. Perruchot, J. F. Watts, S. J. Greaves, *Langmuir* **2003**, *19*, 2072.

[47] J. I. Amalvy, M. J. Percy, S. P. Armes, H. Wiese, *Langmuir* **2001**, *17*, 4770.

[48] R. F. A. Teixeira, H. S. McKenzie, A. A. Boyd, S. A. F. Bon, *Macromolecules* **2011**, *44*, 7415.

[49] M. Chen, S. Zhou, B. You, L. Wu, *Macromolecules* **2005**, *38*, 6411.

[50] S.-W. Zhang, S.-X. Zhou, Y.-M. Weng, L.-M. Wu, *Langmuir* **2005**, *21*, 2124.

[51] Z. H. Cao, G. R. Shan, G. Fevotte, N. Sheibat-Othman, E. Bourgeat-Lami, *Macromolecules* **2008**, *41*, 5166.

[52] I. Tissot, C. Novat, F. Lefebvre, E. Bourgeat-Lami, *Macromolecules* **2001**, *34*, 5737.

[53] M. Chen, L. Wu, S. Zhou, B. You, *Macromolecules* **2004**, *37*, 9613.

[54] R. Atkin, M. Bradley, B. Vincent, *Soft Matter* **2005**, *1*, 160.

[55] J. Wang, H. Li, X. Yang, *Polymers for Advanced Technologies* **2009**, *20*, 965.

[56] X. Cheng, M. Chen, S. Zhou, L. Wu, *Journal of Polymer Science Part A: Polymer Chemistry* **2006**, *44*, 3807.

[57] R. K. Iler, *Journal of colloid and interface science* **1966**, *21*, 569.

[58] G. Decher, *Science* **1997**, *277*, 1232.

[59] G. Decher, J.-D. Hong, *Makromolekulare Chemie. Macromolecular Symposia* **1991**, *46*, 321.

[60] G. Decher, M. Eckle, J. Schmitt, B. Struth, *Current Opinion in Colloid & Interface Science* **1998**, *3*, 32.

[61] G. B. Sukhorukov, E. Donath, S. Davis, H. Lichtenfeld, F. Caruso, V. I. Popov, H. Möhwald, *Polymers for Advanced Technologies* **1998**, *9*, 759.

[62] G. B. Sukhorukov, E. Donath, H. Lichtenfeld, E. Knippel, M. Knippel, A. Budde, H. Möhwald, *Colloids and Surfaces A: Physicochemical and Engineering Aspects* **1998**, *137*, 253.

[63] F. Caruso, *Advanced Materials* **2001**, *13*, 11.

[64] F. Caruso, H. Lichtenfeld, E. Donath, H. Möhwald, *Macromolecules* **1999**, *32*, 2317.

[65] F. Caruso, H. Möhwald, *Langmuir* **1999**, *15*, 8276.

[66] F. Caruso, C. Schüler, D. G. Kurth, *Chemistry of Materials* **1999**, *11*, 3394.

[67] F. L. Caruso, Heinz; Giersig, Michael; Möhwald, Helmuth, *Journal of American Chemical Society* **1998**, *120*, 8523.

[68] F. Caruso, D. Trau, H. Möhwald, R. Renneberg, *Langmuir* **2000**, *16*, 1485.

[69] R. F. A. Teixeira, S. A. F. Bon, "Physical Methods for the Preparation of Hybrid Nanocomposite Polymer Latex Particles", in *Hybrid Latex Particles: Preparation With*, A.M. VanHerk and K. Landfester, Eds., Springer-Verlag Berlin, Berlin, 2010, p. 19.

[70] H. Li, J. Han, A. Panioukhine, E. Kumacheva, *Journal of colloid and interface science* **2002**, *255*, 119.

[71] K. Furusawa, C. Anzai, *Colloids and Surfaces* **1992**, *63*, 103.

[72] A. M. Islam, B. Z. Chowdhry, M. J. Snowden, *Advances in Colloid and Interface Science* **1995**, *62*, 109.

[73] P. D. Yates, G. V. Franks, S. Biggs, G. J. Jameson, *Colloids and Surfaces a-Physicochemical and Engineering Aspects* **2005**, *255*, 85.

[74] R. H. Ottewill, A. B. Schofield, J. A. Waters, N. S. J. Williams, *Colloid Polym Sci* **1997**, *275*, 274.

[75] S. B. Darling, *Progress in Polymer Science* **2007**, *32*, 1152.

[76] I. W. Hamley, *Progress in Polymer Science* **2009**, *34*, 1161.

[77] J. K. Kim, S. Y. Yang, Y. Lee, Y. Kim, *Progress in Polymer Science* **2010**, *35*, 1325.

[78] L. Zhang, A. Eisenberg, *Science* **1995**, *268*, 1728.

[79] Y. Mai, A. Eisenberg, *Chemical Society reviews* **2012**, *41*, 5969.

[80] S. Torza, S. G. Mason, *Journal of colloid and interface science* **1970**, *33*, 67.

[81] D. C. Sundberg, A. P. Casassa, J. Pantazopoulos, M. R. Muscato, B. Kronberg, J. Berg, *Journal of Applied Polymer Science* **1990**, *41*, 1425.

[82] C. S. Chern, *Progress in Polymer Science* **2006**, *31*, 443.

[83] H. J. Jeon, Y. You, M. J. Yoon, J. H. Youk, *Polymer* **2011**, *52*, 3905.

[84] J. S. Kim, H. J. Jeon, K. M. Lee, J. N. Im, J. H. Youk, *Fibers and Polymers* **2010**, *11*, 153.

[85] Q.-Y. Wu, L.-S. Wan, Z.-K. Xu, *Journal of Membrane Science* **2012**, *409–410*, 355.

[86] M. M. Wu, "Acrylonitrile and Acrylonitrile Polymers", in *Encyclopedia of Polymer Science and Technology*, John Wiley & Sons, Inc., 2002.

[87] S. K. Nataraj, K. S. Yang, T. M. Aminabhavi, *Progress in Polymer Science* **2012**, *37*, 487.

[88] K. Landfester, M. Antonietti, *Macromolecular Rapid Communications* **2000**, *21*, 820.

[89] L. Boguslavsky, S. Baruch, S. Margel, *Journal of colloid and interface science* **2005**, *289*, 71.

[90] H. Shiho, J. M. DeSimone, *Macromolecules* **2000**, *33*, 1565.

[91] D. Cho, K. Oh, W. Bae, H. Kim, Y.-W. Lee, *Colloid Polym Sci* **2009**, *287*, 179.

[92] J. C. Ramirez, J. Herrera-Ordonez, V. A. Gonzalez, *Polymer* **2006**, *47*, 3336.

[93] J. C. Ramirez, J. Herrera-Ordonez, *European Polymer Journal* **2007**, *43*, 3819.

[94] R. Arshady, *Colloid Polym Sci* **1992**, *270*, 717.

[95] S. Kawaguchi, K. Ito, "Dispersion Polymerization", in *Polymer Particles*, M. Okubo, Ed., Springer Berlin Heidelberg, 2005, p. 299.

[96] S. Belbekhouche, T. Hamaide, V. Dulong, L. Picton, D. Le Cerf, J. Desbrières, *Polymer International* **2013**, n/a.

[97] E. Kientz, Y. Holl, *Colloids and Surfaces A: Physicochemical and Engineering Aspects* **1993**, *78*, 255.

[98] T. J. Barnes, C. A. Prestidge, *Langmuir* **2000**, *16*, 4116.

[99] O. D. Velev, K. Furusawa, K. Nagayama, *Langmuir* **1996**, *12*, 2385.

[100] K. M. Au, S. P. Armes, *ACS Nano* **2012**, *6*, 8261.

[101] H. Chatham, *Surface and Coatings Technology* **1996**, *78*, 1.

[102] X. Sun, Y. Li, *Angewandte Chemie International Edition* **2004**, *43*, 597.

[103] T. K. Mandal, M. S. Fleming, D. R. Walt, *Nano Letters* **2002**, *2*, 3.

[104] H. Zou, S. P. Armes, *Polymer Chemistry* **2012**, *3*, 172.

[105] L. M. Liz-Marzán, M. Giersig, P. Mulvaney, *Langmuir* **1996**, *12*, 4329.

[106] Y. Kobayashi, H. Katakami, E. Mine, D. Nagao, M. Konno, L. M. Liz-Marzán, *Journal of colloid and interface science* **2005**, *283*, 392.

[107] P. A. Steward, J. Hearn, M. C. Wilkinson, *Advances in Colloid and Interface Science* **2000**, *86*, 195.

[108] A. Aguiar, S. González-Villegas, M. Rabelero, E. Mendizábal, J. E. Puig, J. M. Domínguez, I. Katime, *Macromolecules* **1999**, *32*, 6767.

[109] Y. Chevalier, M. Hidalgo, J. Y. Cavaillé, B. Cabane, *Macromolecules* **1999**, *32*, 7887.

[110] Y.-Q. Li, S.-Y. Fu, Y. Yang, Y.-W. Mai, *Chemistry of Materials* **2008**, *20*, 2637.

[111] A. Lopez, E. Degrandi, E. Canetta, J. L. Keddie, C. Creton, J. M. Asua, *Polymer* **2011**, *52*, 3021.

[112] M. Barrère, K. Landfester, *Macromolecules* **2003**, *36*, 5119.

[113] J. H. Kiefer, J. G., *Polymer* **1996**, *37*, 5715.

[114] J. H. Kiefer, J. G.; Manson, J. A. E.; Leterrier, Y., *Macromolecular* **1996**, *29*, 4158.

[115] E. S. Girard-Reydet, H.; Pascault, J. P.; Keates, P.; Navard, P., *Polymer* **1998**, *39*, 2269.

[116] C. Sawaryn, K. Landfester, A. Taden, *Polymer* **2011**, *52*, 3277.

[117] H. Gerrens, *Journal of Polymer Science Part C: Polymer Symposia* **1969**, *27*, 77.

[118] F. J. Schork, J. Guo, *Macromolecular Reaction Engineering* **2008**, *2*, 287.